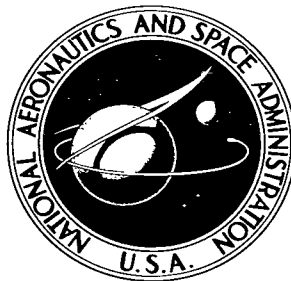


NASA TECHNICAL NOTE



NASA TN D-4233

NASA TN D-4233

c. 1



LOAN COPY: RETURN
AFWL (WLL-2)
KIRTLAND AFB, NM

LARGE-SCALE WIND-TUNNEL INVESTIGATION
OF A V/STOL TRANSPORT MODEL
WITH WING-MOUNTED LIFT FANS AND
FUSELAGE-MOUNTED LIFT-CRUISE
ENGINES FOR PROPULSION

by Jerry V. Kirk, Brent K. Hodder, and Leo P. Hall

*Ames Research Center
Moffett Field, Calif.*



LARGE-SCALE WIND-TUNNEL INVESTIGATION OF A V/STOL
TRANSPORT MODEL WITH WING-MOUNTED LIFT FANS
AND FUSELAGE-MOUNTED LIFT-CRUISE
ENGINES FOR PROPULSION

By Jerry V. Kirk, Brent K. Hodder, and Leo P. Hall

Ames Research Center
Moffett Field, Calif.

NATIONAL AERONAUTICS AND SPACE ADMINISTRATION

For sale by the Clearinghouse for Federal Scientific and Technical Information
Springfield, Virginia 22151 - CFSTI price \$3.00

LARGE-SCALE WIND-TUNNEL INVESTIGATION OF A V/STOL
TRANSPORT MODEL WITH WING-MOUNTED LIFT FANS
AND FUSELAGE-MOUNTED LIFT-CRUISE
ENGINES FOR PROPULSION

By Jerry V. Kirk, Brent K. Hodder, and Leo P. Hall

Ames Research Center

SUMMARY

The low-speed aerodynamic characteristics of a large-scale fan-in-wing V/STOL transport model were investigated. The model had six fans mounted in the wing and two lift-cruise engines mounted forward of the wing in the fuselage. The high mounted wing had an aspect ratio of 3.43, taper ratio of 0.47, and a sweepback at the quarter chord line of 20° . Combinations of two, four, and six fans were investigated as well as the chordwise position of the fans in the wing to determine the interference effects of the fan flow field on the airframe flow field. The effects of operating two lift cruise engines forward of the wing in conjunction with the six lift fans were also studied. The complete configuration with six fans operating and with the fans and lift-cruise engines operating had generally acceptable aerodynamic characteristics.

INTRODUCTION

Ames Research Center is conducting studies of V/STOL transport configurations with lift fans, cruise fans, or combinations of lift fans and cruise fans. Low-speed aerodynamic characteristics are being investigated with large-scale models tested in the 40- by 80-foot wind tunnel. Reference 1 presented results for configurations having lift fans mounted ahead of the wing, rotating cruise fans, and tandem mounted lift fans faired into the wing. This paper presents results obtained from a model with six lift fans in the wing. Fan performance and longitudinal aerodynamic characteristics of the model are shown for various configurations with two, four, and six fans in operation. Results are also presented for the fans located at two different chordwise positions in the wing. Longitudinal aerodynamic characteristics are presented for simulated lift-cruise engines operating in conjunction with the six lift fans. Limited lateral-directional characteristics are presented for the fan only configuration and also for the lift-cruise engine and fan combination.

NOTATION

A	wing aspect ratio
A_f	fan disk area, sq ft
b	wing span, ft
c	wing chord parallel to plane of symmetry, ft
\bar{c}	mean aerodynamic chord, $\frac{2}{S} \int_0^{b/2} c^2 dy$
C_D	drag coefficient, $\frac{D}{qS}$
C_l	rolling-moment coefficient, $\frac{l}{qSb}$
C_L	lift coefficient, $\frac{L}{qS}$
C_m	pitching-moment coefficient, $\frac{M}{qS\bar{c}}$
C_n	yawing-moment coefficient, $\frac{N}{qSb}$
C_y	side-force coefficient, $\frac{Y}{qS}$
D	drag, lb
D_f	diameter of the fan, ft
i_t	horizontal-tail incidence angle, deg
l	rolling moment, ft-lb
L	total lift on model, lb
M	pitching moment, ft-lb
N	yawing moment, ft-lb
P_0	standard atmospheric pressure, 2116 lb/sq ft or 29.92 in. Hg

P_s test section static pressure, lb/sq ft
 P_{TP} engine exit total pressure, in. Hg
 q free-stream dynamic pressure, lb/sq ft
 R Reynolds number or fan radius
rpm corrected fan rotational speed
 S projected wing area, sq ft
 T complete ducted fan or lift-cruise engine thrust in the lift direction
with $\alpha = 0^\circ$, $\beta = 0^\circ$, and $\delta_{NZ} = 0$, $\rho A v_j^2$, lb
 v air velocity, ft/sec
 V free-stream air velocity, knots
 Y side force, lb
 α angle of attack of the wing chord plane, deg
 β_s • sideslip angle, deg
 β_v fan exit-vane deflection angle from the fan axis, deg
 δ relative static pressure, $\frac{P_s}{P_o}$
 δ_f trailing-edge flap deflection measured normal to the hinge line, deg
 δ_{NZ} lift-cruise engine nozzle deflection, 0° in the lift direction
 ϵ average downwash angle at the horizontal tail, deg
 μ tip-speed ratio, $\frac{V}{\omega R}$
 ρ density, lb-sec²/ft⁴
 ω fan rotational speed, radians/sec

Subscripts

j	fan exit
L/C	lift-cruise static thrust
s	lift fan static thrust

MODEL AND APPARATUS

Model

Photographs of the model mounted in the test section of the Ames 40-foot by 80-foot Wind Tunnel are shown in figure 1. Figure 2 is a sketch of the model with pertinent dimensions.

Wing.-- The wing was mounted above the fuselage, and had an aspect ratio of 3.43, a taper ratio of 0.47, a dihedral of -6° , a sweepback of 20° at the quarter chord line, and an NACA 65A-211 airfoil section. An 18-percent chord single-slotted trailing-edge flap extended in two 60-inch and one 56-inch spanwise segments from the fuselage junction to the wing tip. Flap deflections of 0° and 40° were tested. (See fig. 3.)

Fuselage.-- The fuselage was slab sided with rounded corners. It was 427.7 inches long with a maximum depth of 88 inches and a maximum width of 69.6 inches. The inlets for the lift-cruise engines were located in the forward fuselage, and the inlets for the engines driving the lift fans were located above the fuselage in the wing center section (see fig. 2).

Tail.-- The horizontal tail had an aspect ratio of 3.27, taper ratio of 0.33, and dihedral of 22.5° . The horizontal tail was pivoted about the 57-percent chord line. Tail incidence was varied from -15° to $+20^\circ$.

Aspect ratio of the vertical tail was 1.17, and the taper ratio 0.46. Only the horizontal tail was removed during tail-off testing.

Propulsion System

Four YJ85-5 turbojet engines, two simulating lift-cruise engines and two for driving the six X-376 lift fans in the wing, were installed in the fuselage of the model.

Lift-cruise engines.-- Two YJ85-5 engines were mounted in the forward fuselage and exhausted through nozzles on each side of the fuselage. The nozzles were approximately 12.5 inches in diameter and could be vectored from 15° forward of vertical to 90° aft (horizontal). When the model was tested with only the lift fans operating, the lift-cruise nozzles were removed from the model and a fairing was placed over the engine inlets.

Lift-fan installation.- Six X-376 lift fans were installed in the wing of the model. The fans were driven by the airflow from two YJ85-5 turbojet engines. Each engine exhausted into a plenum chamber. From each plenum chamber the exhaust gas was ducted to the three fans in each wing panel. (See fig. 3.) Valves for setting the desired rpm were located above the plenum chamber to divide and control the exhaust flow to each fan. Each plenum chamber also had a tail pipe to allow excess flow from the gas generator to be exhausted overboard. All six fans rotated in a clockwise direction when viewed from above the model.

As shown in figure 2, the inboard and center fans of each wing panel were tested in two chordwise positions in the wing. The outboard fan location was not movable.

The lift fans were completely enclosed within the wing. With the fans in the forward position, inlet radii were quite small (as low as 2.5 in.) in the inboard and center fan locations. In the aft position the minimum inlet radii were 3.5 in. The fans were not equipped with the circular vanes or cross vanes used for the studies of reference 2. During power-off testing, covers were placed over the fans and faired to the wing contour. A cascade of 14 exit vanes was mounted in the exhaust of each fan. The vanes were used for vectoring the fan exhaust and for closing the wing undersurface during power-off testing. Each exit vane airfoil had a chord length of 4.06 inches, a maximum thickness of 10-percent chord at 20-percent chord, and a maximum of 2.3-percent chord camber of the mean line at 35-percent chord. The exit vanes spanned the rotor and the tip turbine sections of the fan and could be deflected from -10° to $+50^{\circ}$.

TESTING AND PROCEDURE

Longitudinal force and moment data are presented for angles of attack from -4° to $+22^{\circ}$. Lateral-directional force and moment data were obtained for sideslip angles of -12° to $+8^{\circ}$. Scale force data were used to measure static lift fan performance. Lift-cruise engine thrust was measured in the same manner. The variation in lift fan performance with forward speed was obtained from survey rakes mounted beneath the three fans in the right-hand wing panel. Fan rpm was varied from 2000 to 3600. Lift-cruise engine thrust was set to balance the pitching moment at hover. Lift-cruise engine nozzle angle was set for zero drag at $\alpha = 0^{\circ}$ at the various forward speeds tested. Airspeed varied from 0 to 125 knots corresponding to a maximum Reynolds number of 14.2 million.

Tests at Zero Angle of Attack

At 0° angle of attack, fan speed, lift-cruise thrust, and wind-tunnel velocity were varied independently. Exit vane angle was varied with combinations of two, four, and six fans and for two flap deflections with the tail

on and off and with the fans in the forward and aft positions. Exit vane angle was also varied with the lift-cruise engines running at various nozzle deflections.

Lift-cruise engine thrust was varied at zero angle of attack at several nozzle angles and fan exit vane settings.

Tests With Variable Angle of Attack

When angle of attack was varied, model and propulsion variables were held constant. Results were obtained for several fan speeds and wind-tunnel airspeeds. Model variables were the same as those listed above.

CORRECTIONS

Force data obtained without fans or lift-cruise engines operating (power off) have been corrected for the effects of wind-tunnel wall interference in the following manner:

$$\begin{aligned}\alpha &= \alpha_u + 0.7800 C_{L_u} \\ C_D &= C_{D_u} + 0.01360 C_{L_u}^2 \\ C_m &= C_{m_u} + 0.01740 C_{L_u} \text{ (tail on tests only)}\end{aligned}$$

In addition a ΔC_D correction of -0.00760 has been applied to all data to account for the tares resulting from exposed tips of the wind-tunnel struts.

Reference 3 presents general criteria for selecting the size of V/STOL models relative to the size of the test section to minimize wall and scale effects. These criteria were developed from comparisons of wind-tunnel and flight-test results. The model of this investigation had a VTOL lifting element area ratio and disk loading closely approximating that of the XV-5A aircraft which, according to reference 3, showed good correlation between uncorrected wind-tunnel results and flight-test results. Therefore, no wind-tunnel wall corrections were applied to the results from the present investigation with the fans and lift-cruise engines operating.

RESULTS

Lift fan tip speed ratio is used as the independent parameter in the presentation of results unless otherwise stated. Figure 4 presents the relationship between tip speed ratio and free stream to fan velocity ratio for the lift fans.

Table I is an index to the figures. The results show lift fan and lift-cruise engine characteristics, longitudinal characteristics at zero angle of attack, downwash at the horizontal tail, horizontal-tail effectiveness, variation of longitudinal characteristics with angle of attack, and lateral-directional characteristics in that order.

Lift Fan and Lift-Cruise Engine Characteristics

Figure 5 presents the static fan thrust as a function of rpm for the fans operating in the forward and aft positions. The variation in fan thrust with forward speed is shown in figure 6. Lift-cruise engine static thrust is shown in figure 7.

Aerodynamic Characteristics With Fan And Lift-Cruise Engine Operation

Zero angle of attack.- The variation of lift coefficient with thrust coefficient, without fans operating, is shown in figure 8 for several nozzle angles. Figures 9 through 11 show the variation of the ratio of lift, drag, and pitching moment to static thrust with tip speed ratio for combinations of two, four, and six fans operating at two different flap deflections. The two and four fan results are for the fans in the aft position, and the six fan data are for the fans in both the forward and aft positions.

Figures 12 through 21 show the variation of lift, drag, and pitching-moment coefficient with tip speed ratio for exit vane deflections from -10° to $+50^\circ$ without the deflected lift-cruise exit nozzles. Figures 12 through 15 are for the six fans forward and figures 16 through 18 are for six fans aft. Two flap deflections are shown with the tail on and off. Data for arrangements with four fans (inboard and center, inboard and outboard) are presented in figures 19 and 20 for the fans aft. Figure 21 shows results for two fans aft, the tail off, and two flap deflections.

Results with both lift fans and lift-cruise engines operating are shown in figures 22 and 23. To obtain the results in figure 22, the level of lift-cruise thrust was defined by hover balance, and nozzle angle is that required to trim drag without the fans operating. From these test conditions, fan tip speed ratio and exit louver angle were varied. The data in figure 23 were obtained at the same test conditions as that in figure 22, but lift-cruise thrust was varied rather than lift-fan parameters.

The variation in average downwash at the horizontal tail is presented in figure 24. (On this and following figures, the abbreviation L/C is used for lift-cruise.) Figures 25 through 27 show the horizontal-tail effectiveness for six fans only and for six fans operating in conjunction with the lift-cruise engines.

Variable angle of attack.- The variation in longitudinal aerodynamic characteristics with angle of attack is shown in figures 28 through 35. Power-off data at two flap deflections with the horizontal tail on and off

are shown in figure 28. Results with two and four fans aft at two flap deflections with the tail off are shown in figures 29 through 31. Figure 29 is for the two-fan arrangement, figure 30 for four fans (inboard and center) and figure 31 for four fans (inboard and outboard).

Low-speed results for six fans in the forward and aft position, tail on, with the flaps deflected 40° , are plotted in figure 32 as the ratio of forces and moments to static thrust. Results are shown in figure 33 for six fans forward, the tail on and off, and flaps deflected 40° . Low tunnel speed (low tip speed) data are shown as the ratio of forces and moments to static thrust, while the higher speed results are shown in coefficient form. Figure 34 presents similar results for the fans aft arrangement.

Longitudinal characteristics with six fans forward and aft in conjunction with the lift-cruise engines are shown in figure 35. All results are with the flaps deflected 40° . With the fans forward the data are for the tail off while with the fans aft the data are for the tail on and off.

Aerodynamic characteristics with sideslip.- The variation in lateral-directional characteristics with sideslip angle at 0° and 8° angle of attack is shown in figures 36 through 39. Power-off results are shown in figure 36. Results with six fans aft are shown in figure 37 with the tail on and flaps deflected 40° . Low-speed data are shown as forces and moments. Corresponding results are presented in figures 38 and 39 for the six fans operating with the lift-cruise engines.

DISCUSSION

Fan Performance

Performance of the lift fans in the forward and aft positions was measured statically and with forward speed. Static measurements were obtained from the force balance while the variation in fan thrust with forward speed was measured with pressure rakes mounted beneath the three fans in the right-hand wing.

At zero forward speed, measured fan thrust was nearly the same for both the forward and aft fan positions (fig. 5). These data compare very favorably with the results of reference 4 for which the fans were mounted in folding pods on the fuselage.

The variation of fan thrust with forward speed (see fig. 6) showed large dependence on chordwise placement of the fans in the wing. For the six-fan arrangement, fan thrust decreased continually with increased forward speed (tip speed ratio). In the six fans forward arrangement, which had the largest decrement in thrust with forward speed, being approximately 0.6 of the static value at a tip speed ratio of 0.28, the sharp inlet radius on the inboard fans caused flow separation over the inlet and poor fan performance as forward speed increased. The inlet radius of the inboard fans in the aft position was more generous; even so, the fan performance at forward speed is the poorest

measured to date for fan-in-wing installations. If these results are used to calculate airplane performance, they should be modified to reflect more representative fan performance such as that with the circular vanes and cross vanes of reference 2.

Outboard fan performance was the same with the inboard and center fans in either the forward or aft positions; however, performance of the outboard fan was somewhat lower than that of the other two fans in either chordwise position.

Interference Effects

Effects of chordwise fan location.- Fan thrust, total model lift, and power-off lift are shown in figure 40 as a function of free-stream to fan velocity ratio for two flap deflections with six fans forward and aft. Comparison of the difference between fan thrust plus power-off lift and total measured lift at a velocity ratio of 0.4, with the flaps up and the exit vane deflected 0° , shows that the induced effects with the fans forward are approximately 71 percent of those with fans aft. Similar results are shown with the flaps deflected 40° where induced lift with the fans forward is approximately 61 percent of that with the fans aft. These results agree with those of reference 4 which showed large positive induced effects with the fans mounted near the wing trailing edge.

Effect of spanwise fan location.- Induced lift is dependent upon fan area to wing area ratio, wing geometry, fan location, and fan distribution (ref. 5). To evaluate the effect of fan distribution with the fans in the aft location, the direct effect of area ratio can be removed by comparing the product of the ratio of induced lift to static thrust and the fan to wing area ratio. Figure 41 shows the variation of this value with flight velocity ratio for three fan arrangements. The maximum induced lift is obtained by distributing the fans spanwise in the wing.

From the results in figures 40 and 41 it would appear that to obtain maximum induced lift, fans should be distributed spanwise near the wing trailing edge.

Flap effectiveness.- With the flaps deflected 40° , the difference between total lift and power-off lift plus fan thrust is approximately 50 percent of that for the flaps up condition for both fans forward and fans aft arrangements (fig. 40). This loss is attributed to a loss in flap effectiveness with fan operation. The reason for this loss is not fully understood, but as stated in reference 5, factors which might contribute to a loss in flap effectiveness are blockage of the flow below the flap by the fan exhaust and pre-turning of the flow above the flap by the fan.

Lift-cruise engine effects.- References 1, 2, and 4 reported adverse effects on lift when the fans operated forward of the wing. The variation in lift coefficient with lift-cruise engine thrust coefficient with the lift-cruise engines operating ahead of the wing is shown in figure 8. A comparison of the measured lift with power off lift plus the product of the lift-cruise

engine thrust coefficient and the cosine of the nozzle angle at 30 knots with the nozzles deflected 10° shows the measured lift of the present model to be approximately 93 percent of the power off lift-cruise engine thrust coefficient. Similar results, different in magnitude, can be computed for other forward speeds and nozzle angles tested. Downwash from the engine exhaust apparently unloaded the wing causing the loss in lift.

Pitching-moment variation.- Figure 42 shows the variation of moment, normalized by lift and fan diameter, with velocity ratio for the six fans forward and aft arrangement and two flap deflections. The largest variation in moment with forward speed occurs with the fans aft. As with induced lift, chordwise placement of the fans significantly affects the variation of moment with forward speed. The results indicate that high induced lift will cause corresponding large moments.

With the trailing-edge flaps deflected, the nose-down pitching moment from the flap produced curves which tended to level off as forward speed was increased; thus the trailing-edge flap reduced the moments required for trim.

Ames Research Center
National Aeronautics and Space Administration
Moffett Field, Calif., 94035, Aug. 17, 1967
721-03-00-06-00-21

REFERENCES

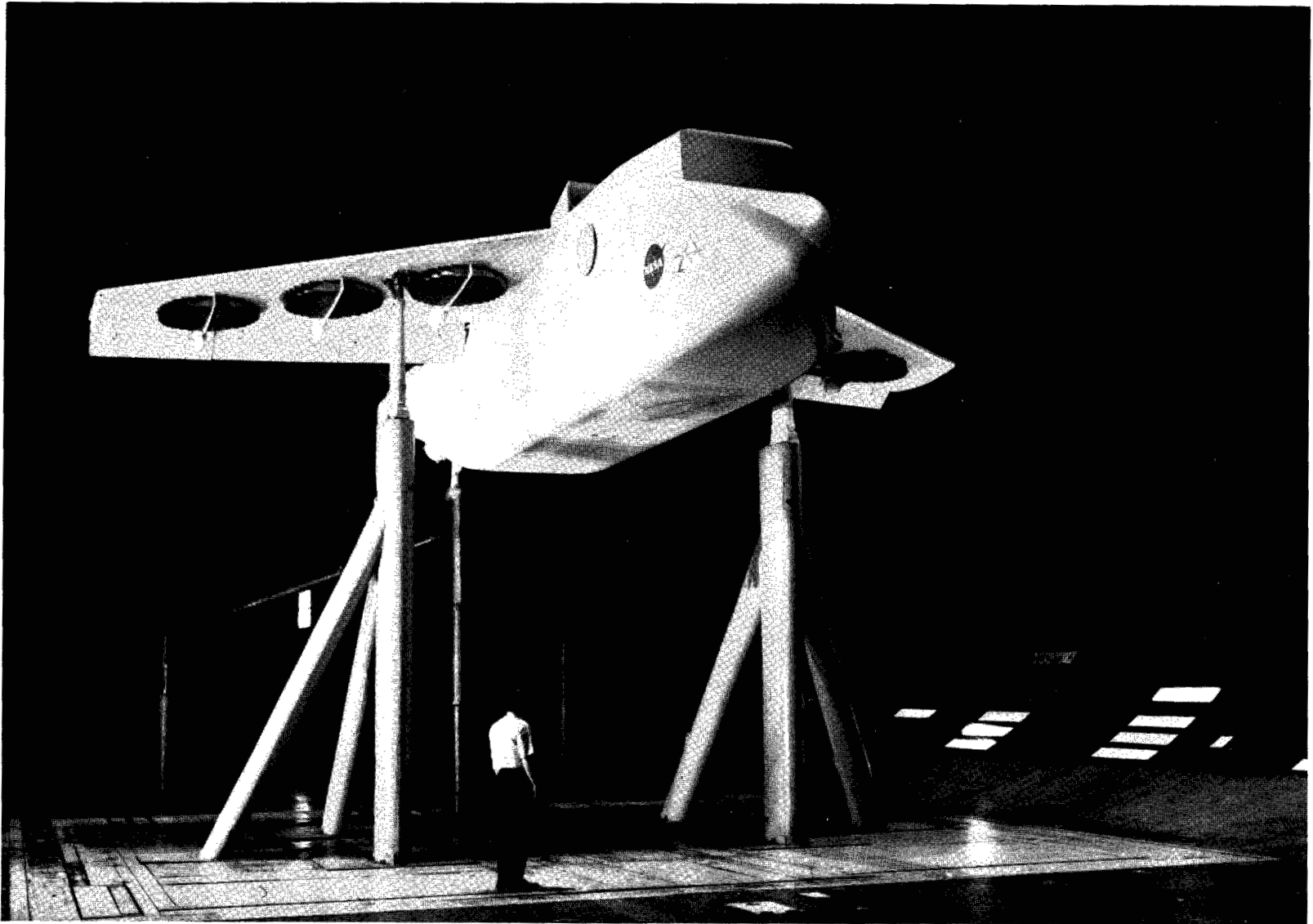
1. Hickey, David H.; Kirk, Jerry V.; and Hall, Leo P.: Aerodynamic Characteristics of a V/STOL Transport Model With Lift and Lift-Cruise Fan Power Plants. Paper 7, NASA SP-116, 1966.
2. Kirk, Jerry V.; Hickey, David H.; and Hall, Leo P.: Aerodynamic Characteristics of a Full-Scale Fan-In-Wing Model Including Results in Ground Effect With Nose-Fan Pitch Control. NASA TN D-2368, 1964.
3. Cook, Woodrow L.; and Hickey, David H.: Comparison of Wind Tunnel and Flight-Test Aerodynamic Data in the Transition Flight Speed Range for Five V/STOL Aircraft. Paper 26, NASA SP-116, 1966.
4. Hall, Leo P.; Hickey, David H.; and Kirk, Jerry V.: Aerodynamic Characteristics of a Large-Scale V/STOL Transport Model With Lift and Lift-Cruise Fans. NASA TN D-4092, 1967.
5. Goldsmith, Robert H.; and Hickey, David H.: Characteristics of Lifting-Fan V/STOL Aircraft. Astronautics and Aerospace Engineering, vol. 1, no. 9, Oct. 1963.

TABLE I.- LIST OF FIGURES

Figure	α , deg	β_v , deg	V, knots	δ_{NZ} , deg	i_t , deg	δ_f , deg	β_s , deg	Remarks
Fan and lift-cruise engine characteristics								
4	0	0	Variable	Off	-	-	0	Relationship of velocity ratio to tip-speed ratio Fan rpm variable
5(a)	↓	↓	0	↓	-	-	↓	
5(b) 5(c)			↓					
6			Variable	↓	-	-		Effect of forward speed on fan thrust
7		90	0	10,20	-	-		Lift-cruise engine static performance
8	↓	90	Variable	Variable	-	40	↓	Variation in lift coefficient with lift-cruise engine operation
Longitudinal data at zero angle of attack (lift fans operating) $L/T_s, D/T_s, M/T_s D_f$ vs μ								
9	0	0	Variable	Off	On,Off	0	0	Effect of fan position and no. of fans operating
10	↓	↓	↓	↓	Off	40	↓	
11					0	40		
Longitudinal data at zero angle of attack (lift fans operating) C_L, C_D, C_m vs μ								
12(a)	0	Variable	Variable	Off	Off	0	0	Six fans forward
12(b)					Off	40		Six fans aft
13(a)								
13(b)					0	0		
14(a)								
14(b)					0	40		
15					0	40		
16(a)					0	0		
16(b)								
17(a)					Off	40		
17(b)								
18(a)					0	40		
18(b)								
19(a)					Off	0		Four fans aft (inboard and center)
19(b)								Four fans aft (inboard and outboard)
19(c)						40		
20(a)						40		
20(b)								
21(a)						0		Two fans aft (inboard)
21(b)						40		Six fans aft
22(a)				Variable	0			
22(b)					Off			
23(a)					0			Average downwash at the horizontal tail
23(b)					0			
24	↓	0	↓	Off,On	0	↓	↓	

TABLE I.- LIST OF FIGURES - Concluded

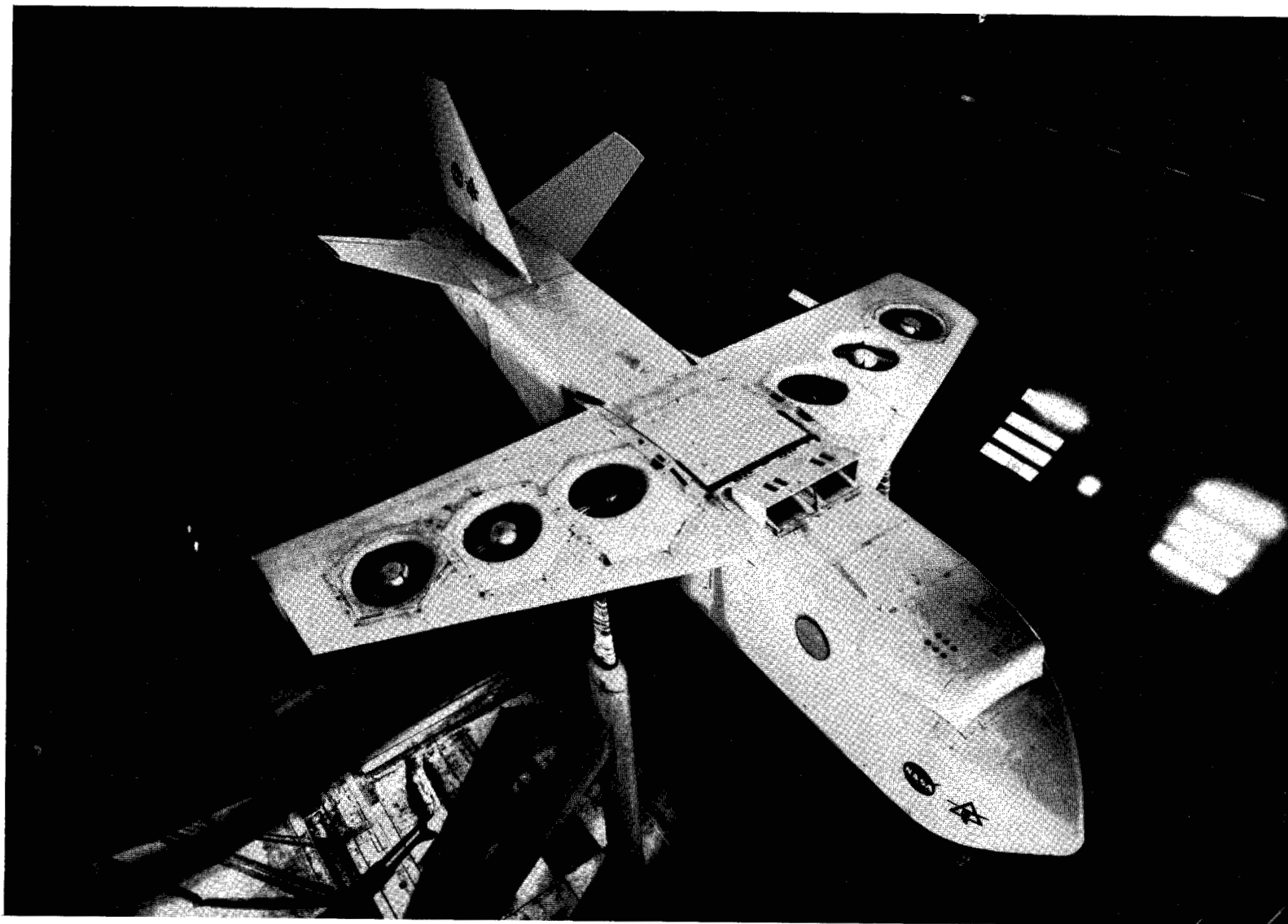
Figure	α , deg	β_v , deg	V, knots	δ_{WZ} , deg	i_t , deg	δ_F , deg	β_B , deg	Remarks
Horizontal tail effectiveness								
25	0	Variable	Variable	Off	Variable	40	0	Six fans aft
26	0,10	↓	↓	Variable	↓	↓	↓	↓
27	0	↓	↓	Variable	↓	↓	↓	↓
Longitudinal data at variable angle of attack (lift fans operating)								
28	Variable	90,0	80	Off	Off,0	40,0	0	Power off, inlets sealed
29(a)	↓	0,20	40,80	↓	Off	40,0	↓	Two fans aft (inboard)
29(b)	↓	0	30,60	↓	↓	40	↓	↓
30(a)	↓	5,40	40,80	↓	↓	0	↓	Four fans aft (inboard and center)
30(b)	↓	0,5	30,40	↓	↓	40	↓	↓
30(c)	↓	18,30,20	60,80	↓	↓	↓	↓	↓
31(a)	↓	0,5	30,40	↓	↓	↓	↓	Four fans aft (inboard and outboard)
31(b)	↓	15,32,20	60,80	↓	↓	↓	↓	↓
32	↓	10,12,9,15	30,40	↓	0	↓	↓	Six fans forward and aft
33(a)	↓	9,15,0,0	30,40	↓	Off	↓	↓	Six fans forward
33(b)	↓	90,35,25	80,60	↓	↓	↓	↓	↓
33(c)	↓	0,90,50	100,80,60	↓	↓	↓	↓	↓
33(d)	↓	90,20,35	80,60	↓	0	↓	↓	↓
34(a)	↓	30,11	80,40	↓	Off	0	↓	Six fans aft
34(b)	↓	22,40,33	60,80	↓	Off	40	↓	↓
34(c)	↓	20,40,33, 22	80,60	↓	0	↓	↓	↓
35(a)	↓	20	60	25	Off	↓	↓	Six fans forward
35(b)	↓	26,19,12	80,60,40	30,18, 9.5	Off	↓	↓	Six fans aft
35(c)	↓	26,30,0	80,100, 125	30,45, 67	0	↓	↓	↓
35(d)	↓	10,18	40,60	9.5,18	0	↓	↓	↓
Lateral-directional data (lift fans operating)								
36	0.5,9	90	80	Off	0	40	Variable	Power off, inlets sealed
37(a)	0	9,12	30,40	Off	↓	↓	↓	Six fans aft
37(b)	0	22,33,40, 90	60,80	↓	↓	↓	↓	↓
37(c)	8	10,15	30,40	↓	↓	↓	↓	↓
37(d)	8	22,33,40, 90	60,80	↓	↓	↓	↓	↓
38(a)	0	5,10	30,40	6,9.5	↓	↓	↓	↓
38(b)	0	18,26,30, 0	60,80 100,125	18,30, 45,67	↓	↓	↓	↓
39	0,8	26	80	30	↓	↓	↓	↓



(a) 3/4 front view.

A-37161

Figure 1.- Photographs of the model mounted in the Ames 40- by 80-Foot Wind Tunnel.



(b) Top view showing fans in aft position.

A-37207.1

Figure 1.- Concluded.

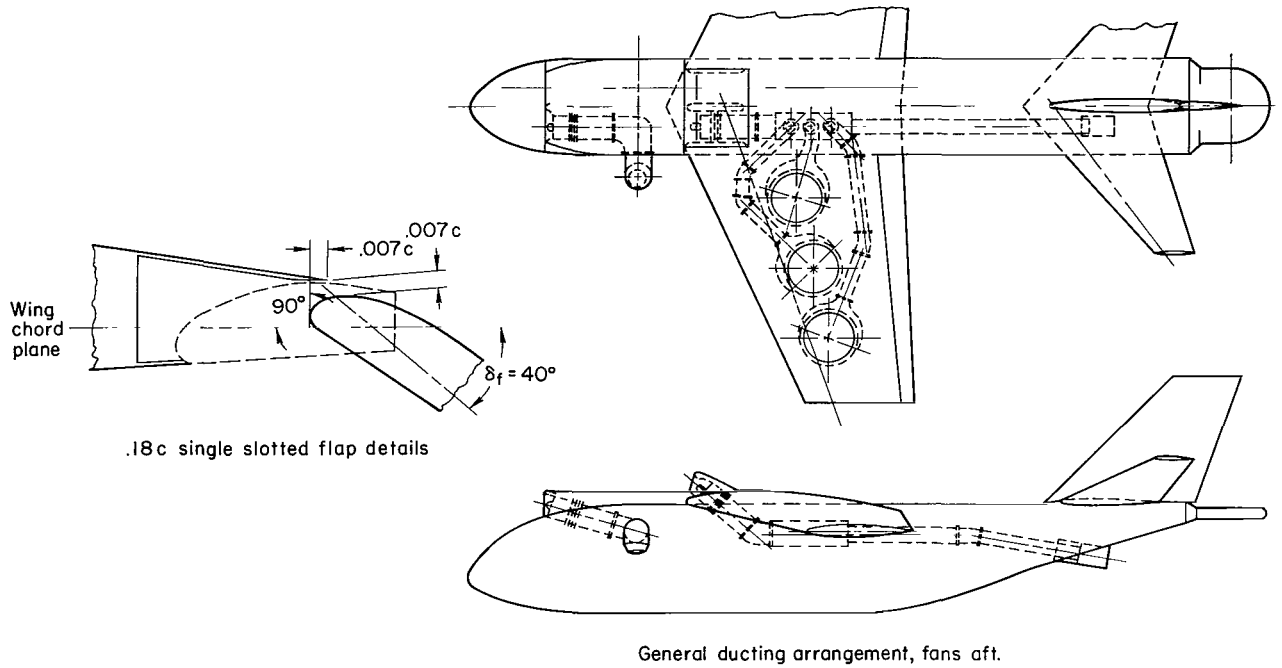


Figure 3.- Details of the trailing-edge flap and the general ducting arrangement.

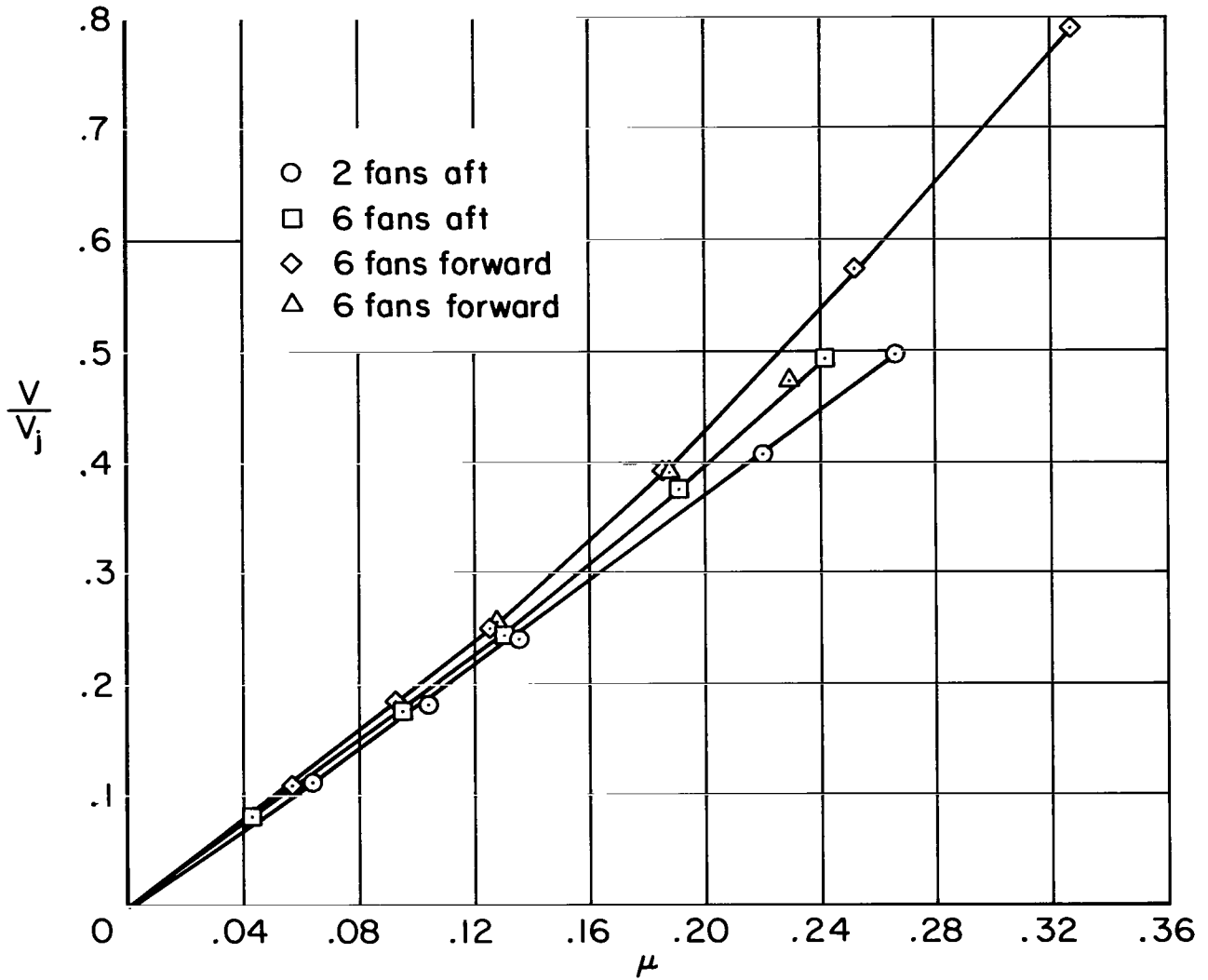
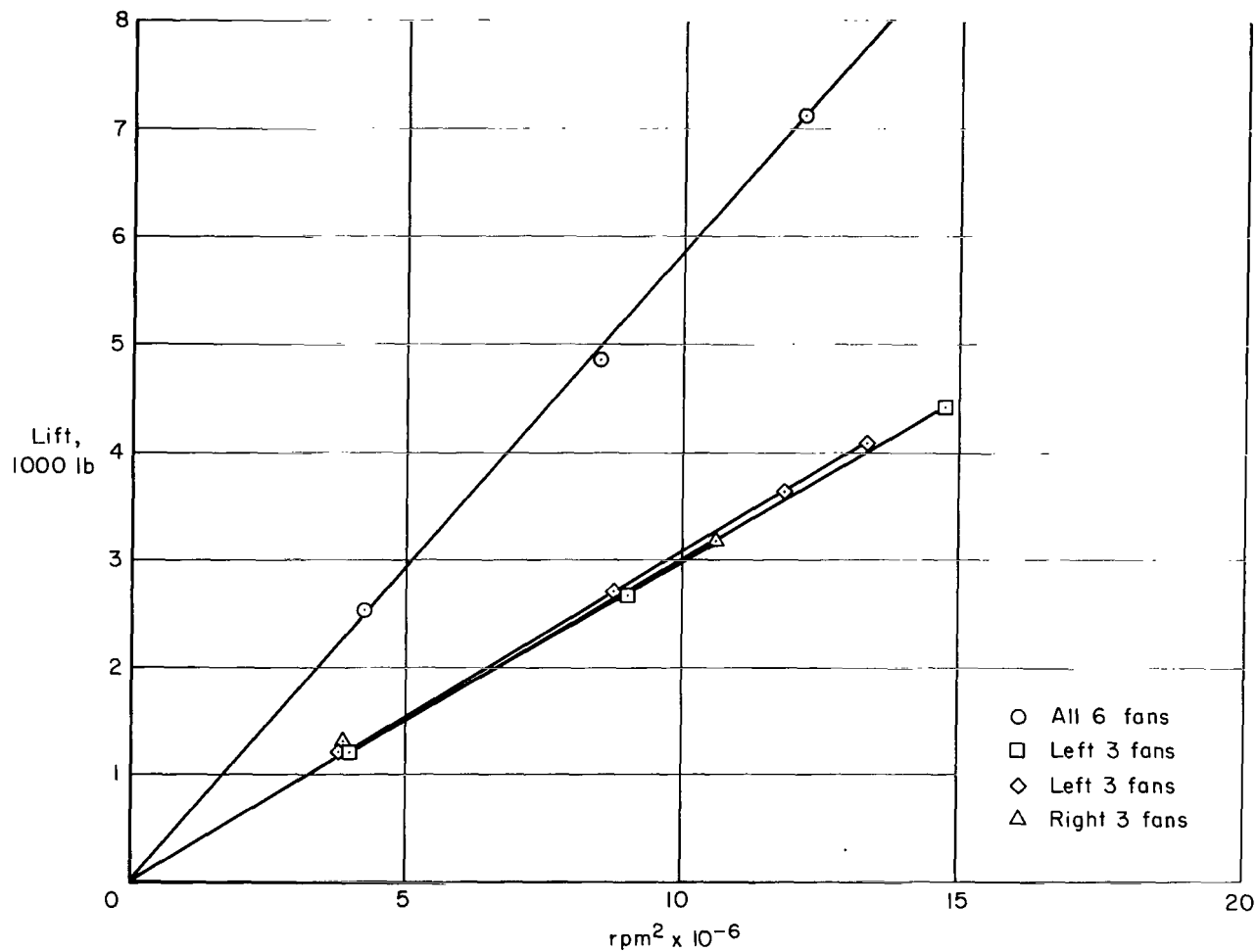
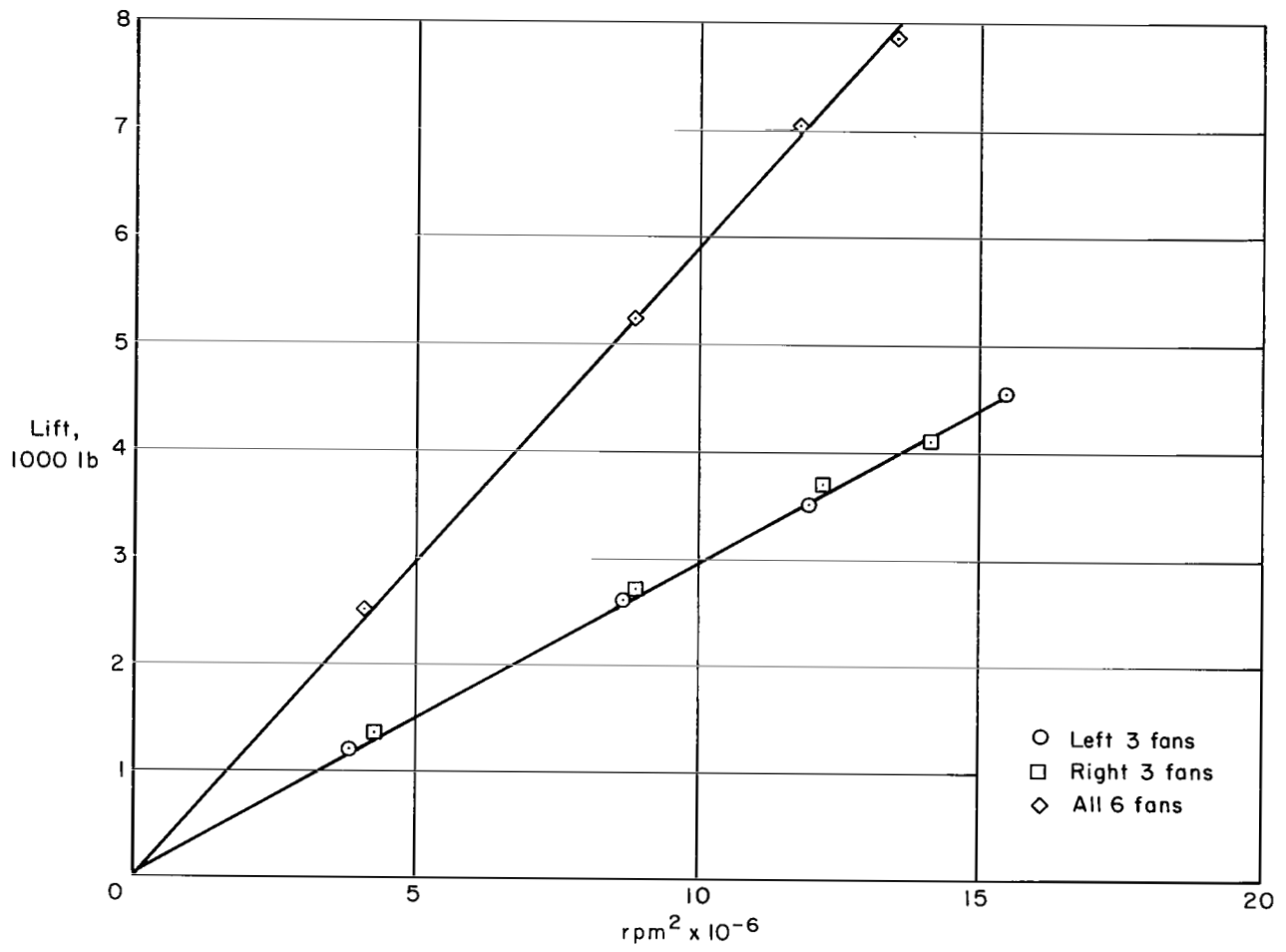


Figure 4.- The variation of average velocity ratio with tip-speed ratio;
 $\alpha = 0^\circ$, $\beta_v = 0^\circ$.



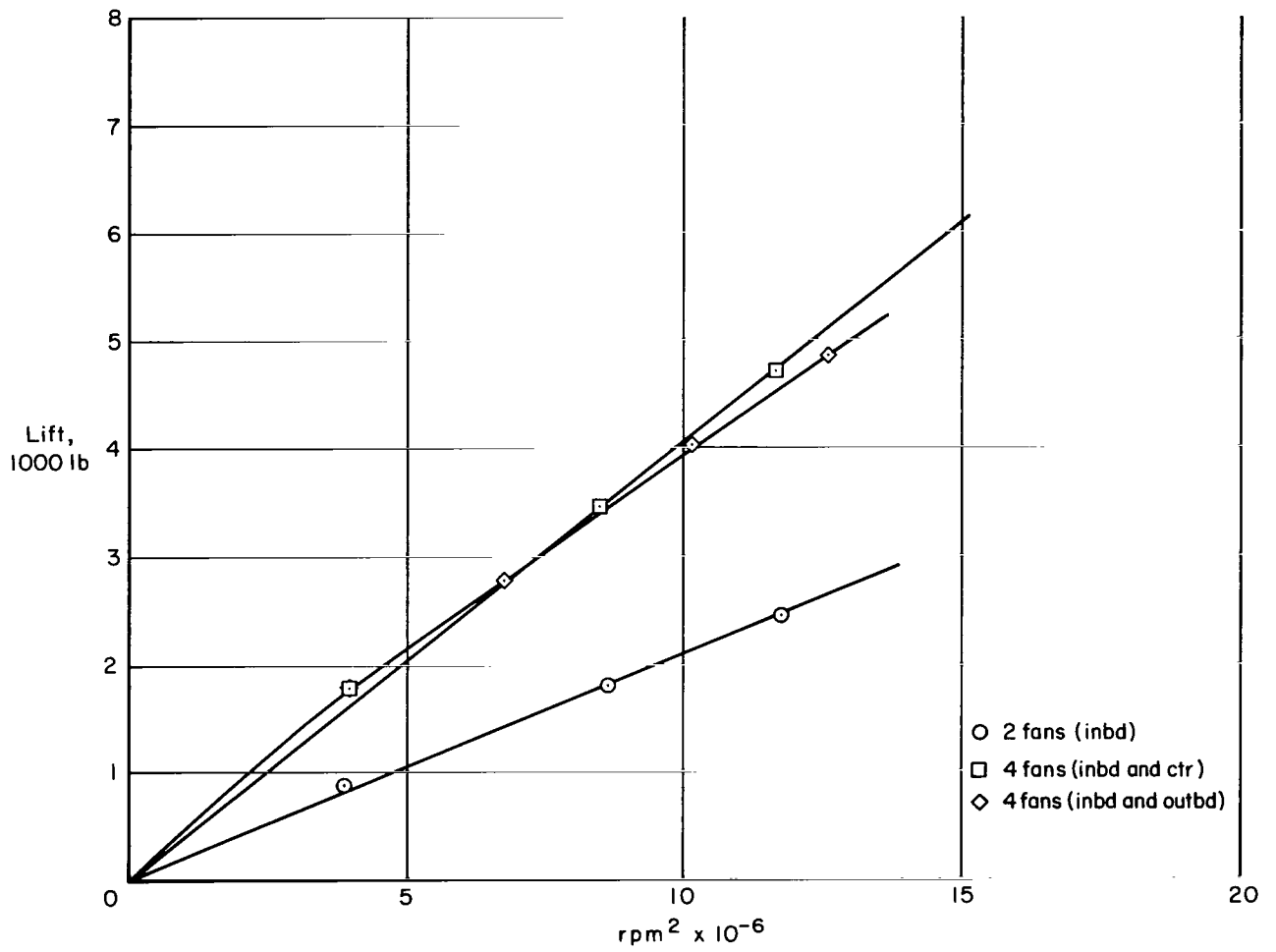
(a) Six fans forward.

Figure 5.- Zero airspeed performance of the model with fan operation;
 $\alpha = 0^\circ$, $\beta_V = 0^\circ$.



(b) Six fans aft.

Figure 5.- Continued.



(c) Two and four fans aft.

Figure 5.- Concluded.

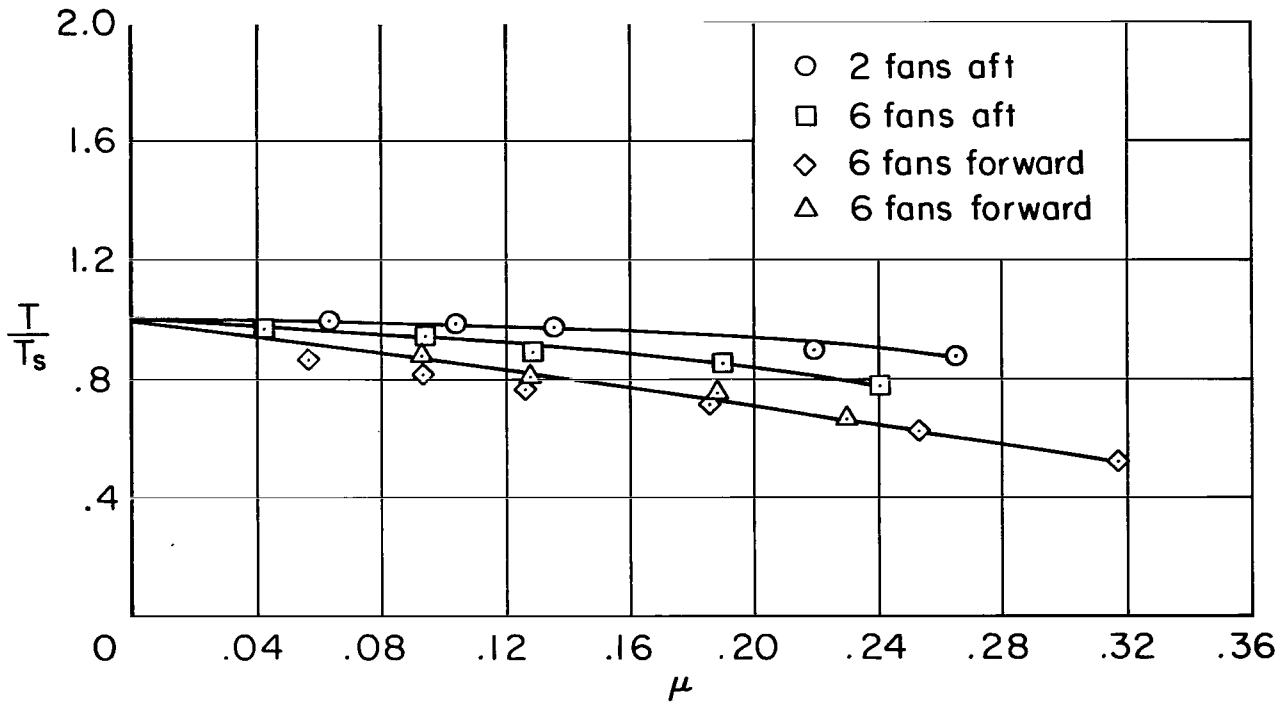


Figure 6.- The effect of forward speed (tip-speed ratio) on average fan thrust; $\alpha = 0^\circ$, $\beta_v = 0^\circ$.

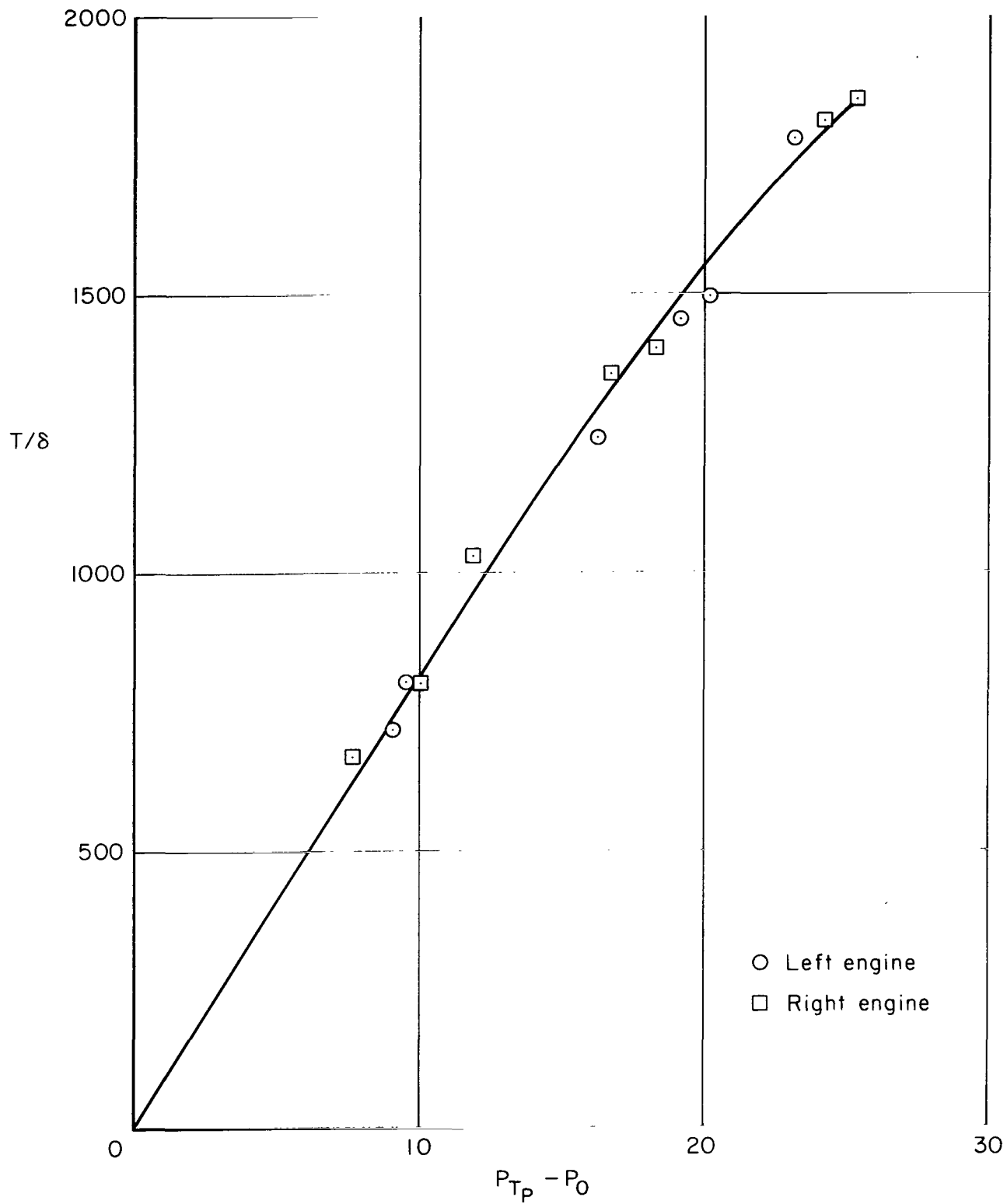


Figure 7.- Zero airspeed performance of the model with the lift-cruise engines operating; $\alpha = 0^\circ$.

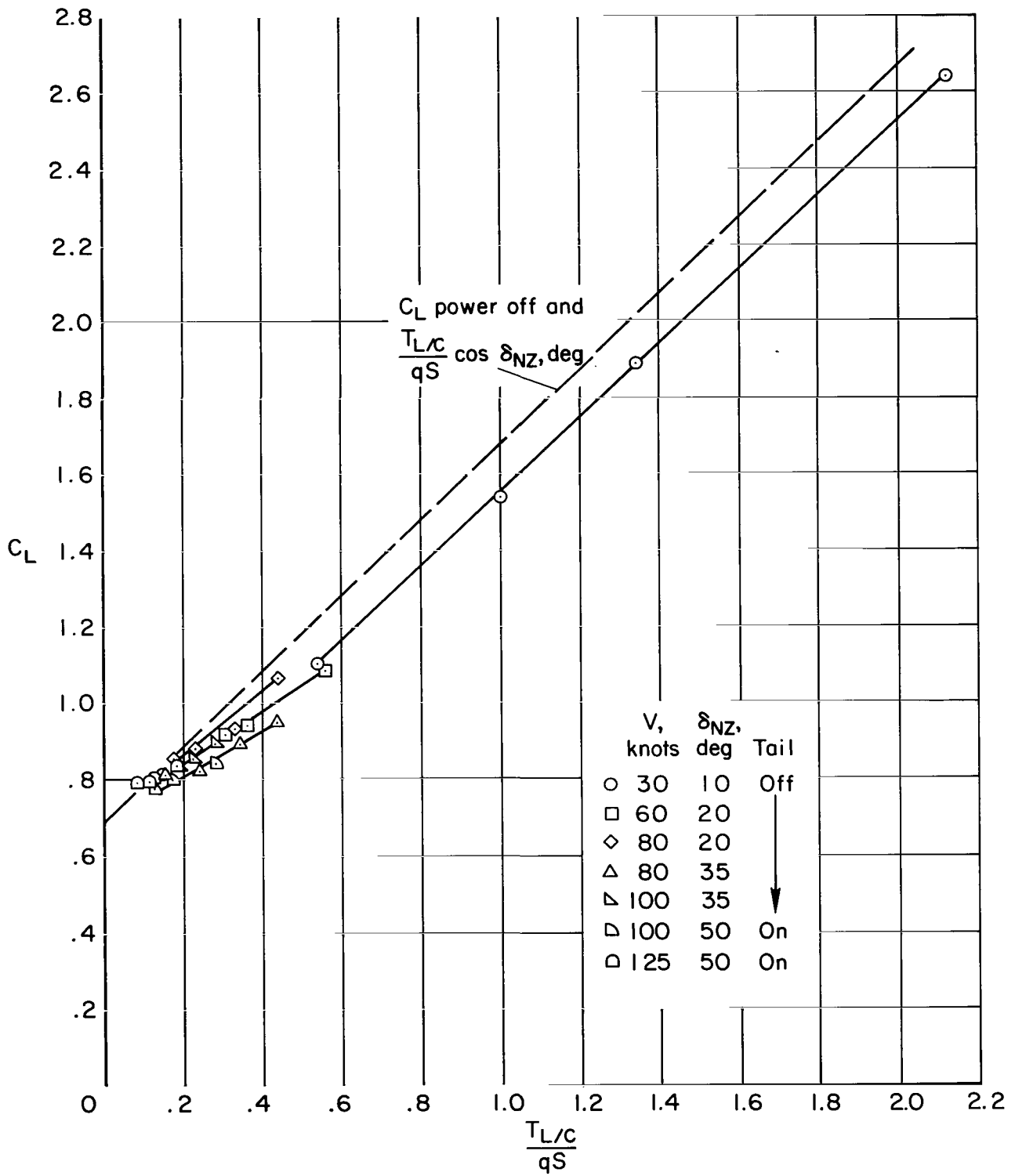


Figure 8.- The variation in lift coefficient with lift-cruise engine operation; $\alpha = 0^\circ$, $\beta_V = 90^\circ$, $\delta_F = 40^\circ$, fan inlets covered.

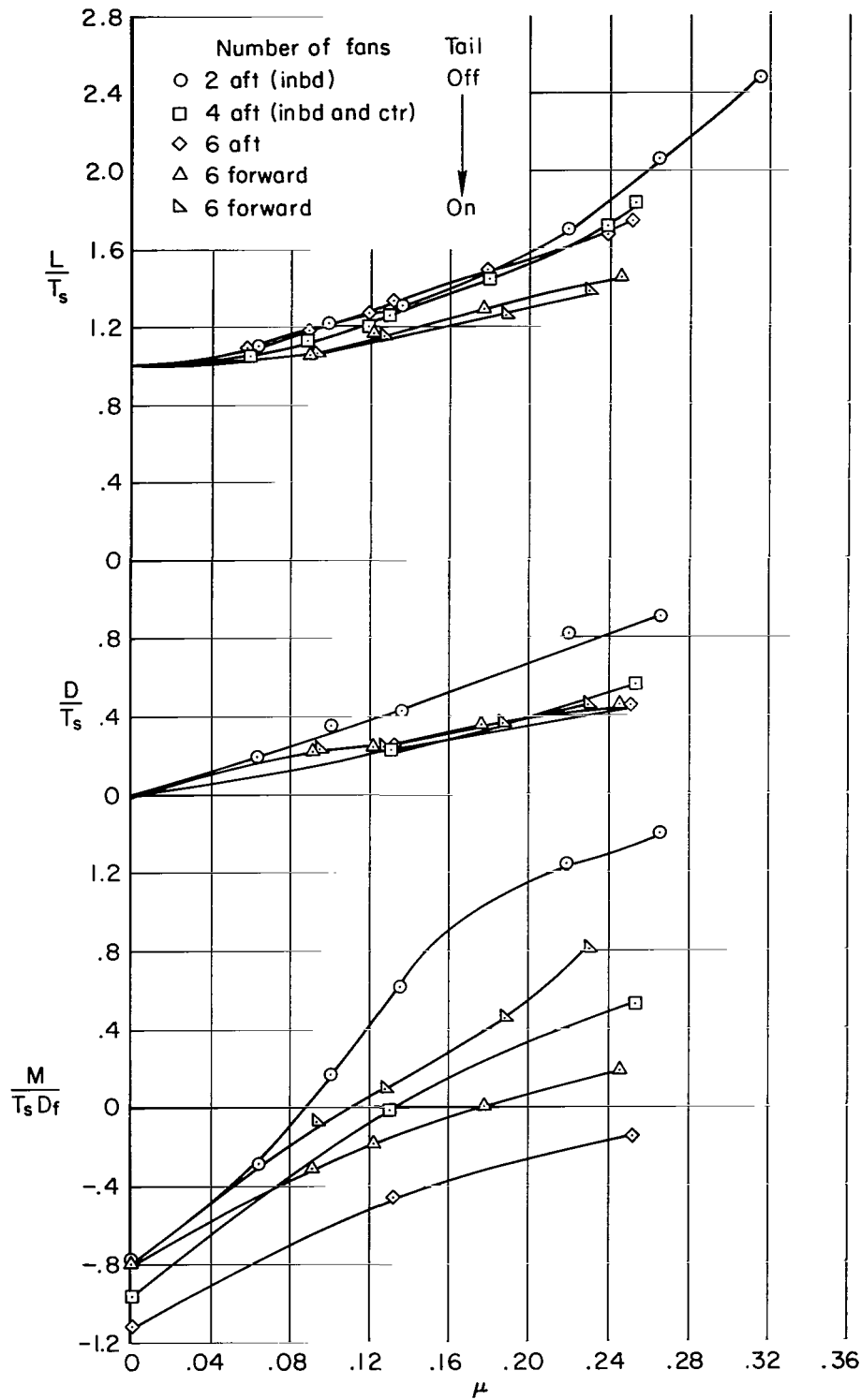


Figure 9.- The variation of longitudinal characteristics with tip-speed ratio; $\alpha = 0^\circ$, $\beta_v = 0^\circ$, $\delta_f = 0^\circ$, lift-cruise nozzles off, 3600 rpm.

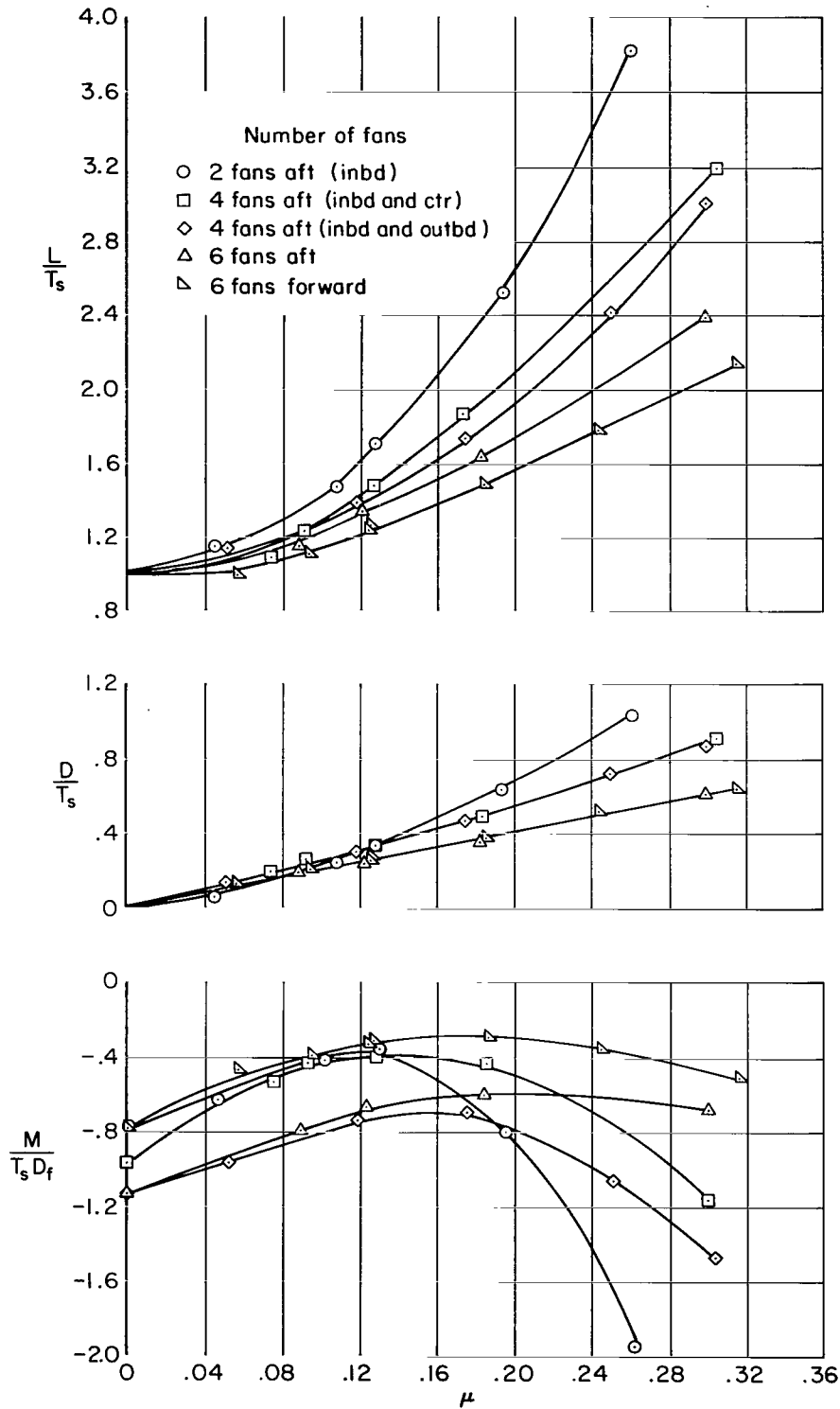


Figure 10.- The variation of longitudinal characteristics with tip-speed ratio; $\alpha = 0^\circ$, $\beta_V = 0^\circ$, $\delta_f = 40^\circ$, tail off, lift-cruise nozzles off, 3600 rpm.

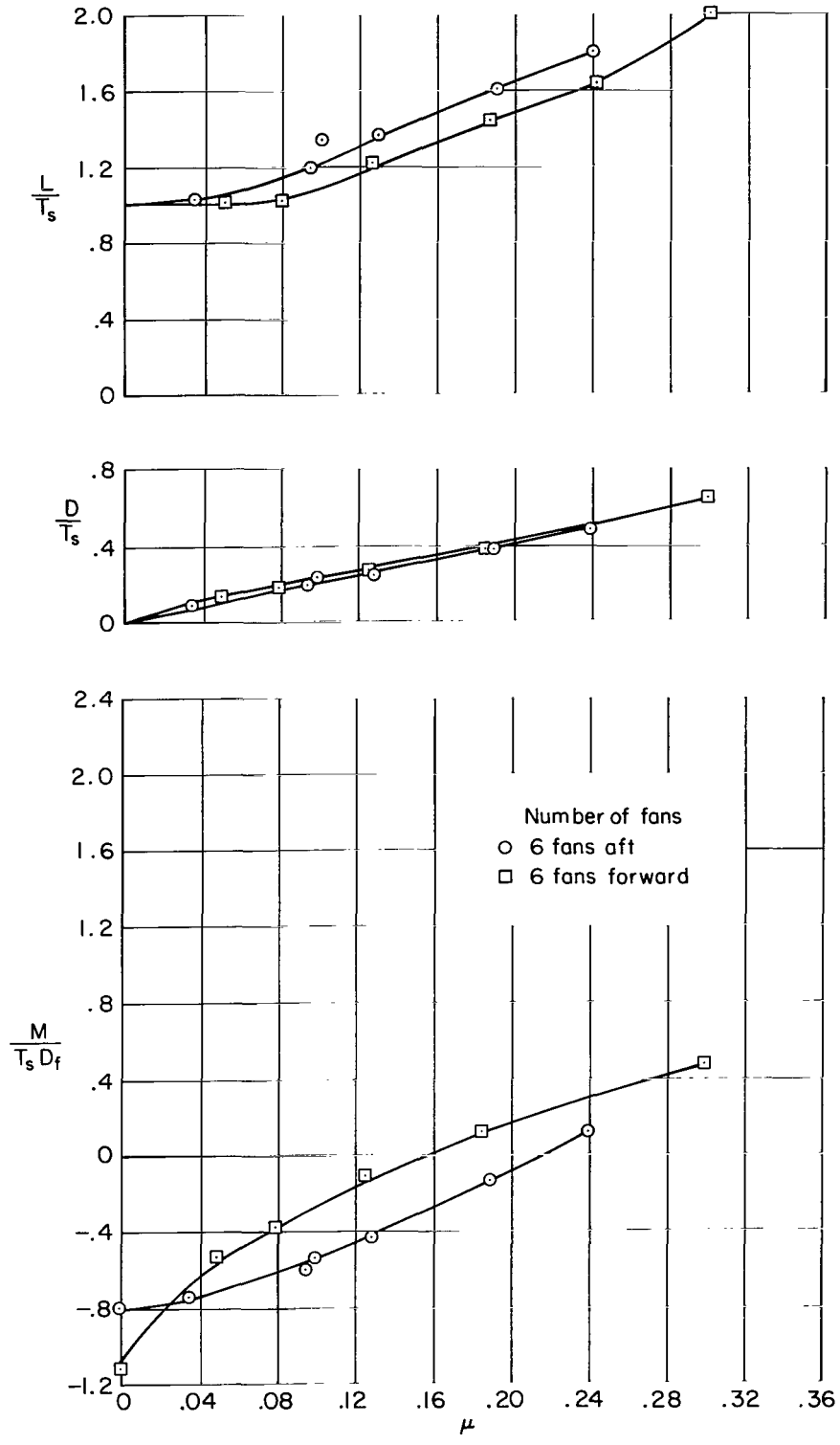
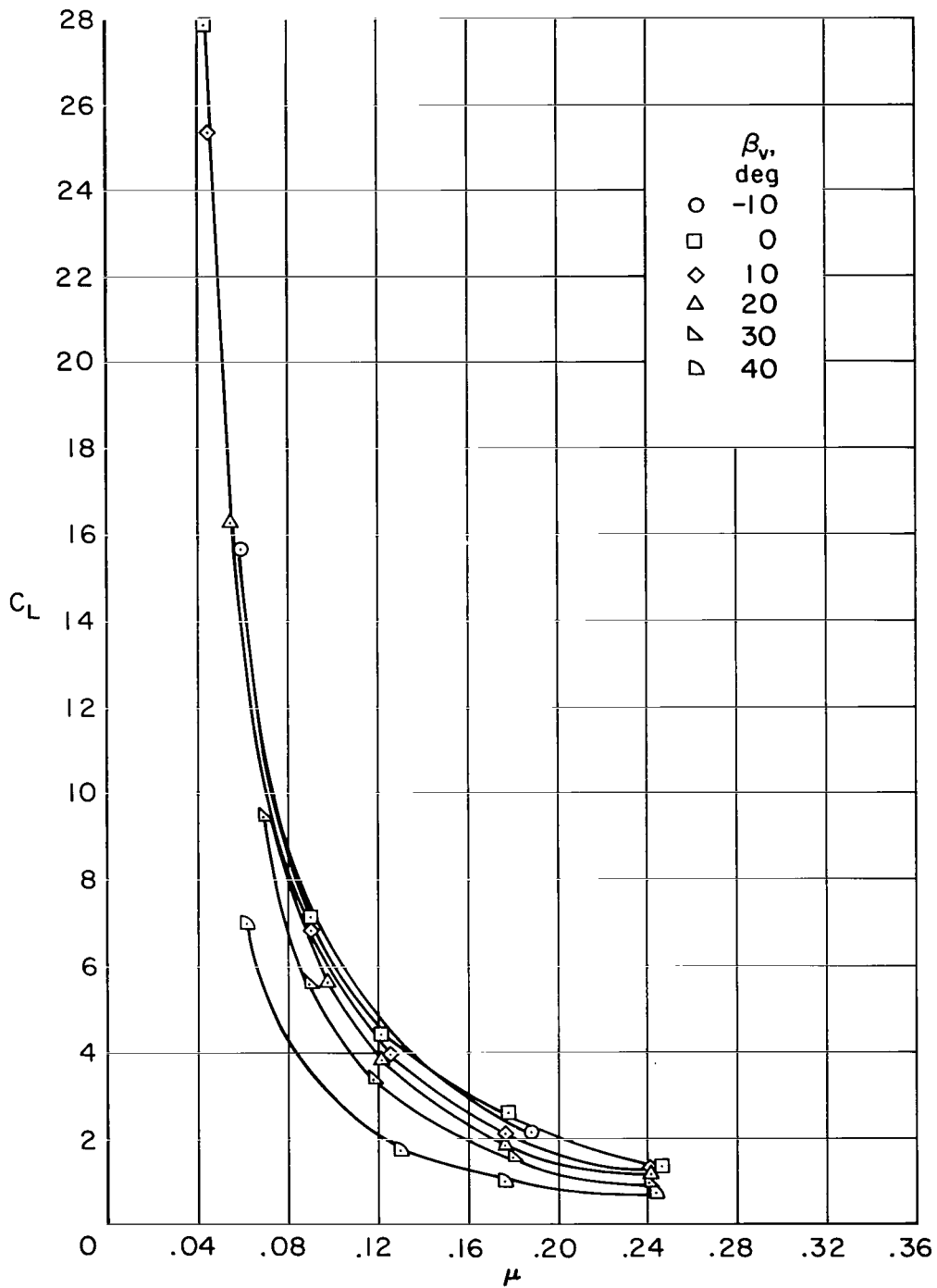
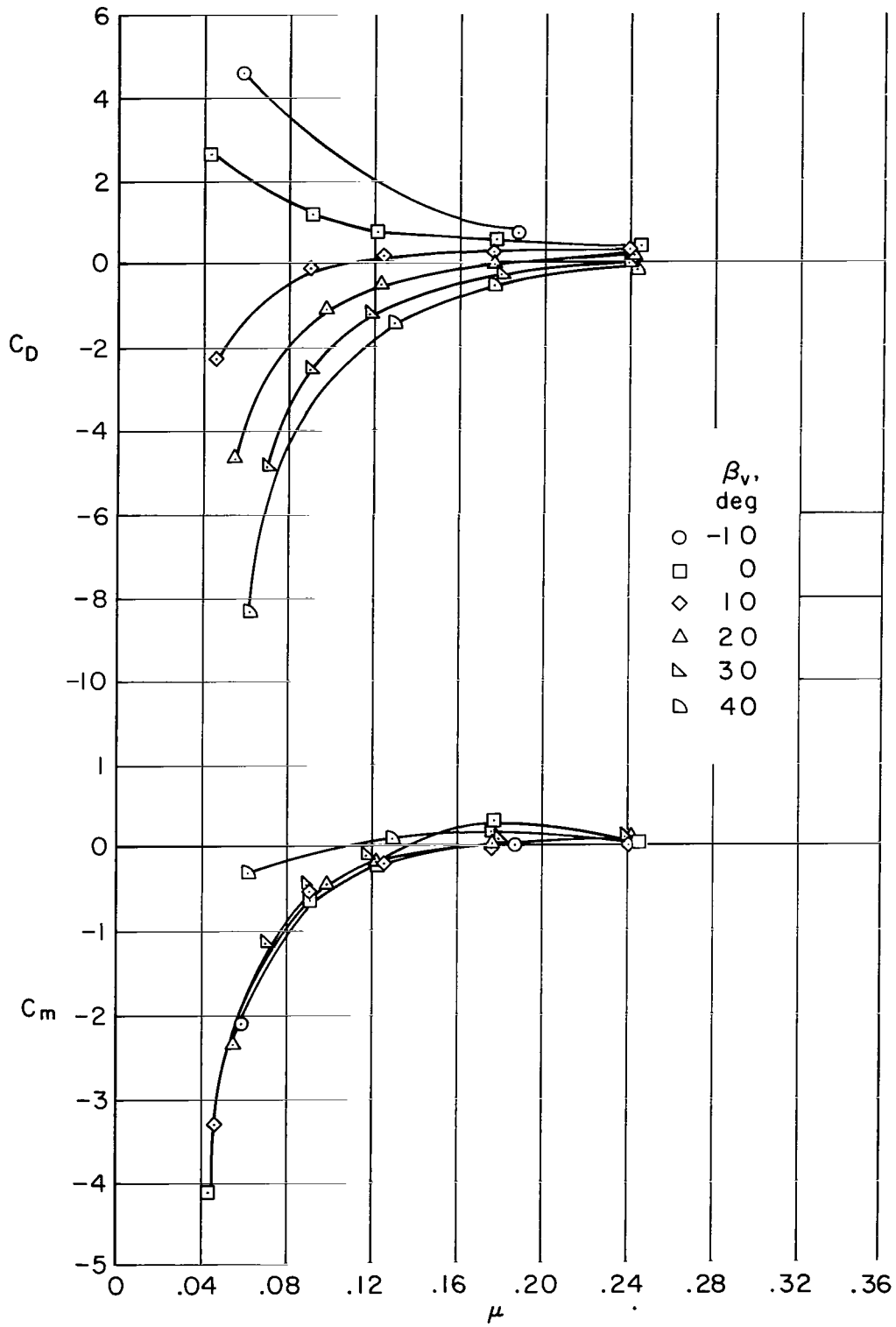


Figure 11.- The variation of longitudinal characteristics with tip-speed ratio; $\alpha = 0^\circ$, $\beta_v = 0^\circ$, $\delta_f = 40^\circ$, tail on, $i_t = 0^\circ$, lift-cruise nozzles off, 3600 rpm.



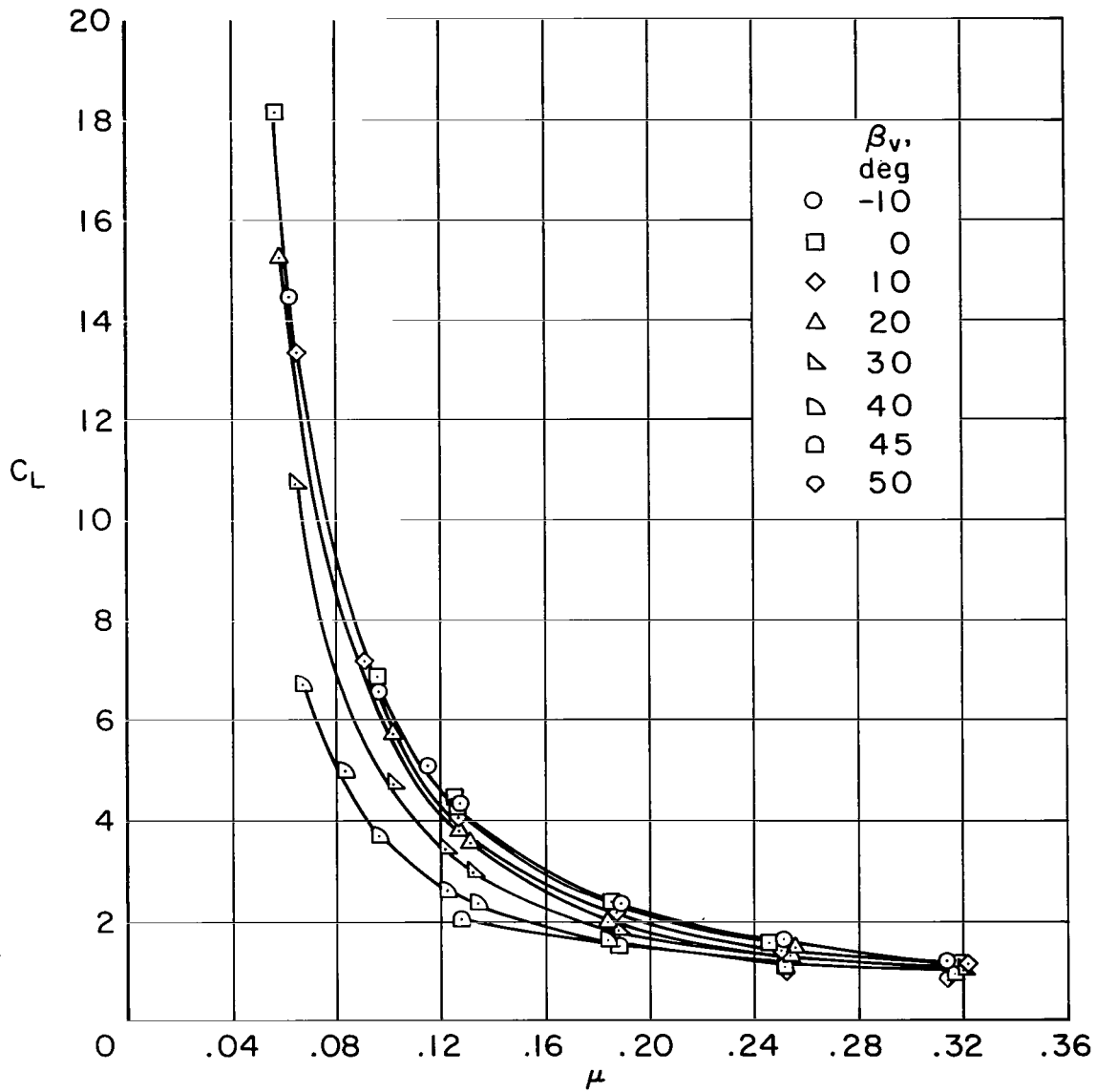
(a) C_L versus tip-speed ratio.

Figure 12.- The variation of longitudinal characteristics with tip-speed ratio; $\alpha = 0^\circ$, $\delta_f = 40^\circ$, tail off, six fans forward, lift-cruise nozzles off, 3600 rpm.



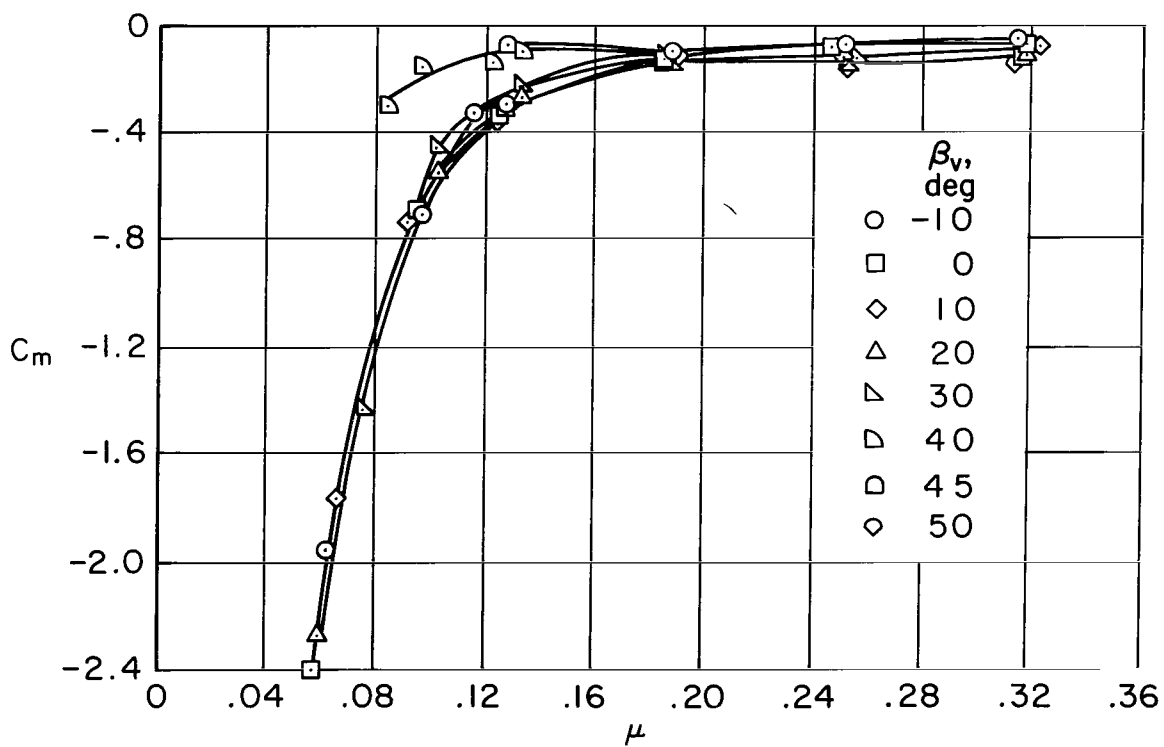
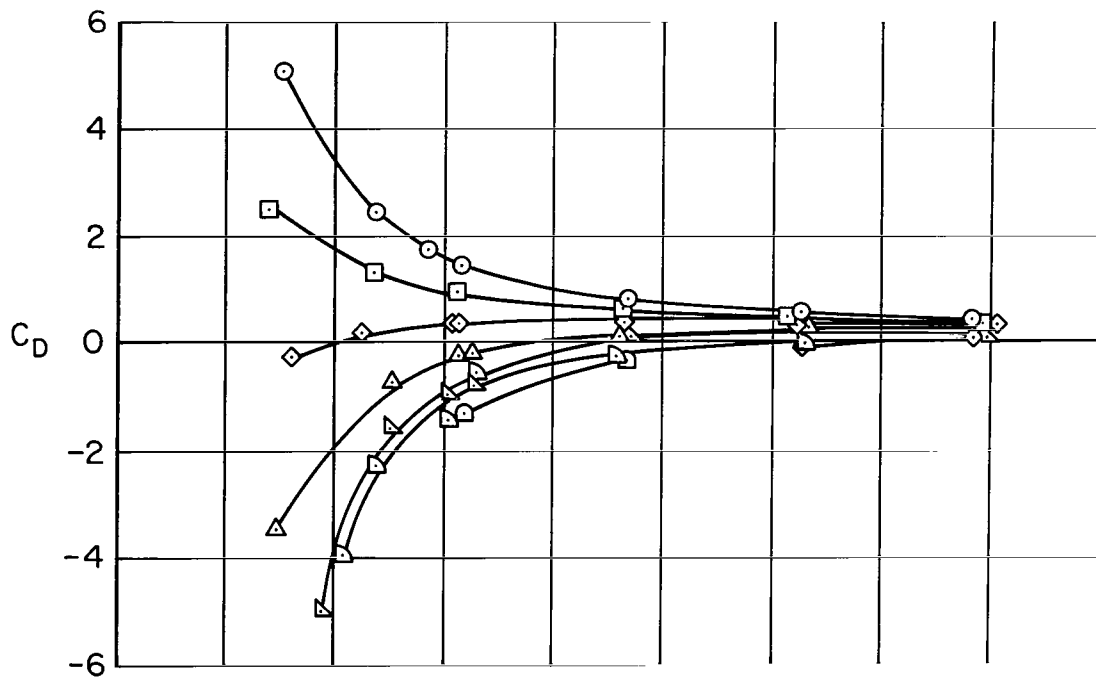
(b) C_D , C_m versus tip-speed ratio.

Figure 12.- Concluded.



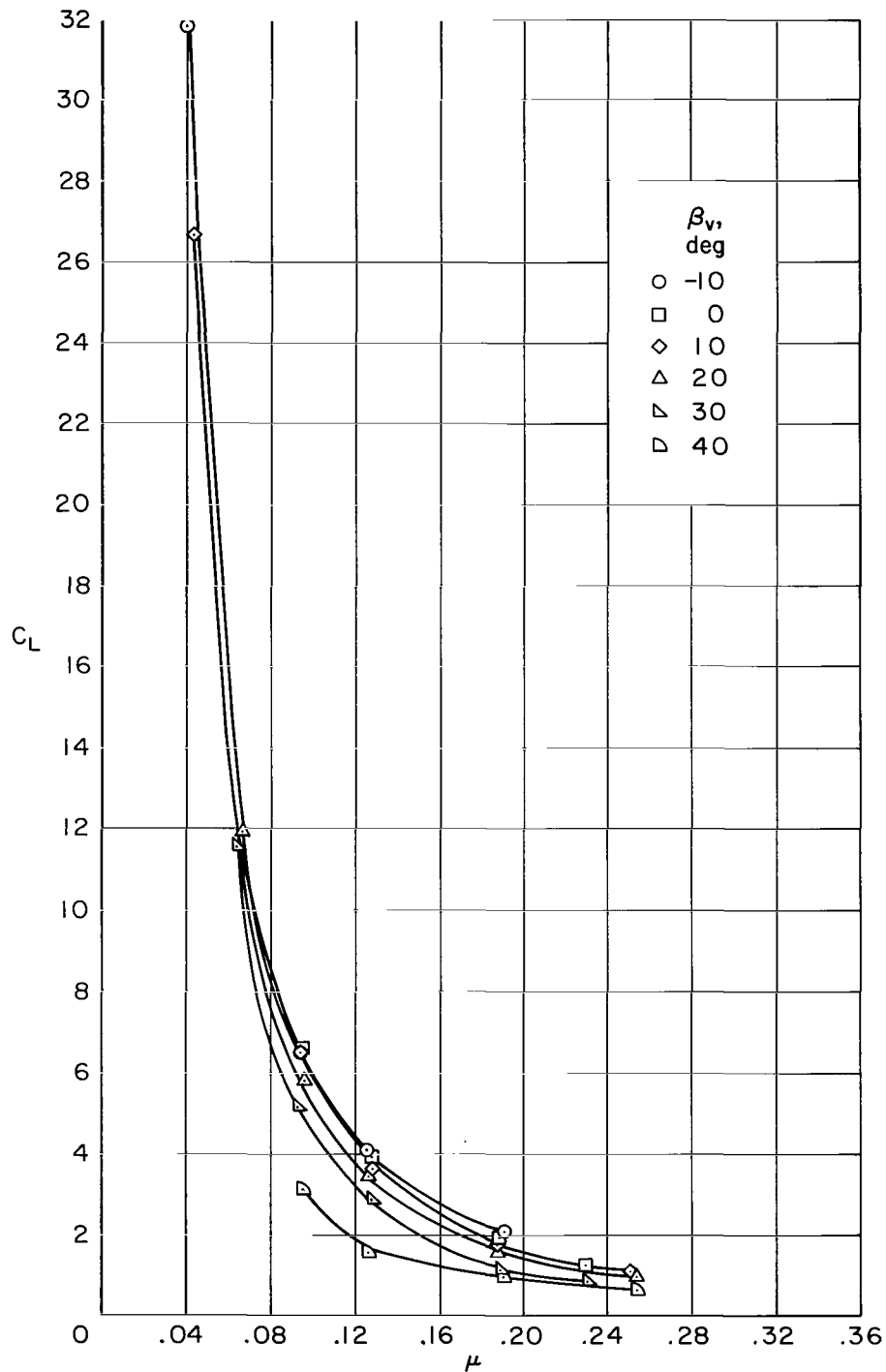
(a) C_L versus tip-speed ratio.

Figure 13.- The variation of longitudinal characteristics with tip-speed ratio; $\alpha = 0^\circ$, $\delta_f = 40^\circ$, tail off, six fans forward, lift-cruise nozzles off, 3600 rpm.



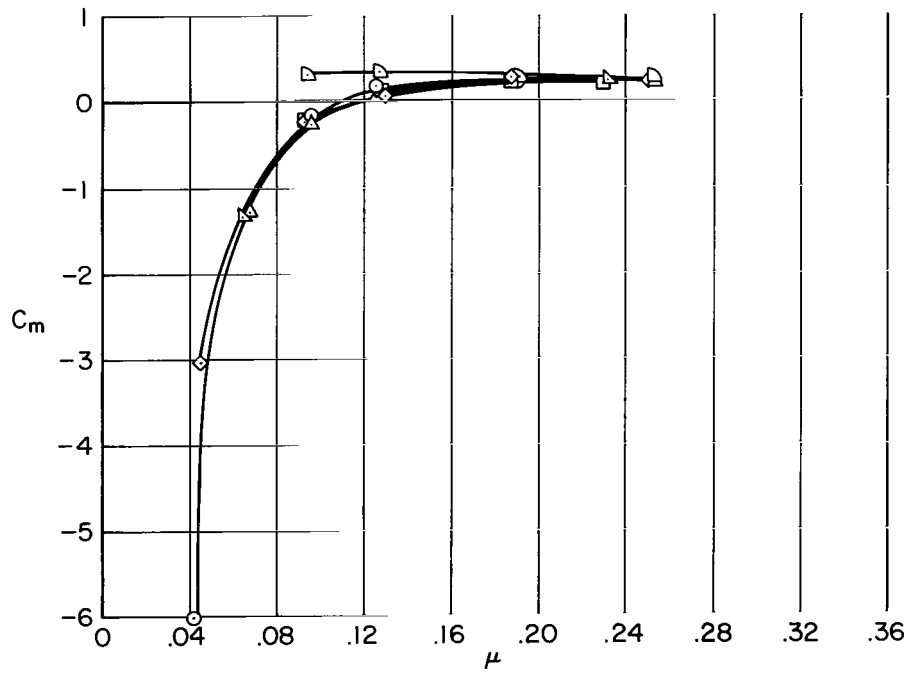
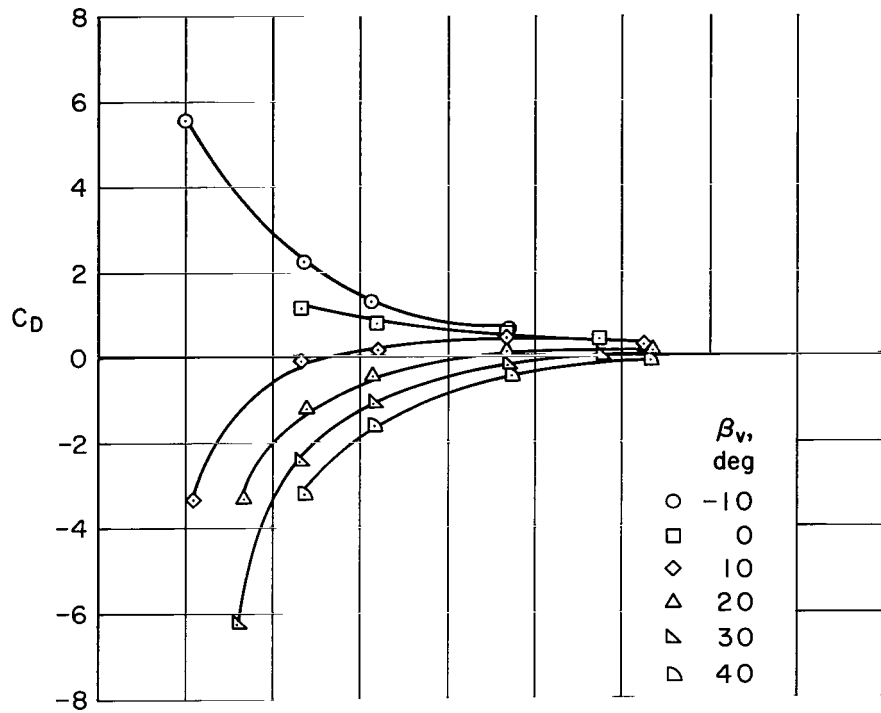
(b) C_D , C_m versus tip-speed ratio.

Figure 13.- Concluded.



(a) C_L versus tip-speed ratio.

Figure 14.- The variation of longitudinal characteristics with tip-speed ratio; $\alpha = 0^\circ$, $\delta_f = 0^\circ$, tail on, $i_t = 0^\circ$, six fans forward, lift-cruise nozzles off, 3600 rpm.



(b) C_D , C_m versus tip-speed ratio.

Figure 14.- Concluded.

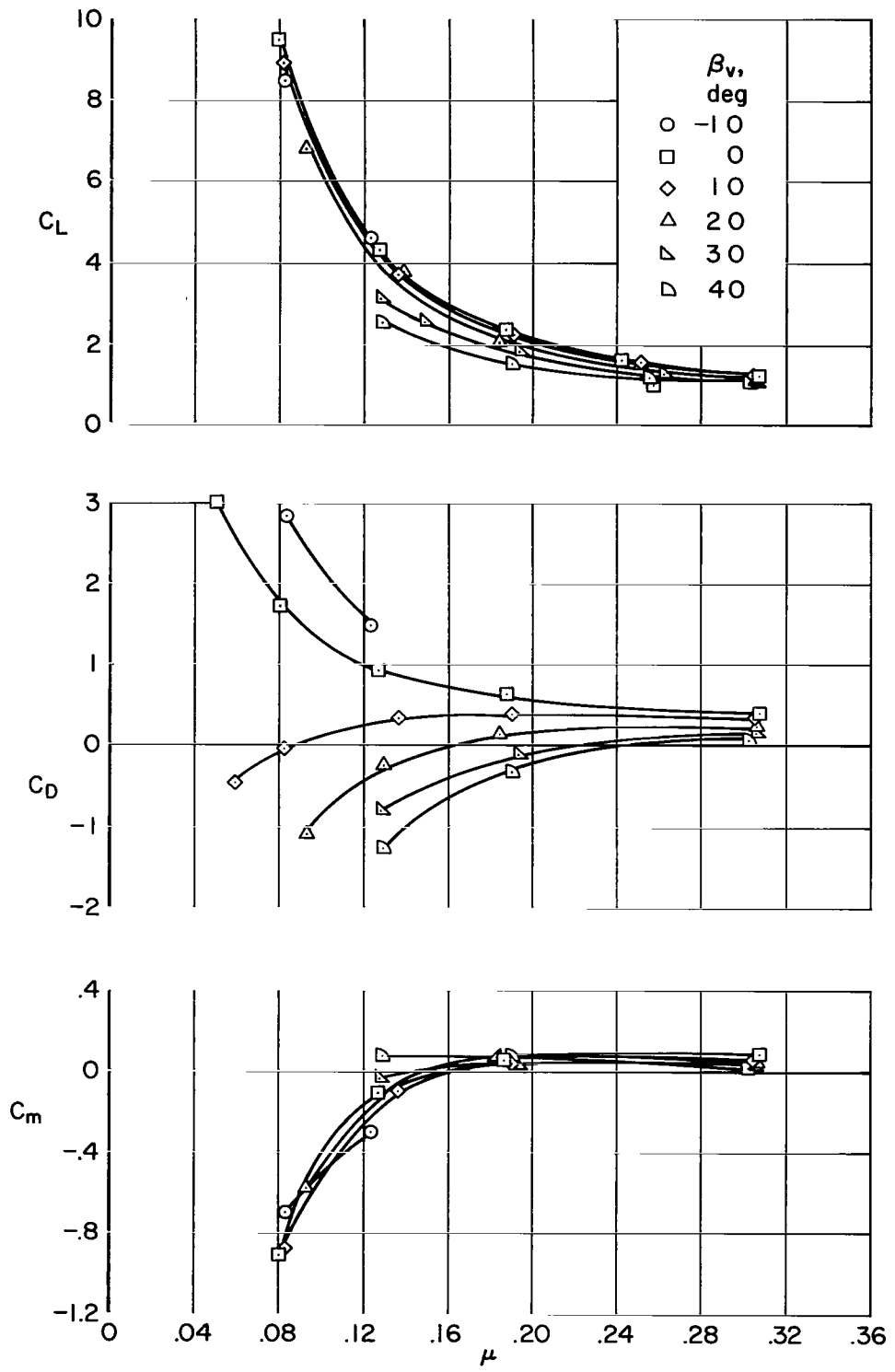
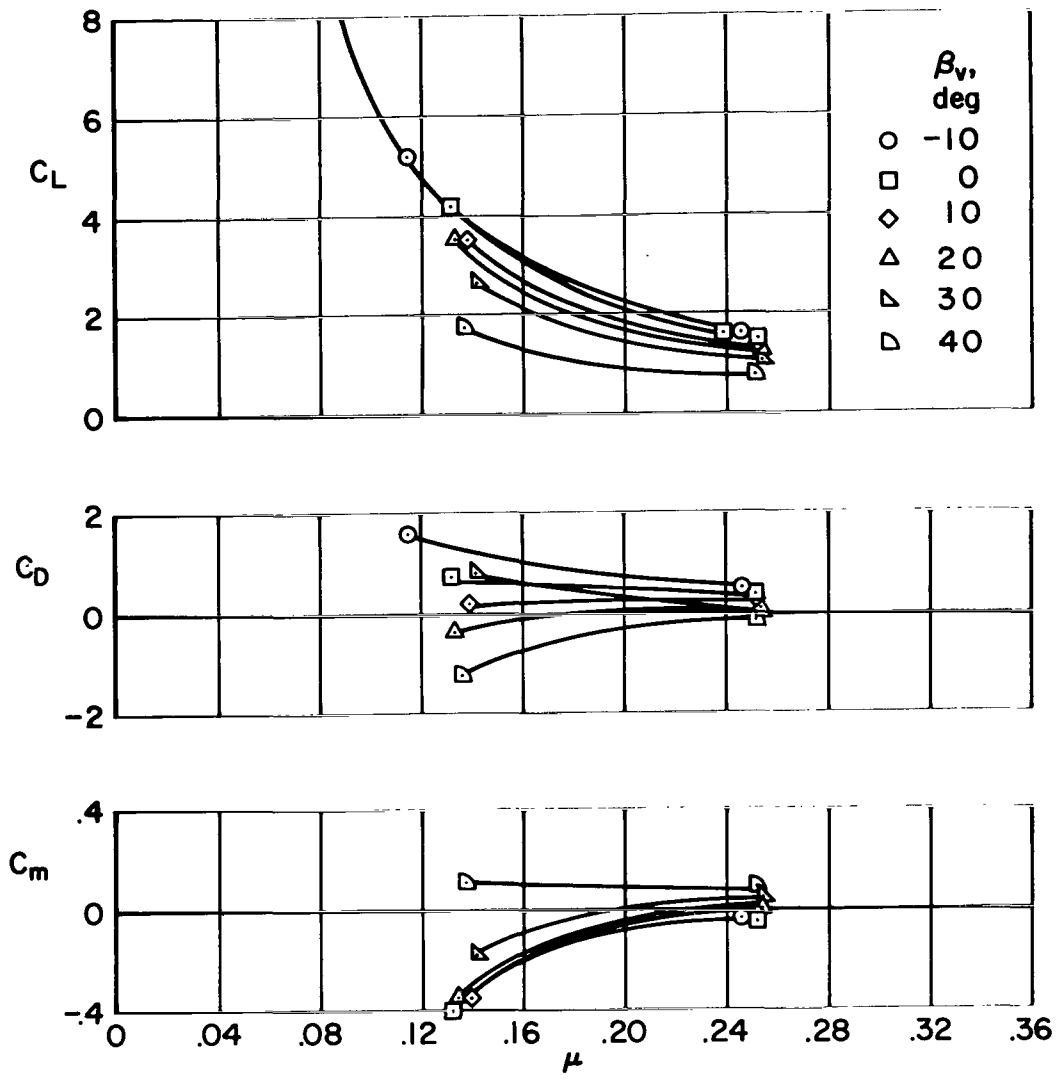
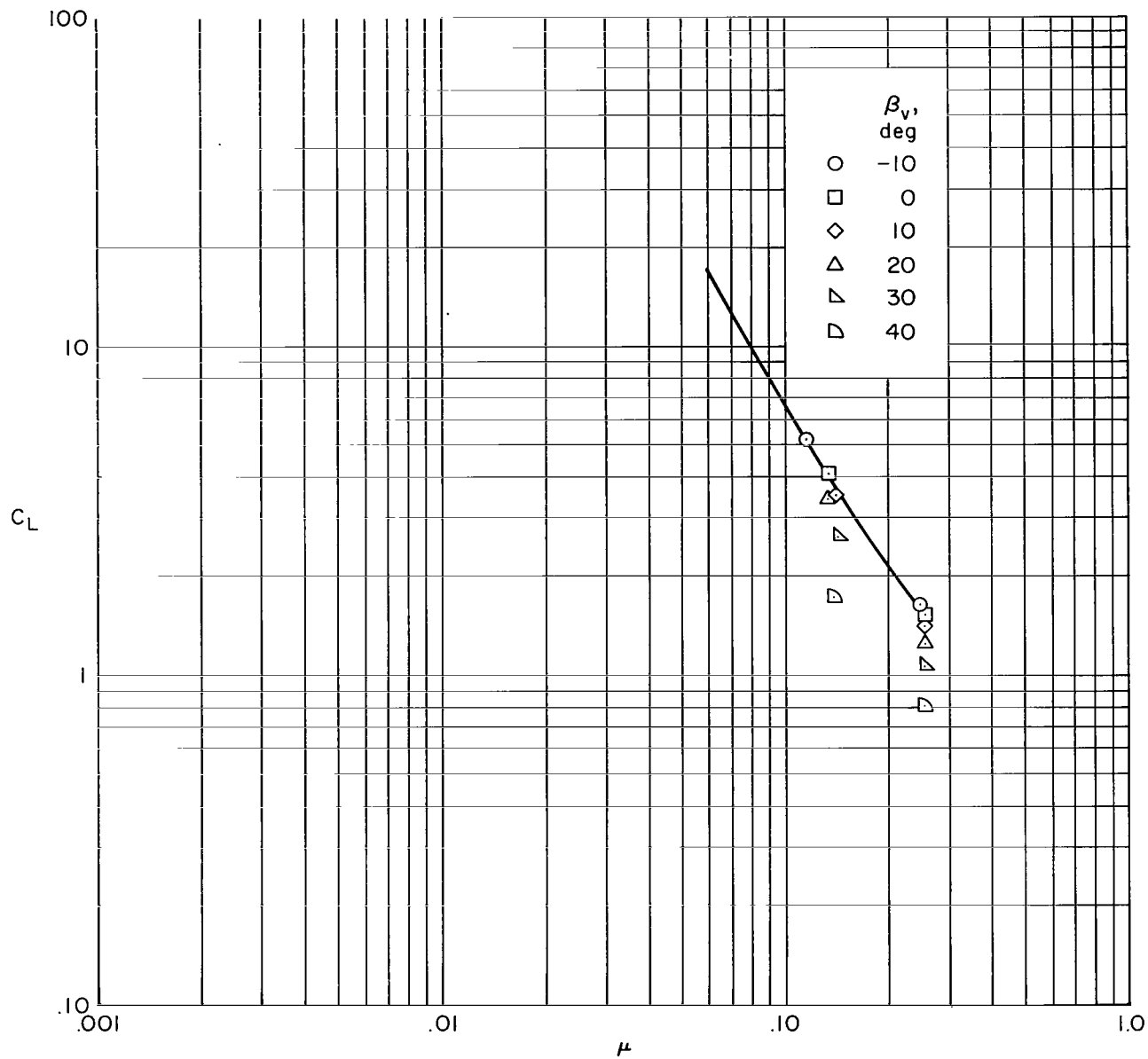


Figure 15.- The variation of longitudinal characteristics with tip-speed ratio; $\alpha = 0^\circ$, $\delta_F = 40^\circ$, tail on, $i_t = 0^\circ$, six fans forward, lift-cruise nozzles off, 3600 rpm.



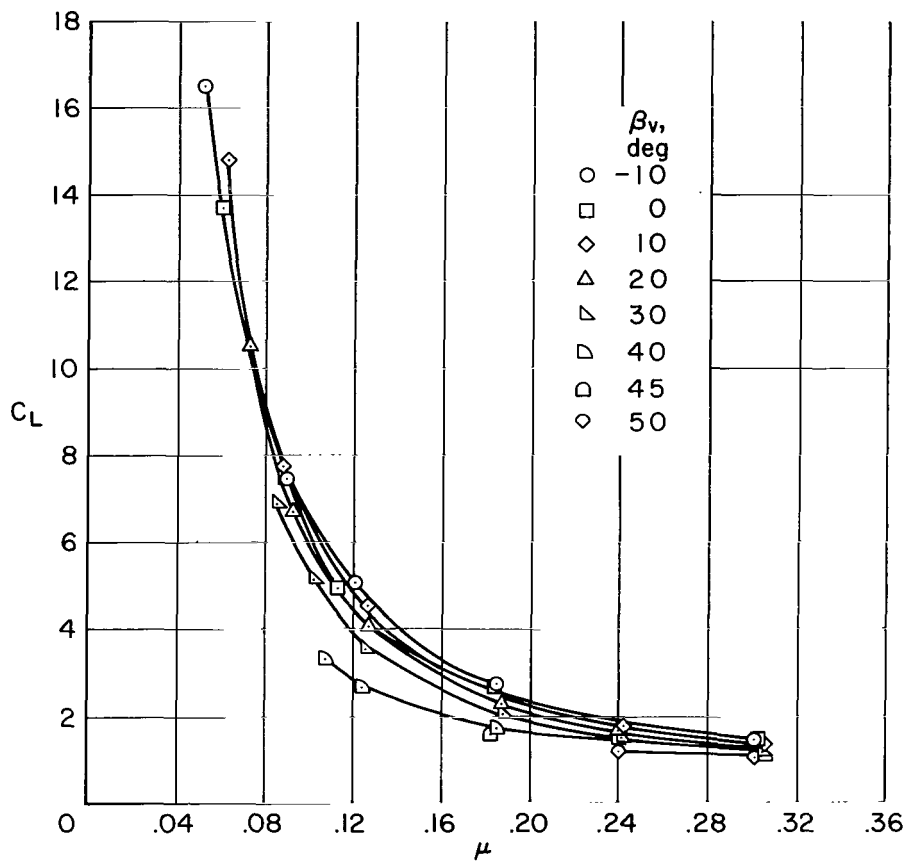
(a) Standard scale.

Figure 16.- The variation of longitudinal characteristics with tip-speed ratio; $\alpha = 0^\circ$, $\delta_f = 0^\circ$, tail off, six fans aft, lift-cruise nozzles off, 3600 rpm.



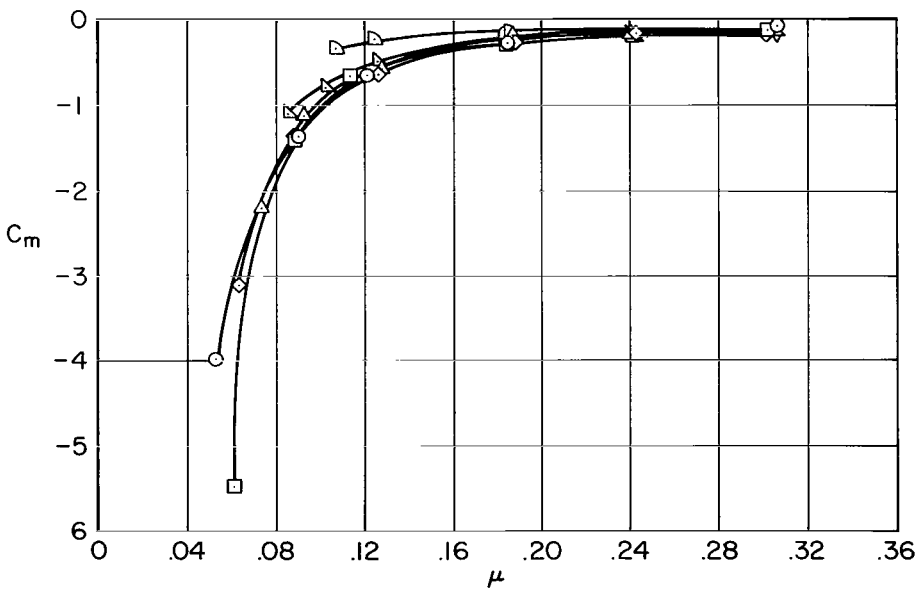
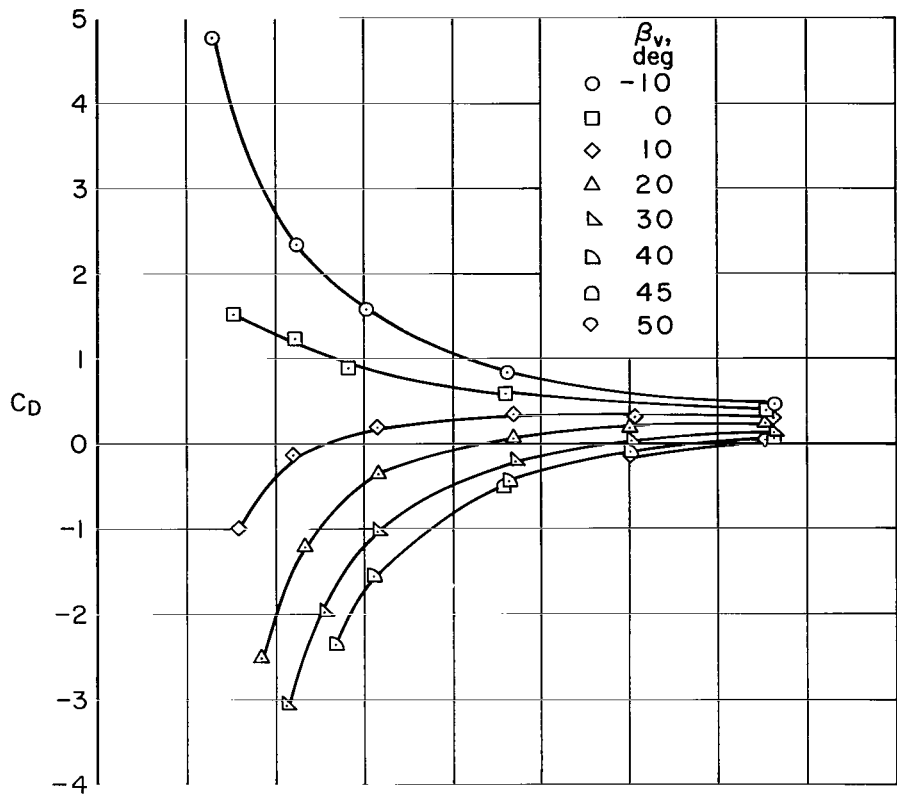
(b) Logarithm scale.

Figure 16.- Concluded.



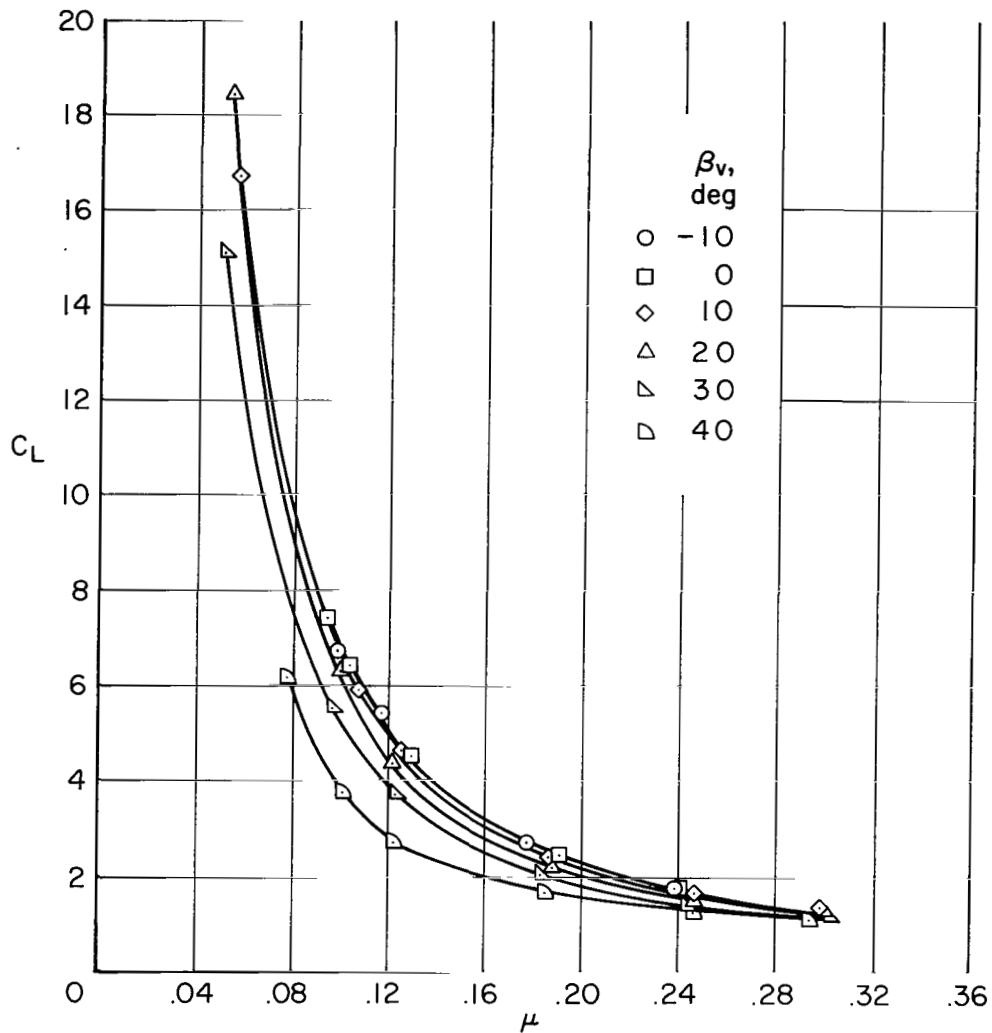
(a) C_L versus tip-speed ratio.

Figure 17.- The variation of longitudinal characteristics with tip-speed ratio; $\alpha = 0^\circ$, $\delta_f = 40^\circ$, tail off, six fans aft, lift-cruise nozzles off, 3600 rpm.



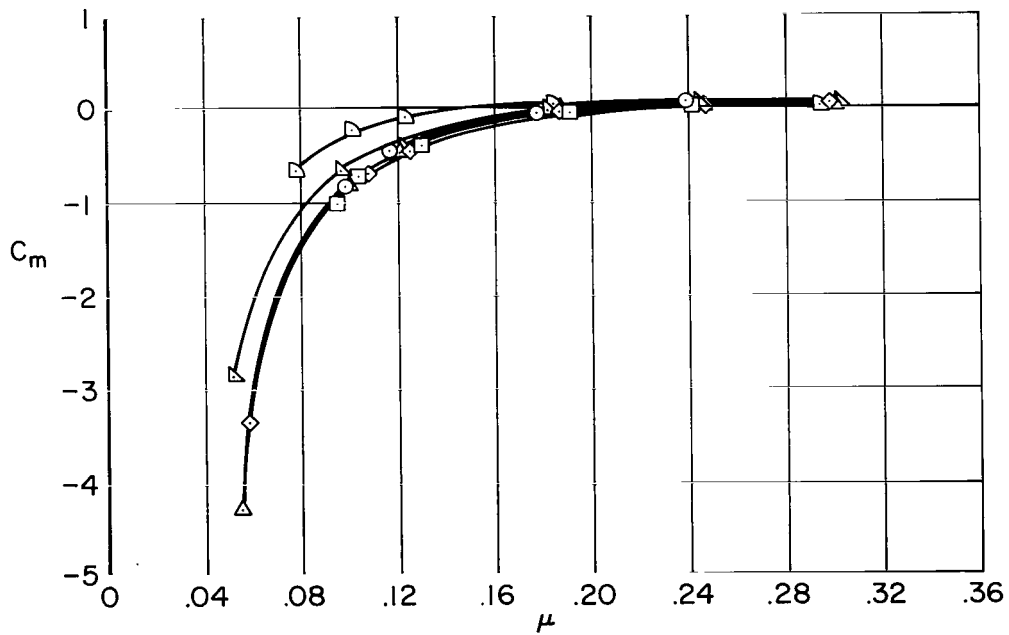
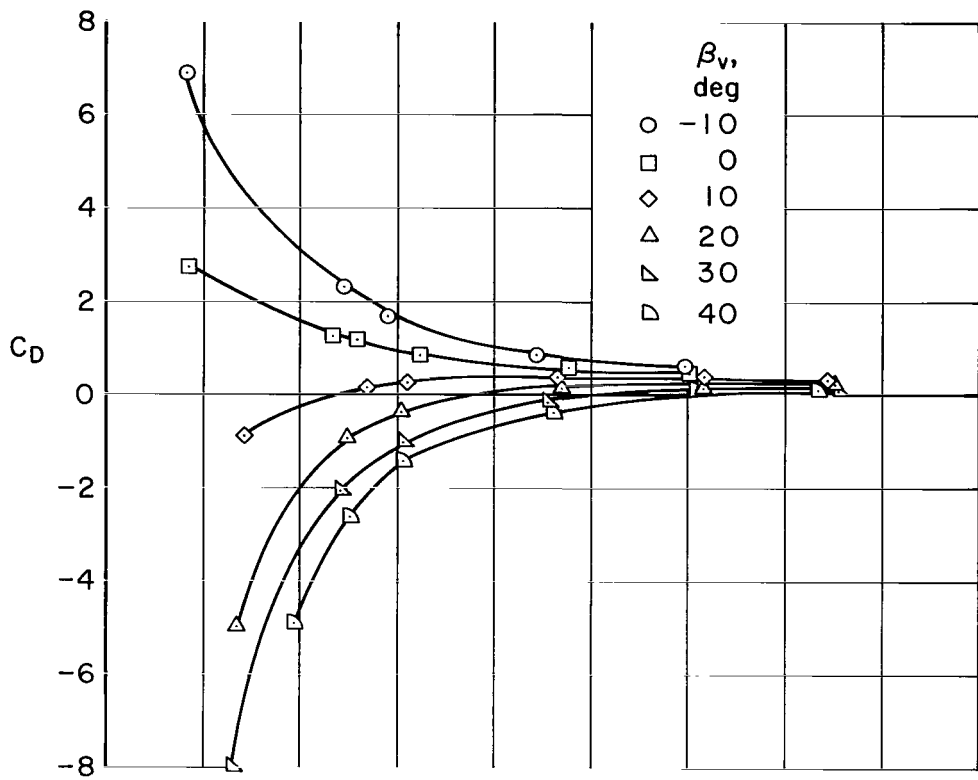
(b) C_D , C_m versus tip-speed ratio.

Figure 17.- Concluded.



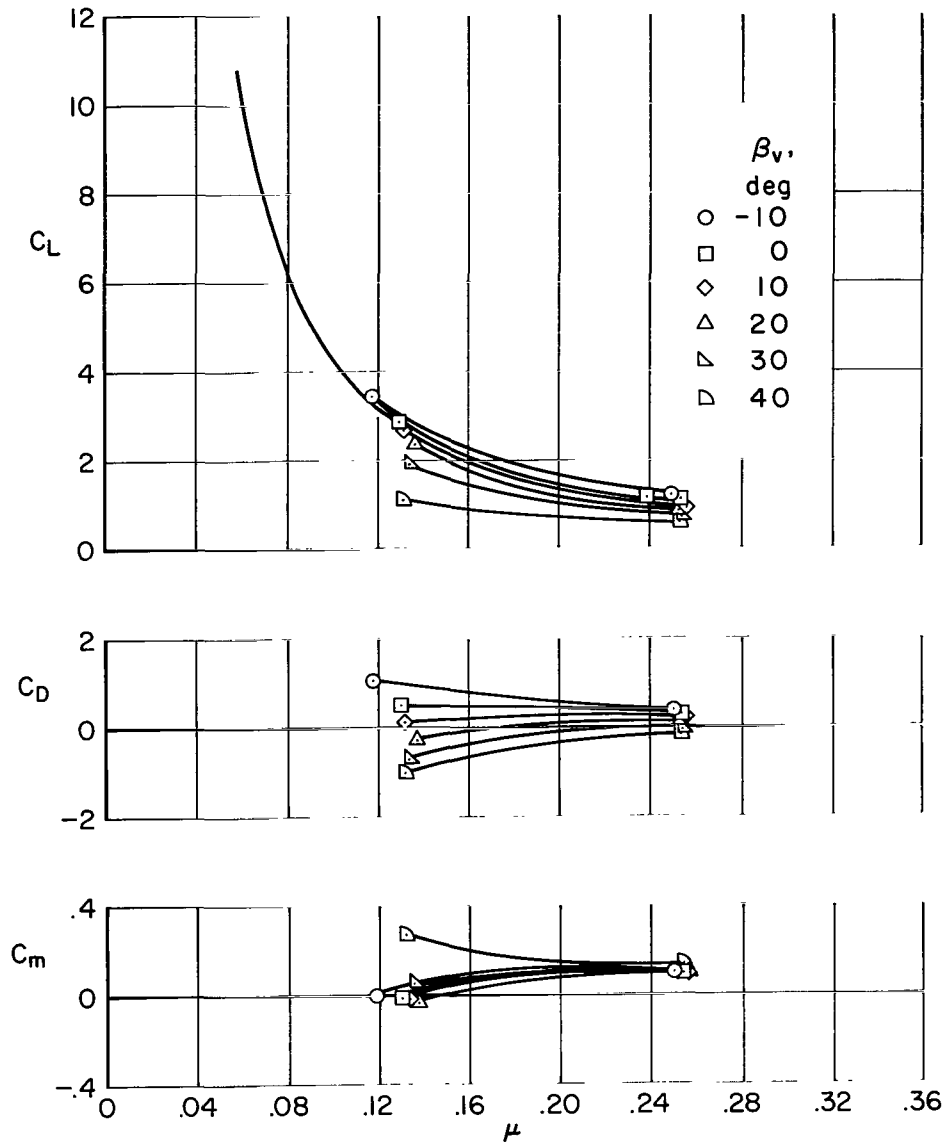
(a) C_L versus tip-speed ratio.

Figure 18.- The variation of longitudinal characteristics with tip-speed ratio; $\alpha = 0^\circ$, $\delta_f = 40^\circ$, tail on, $i_t = 0^\circ$, six fans aft, lift-cruise nozzles off, 3600 rpm.



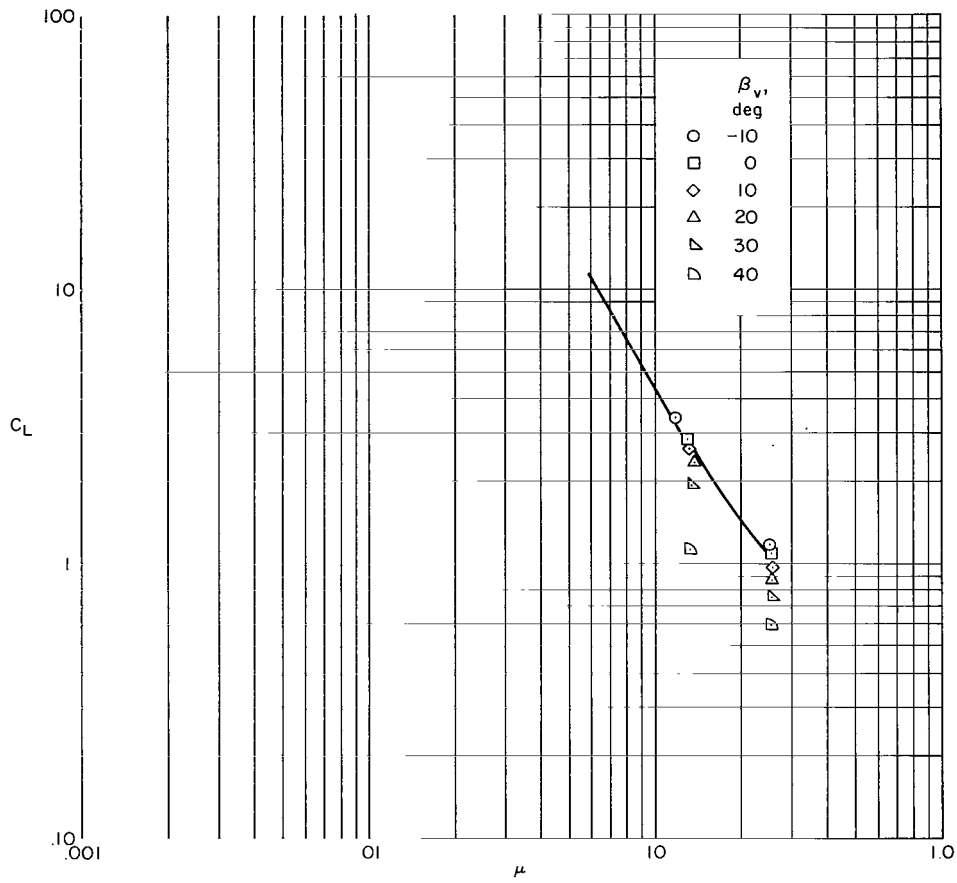
(b) C_D , C_m versus tip-speed ratio.

Figure 18.- Concluded.



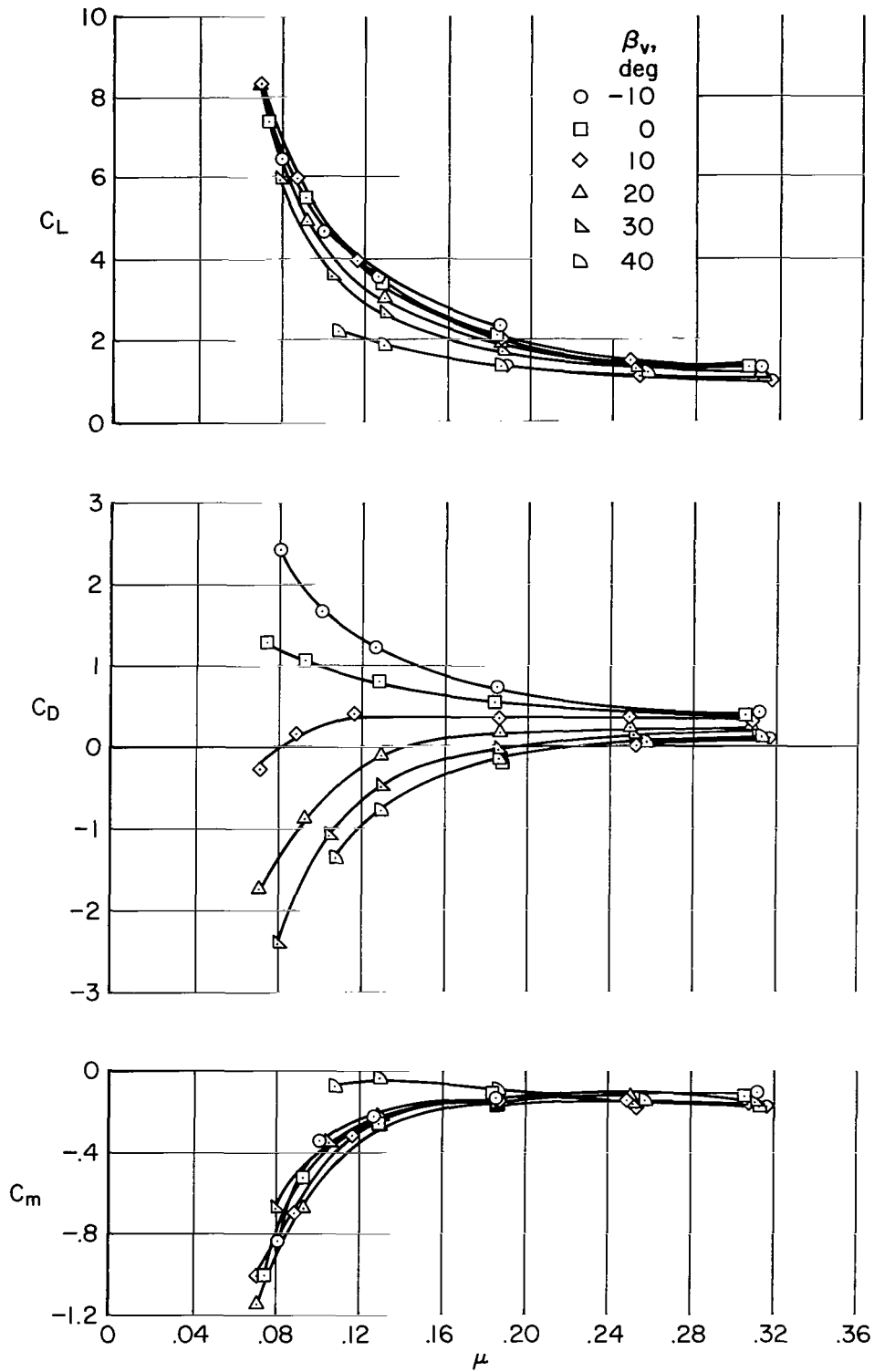
(a) $\delta_f = 0^\circ$, standard scale.

Figure 19.- The variation of longitudinal characteristics with tip-speed ratio; $\alpha = 0^\circ$, tail off, four fans aft (inboard and center), lift-cruise nozzles off, 3600 rpm.



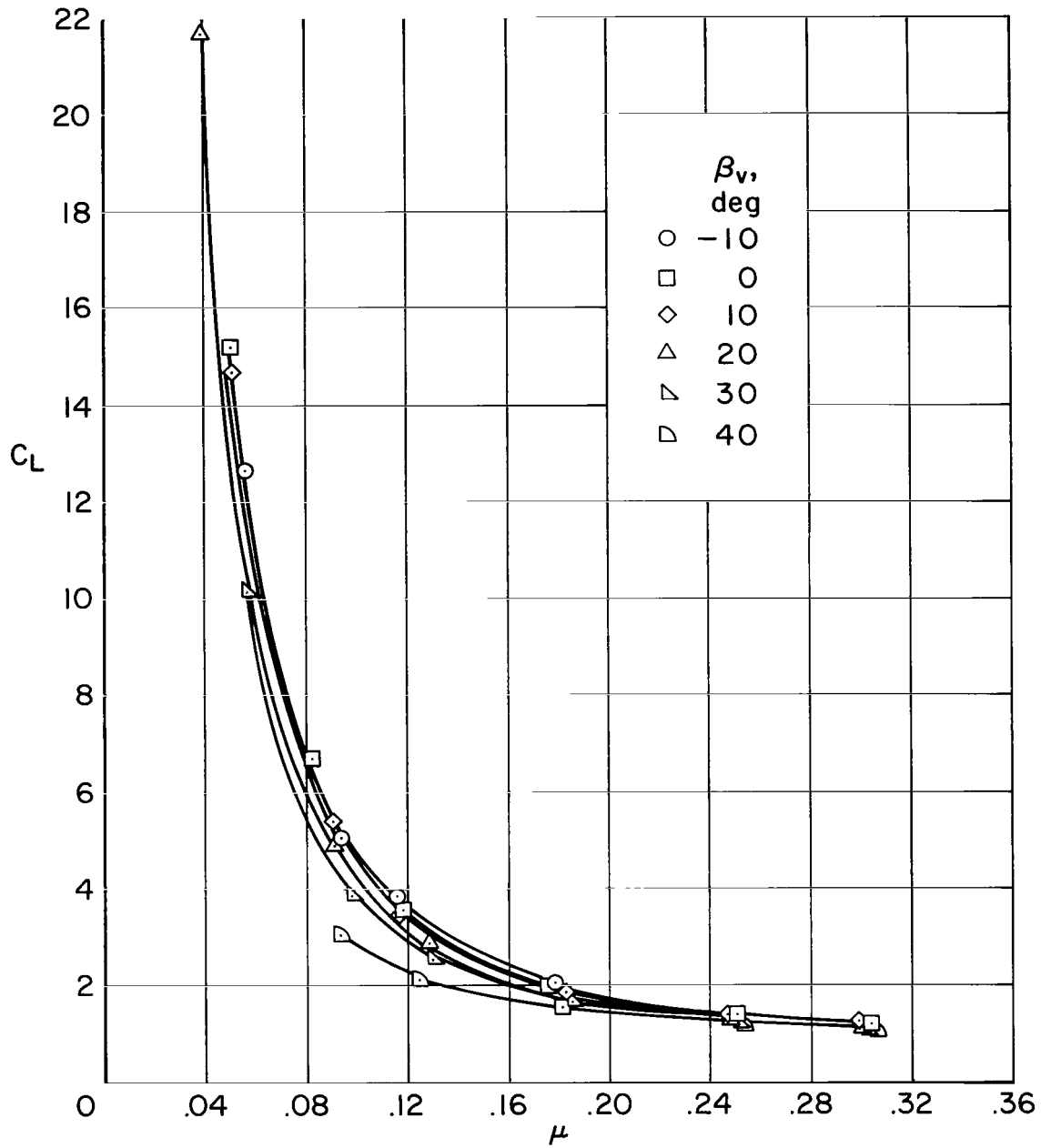
(b) $\delta_f = 0^\circ$, logarithm scale.

Figure 19.- Continued.



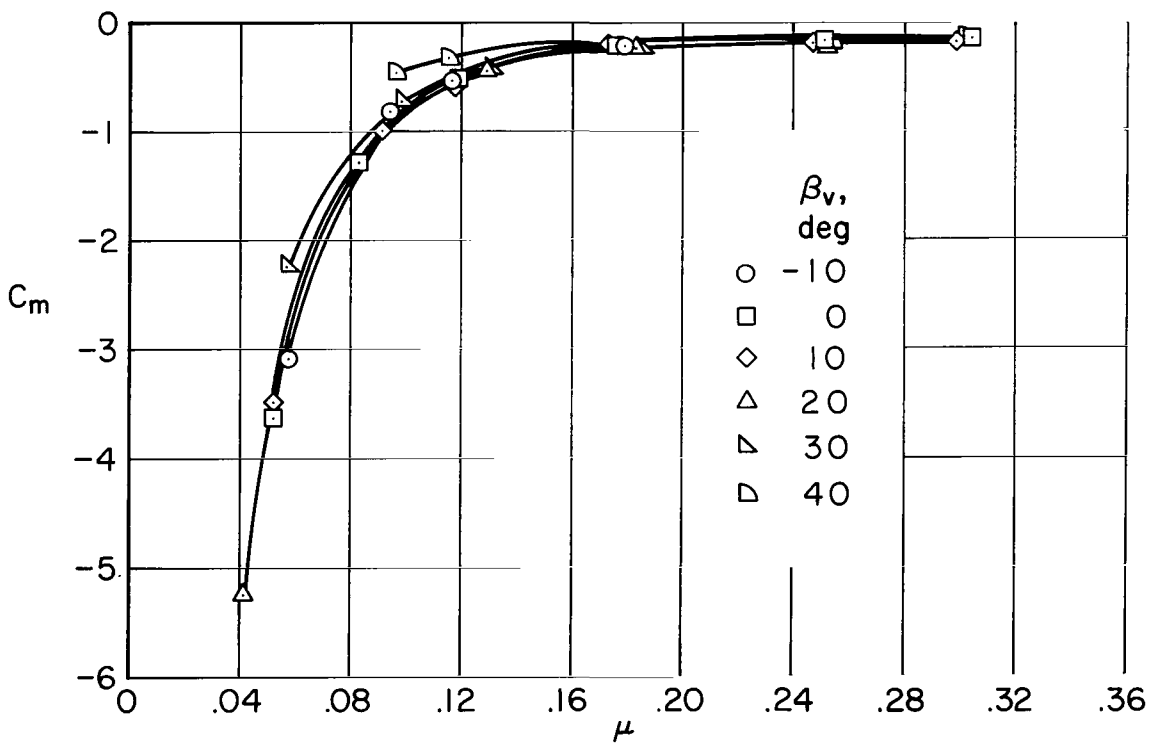
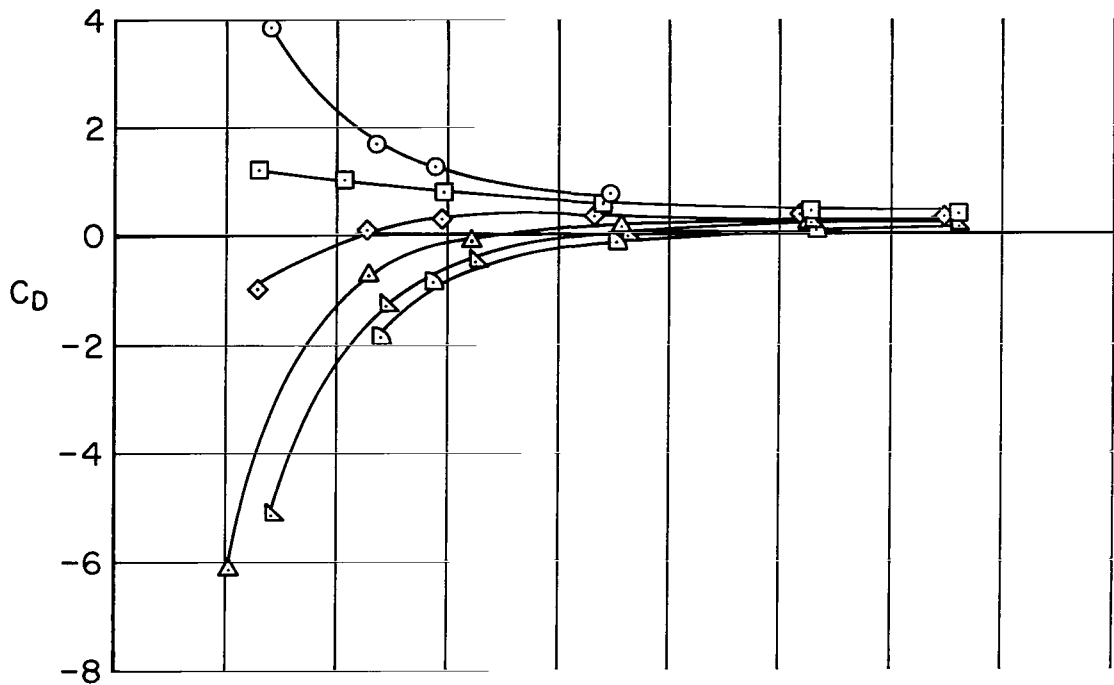
(c) $\delta_f = 40^\circ$, standard scale.

Figure 19.- Concluded.



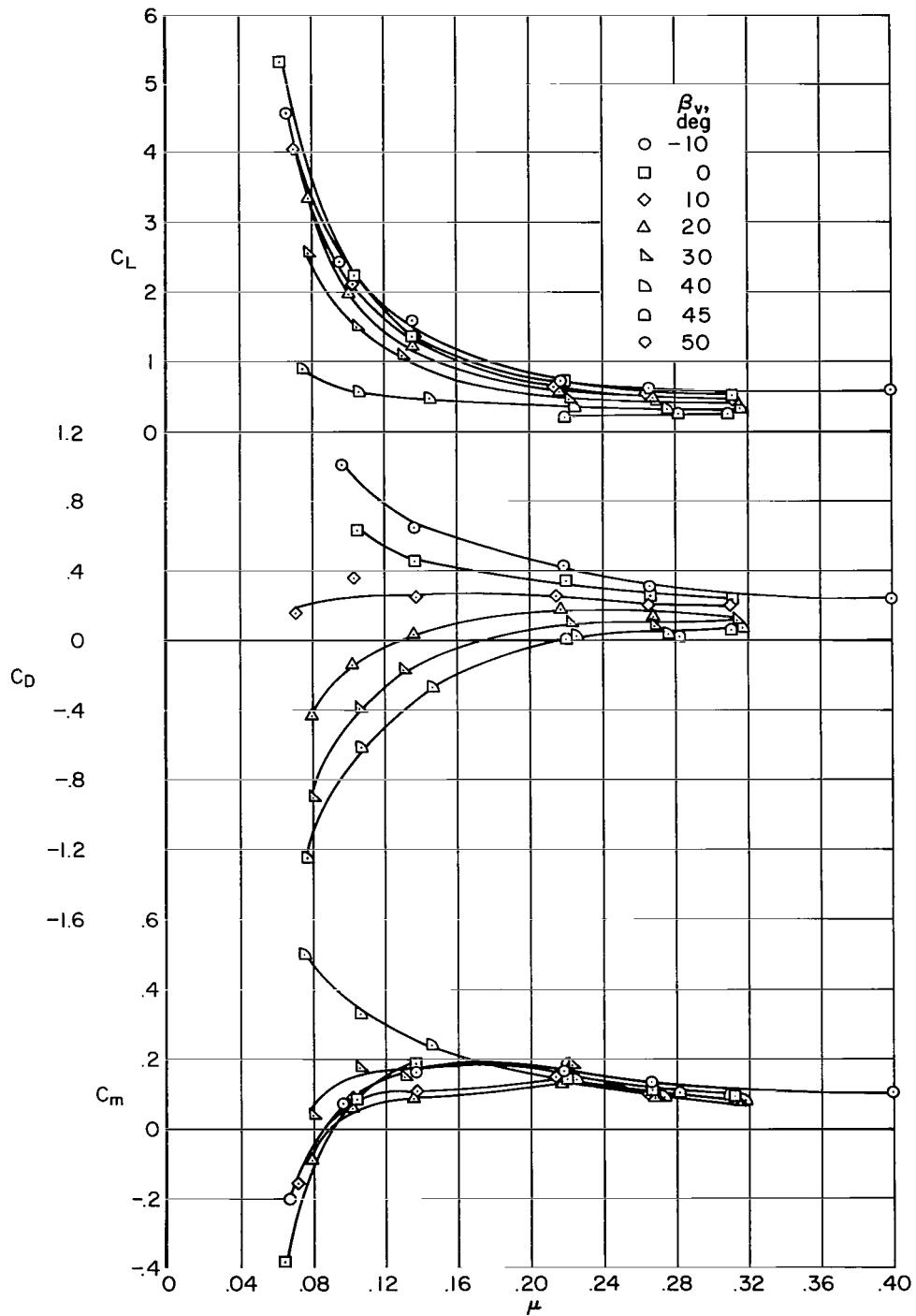
(a) C_L versus tip-speed ratio.

Figure 20.- The variation of longitudinal characteristics with tip-speed ratio; $\alpha = 0^\circ$, $\delta_f = 40^\circ$, tail off, four fans aft (inboard and outboard), lift-cruise nozzles off, 3600 rpm.



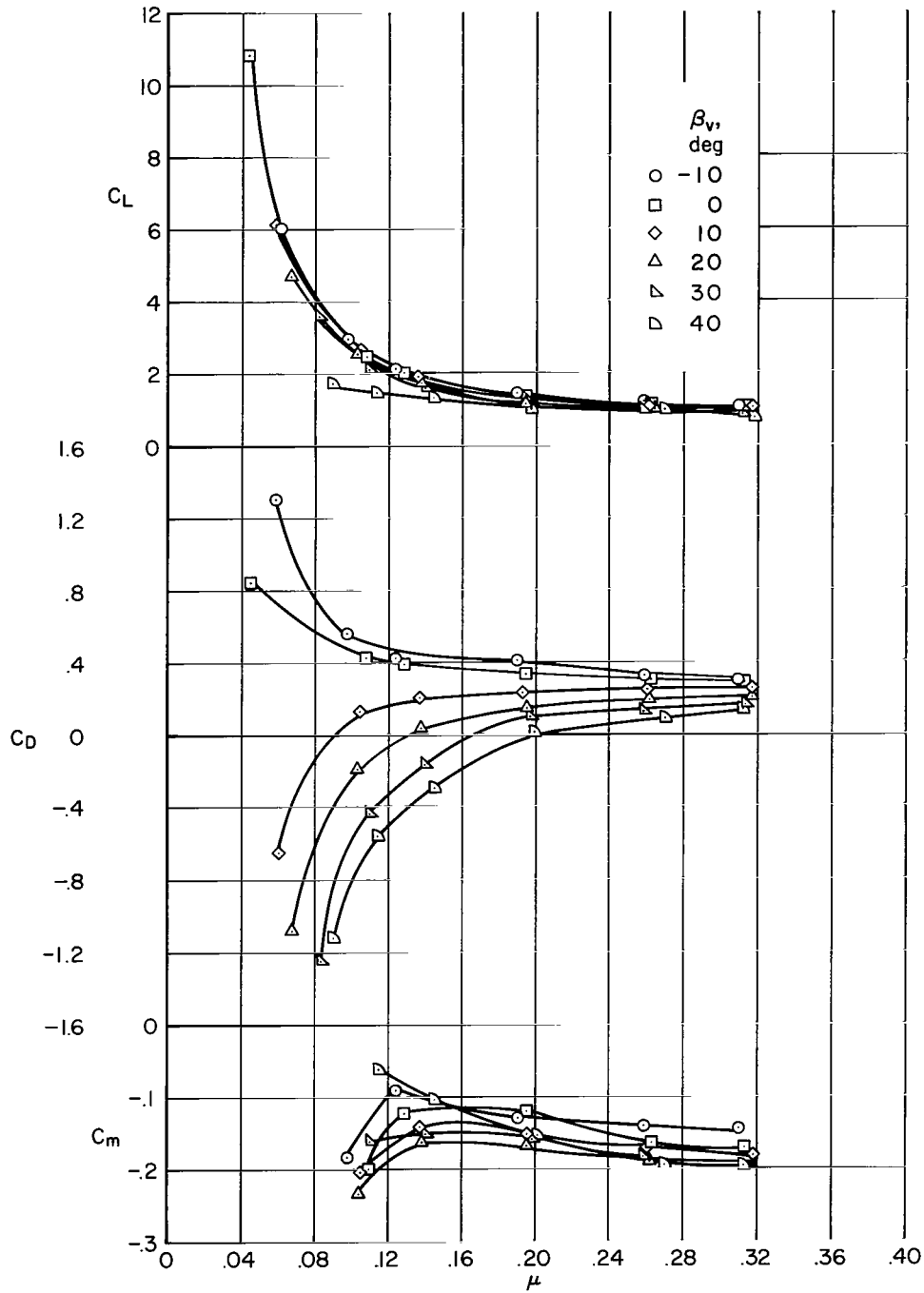
(b) C_D , C_m versus tip-speed ratio.

Figure 20.- Concluded.



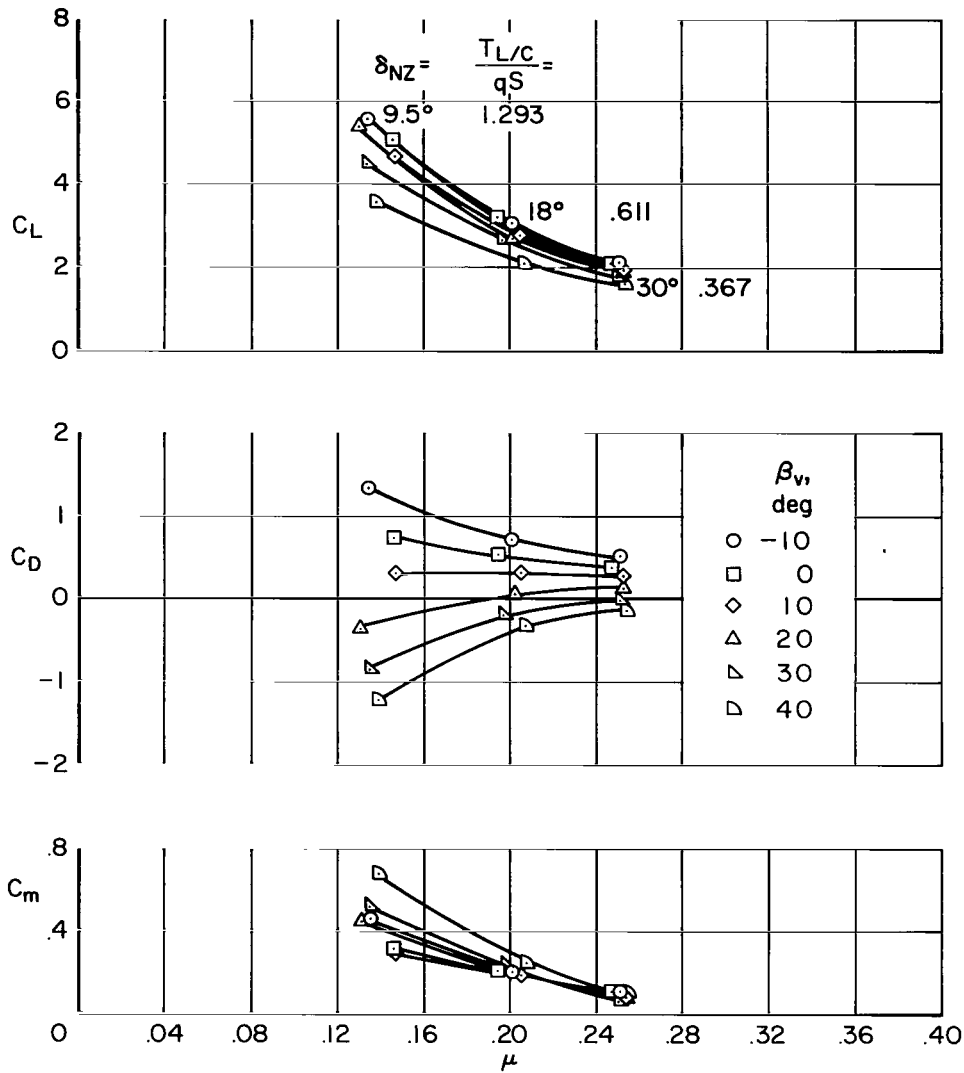
(a) $\delta_F = 0^\circ$

Figure 21.- The variation of longitudinal characteristics with tip-speed ratio; $\alpha = 0^\circ$, tail off, two fans aft (inboard), lift-cruise nozzles off, 3500 rpm.



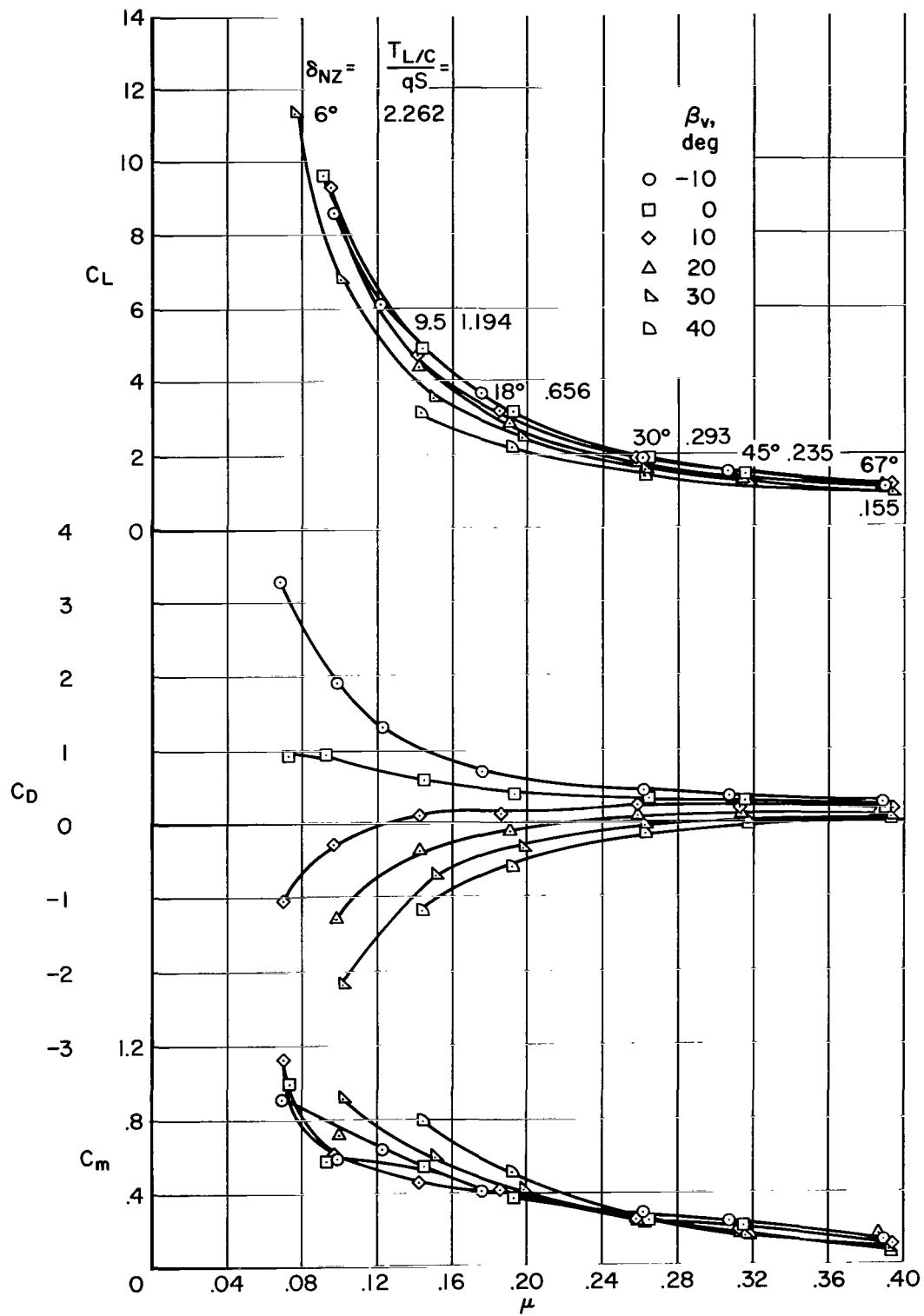
(b) $\delta_F = 40^\circ$

Figure 21.- Concluded.



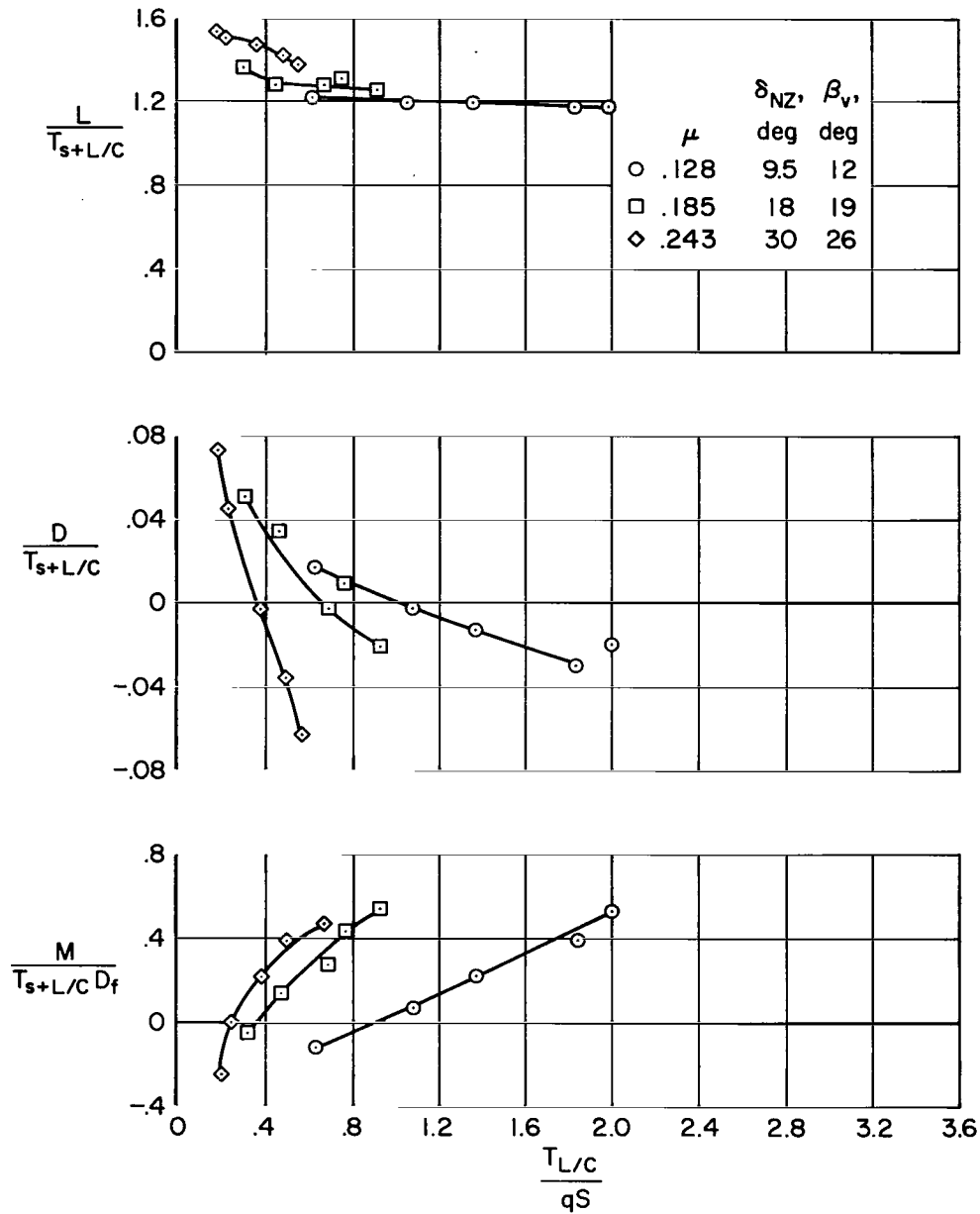
(a) Tail off.

Figure 22.- The variation of longitudinal characteristics with tip-speed ratio; $\alpha = 0^\circ$, $\delta_f = 40^\circ$, six fans aft, lift-cruise nozzles on, 2950 rpm, lift-cruise thrust = 1000 lb/engine.



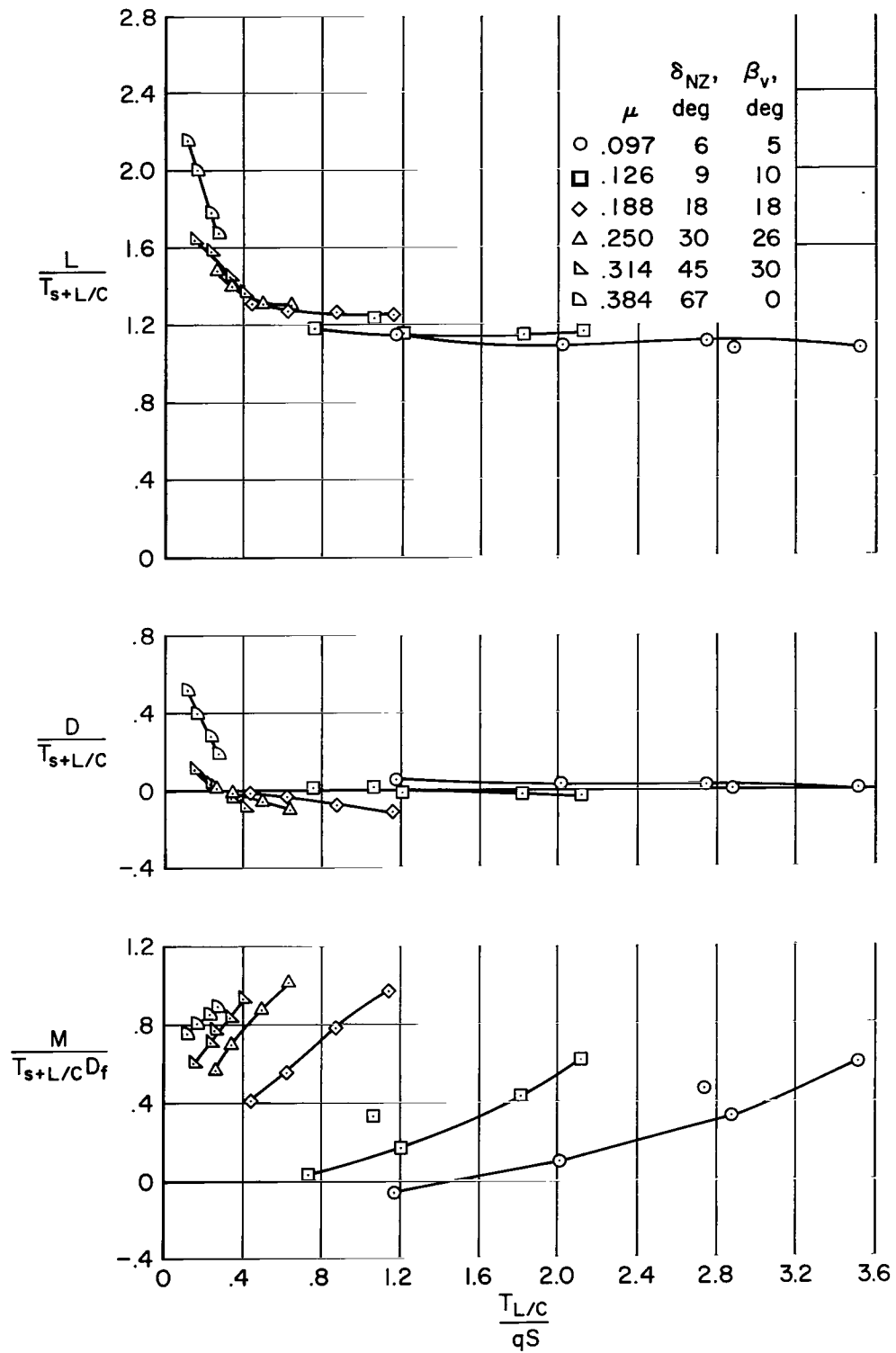
(b) Tail on, $i_t = 0^\circ$.

Figure 22.- Concluded.



(a) Tail off.

Figure 23.- The variation of longitudinal characteristics with lift-cruise thrust coefficient; $\alpha = 0^\circ$, $\delta_f = 40^\circ$, six fans aft, lift-cruise nozzles on, 2950 rpm.



(b) Tail on, $i_t = 0^\circ$.

Figure 23.- Concluded.

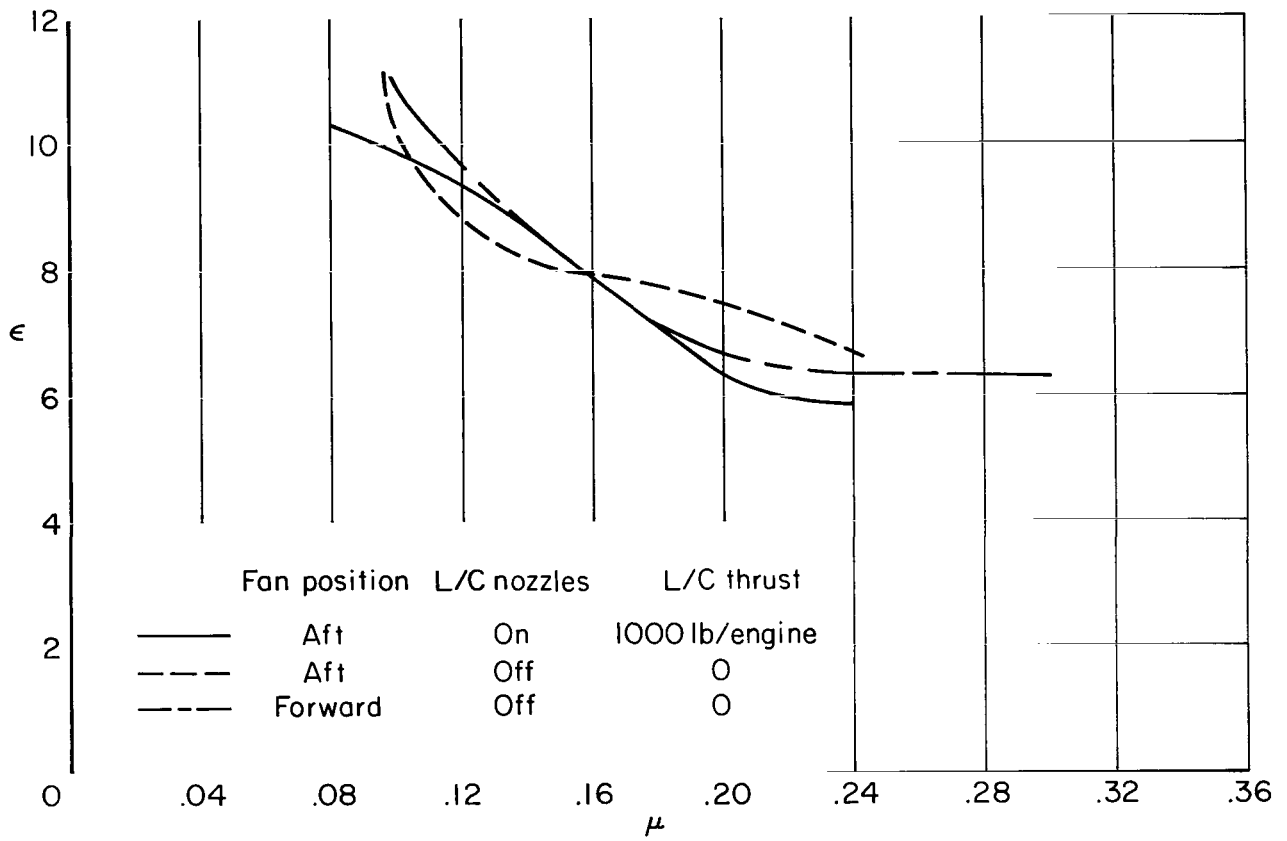


Figure 24.- The variation in average downwash at the horizontal tail with tip-speed ratio; $\alpha = 0^\circ$, $\delta_f = 40^\circ$, $\beta_v = 0^\circ$, six fans operating, 3600 rpm.

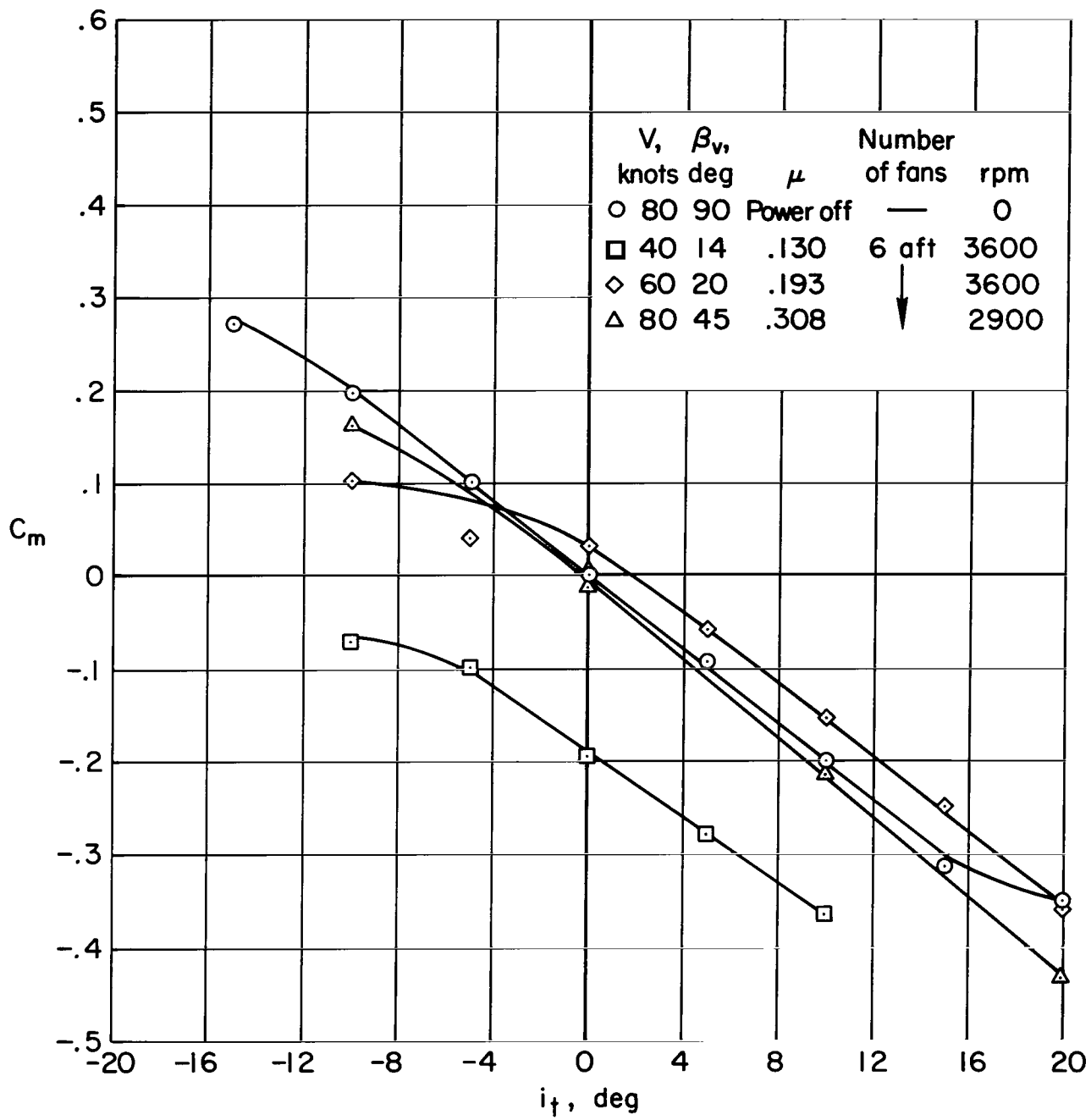


Figure 25.- Horizontal-tail effectiveness; $\alpha = 0^\circ$, $\delta_f = 40^\circ$, lift-cruise nozzles off.

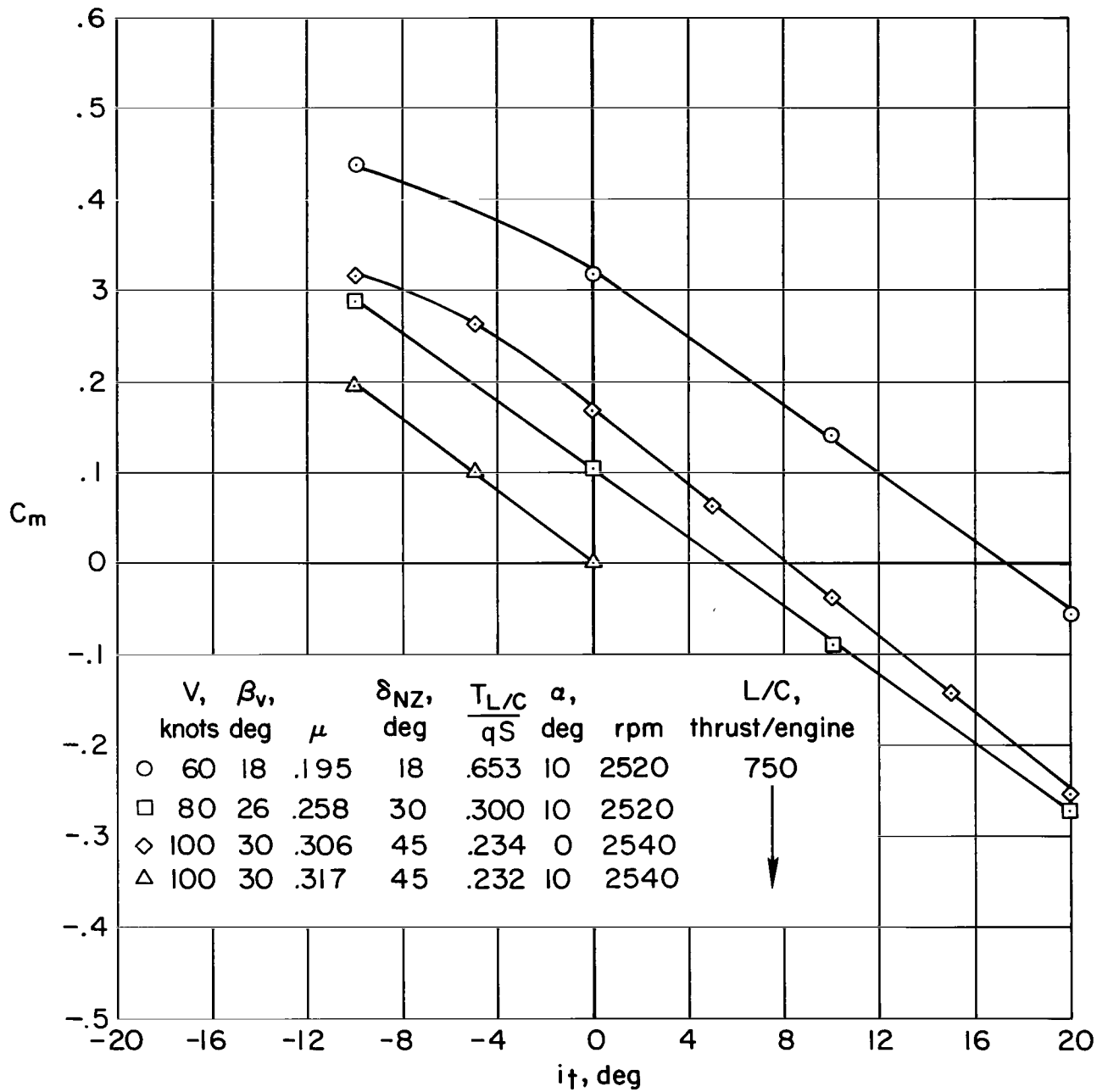


Figure 26.- Horizontal tail effectiveness; $\delta_f = 40^\circ$, six fans aft, lift-cruise nozzles on.

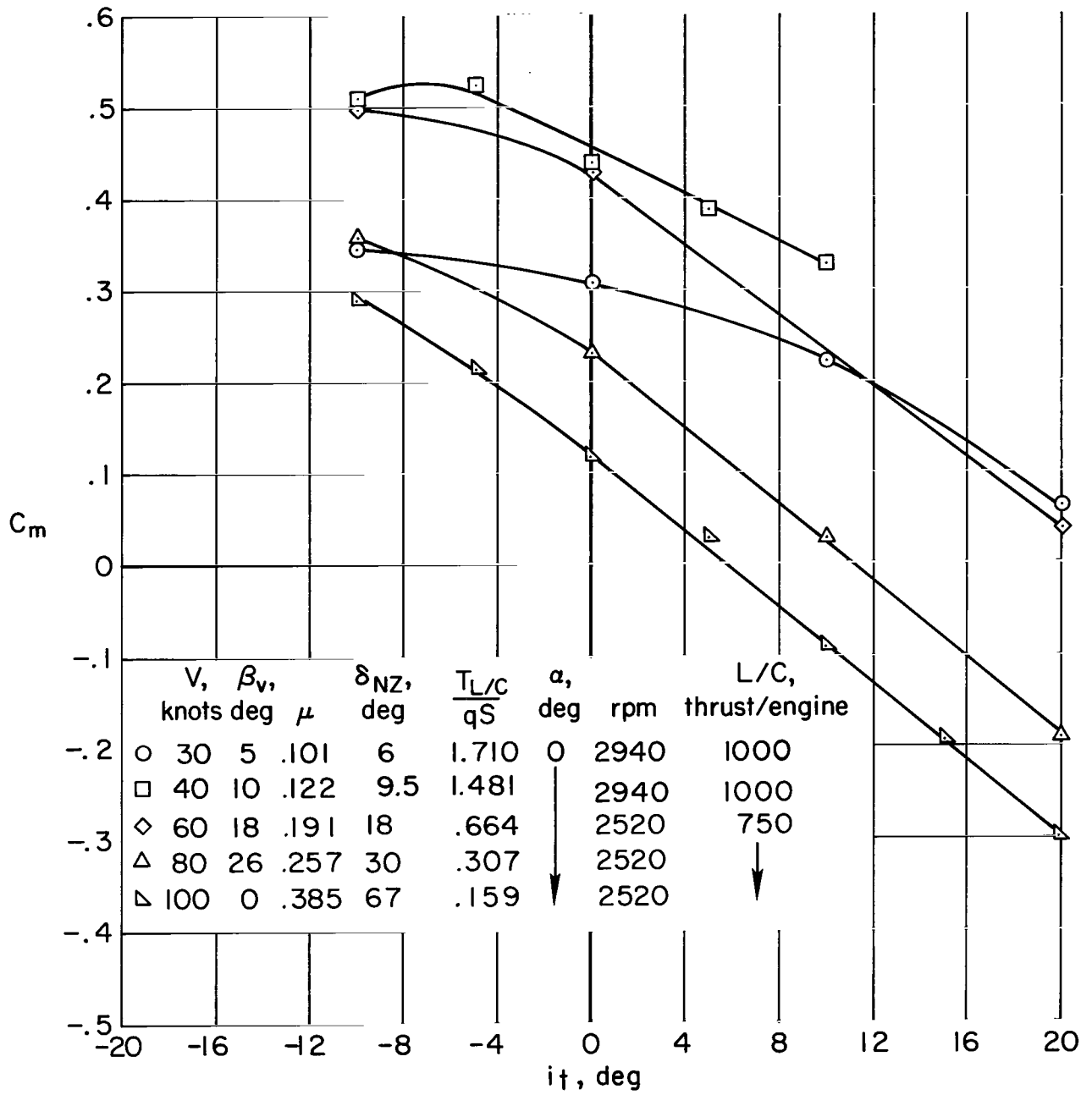


Figure 27.- Horizontal tail effectiveness; $\delta_f = 40^\circ$, six fans aft, lift-cruise nozzles on.

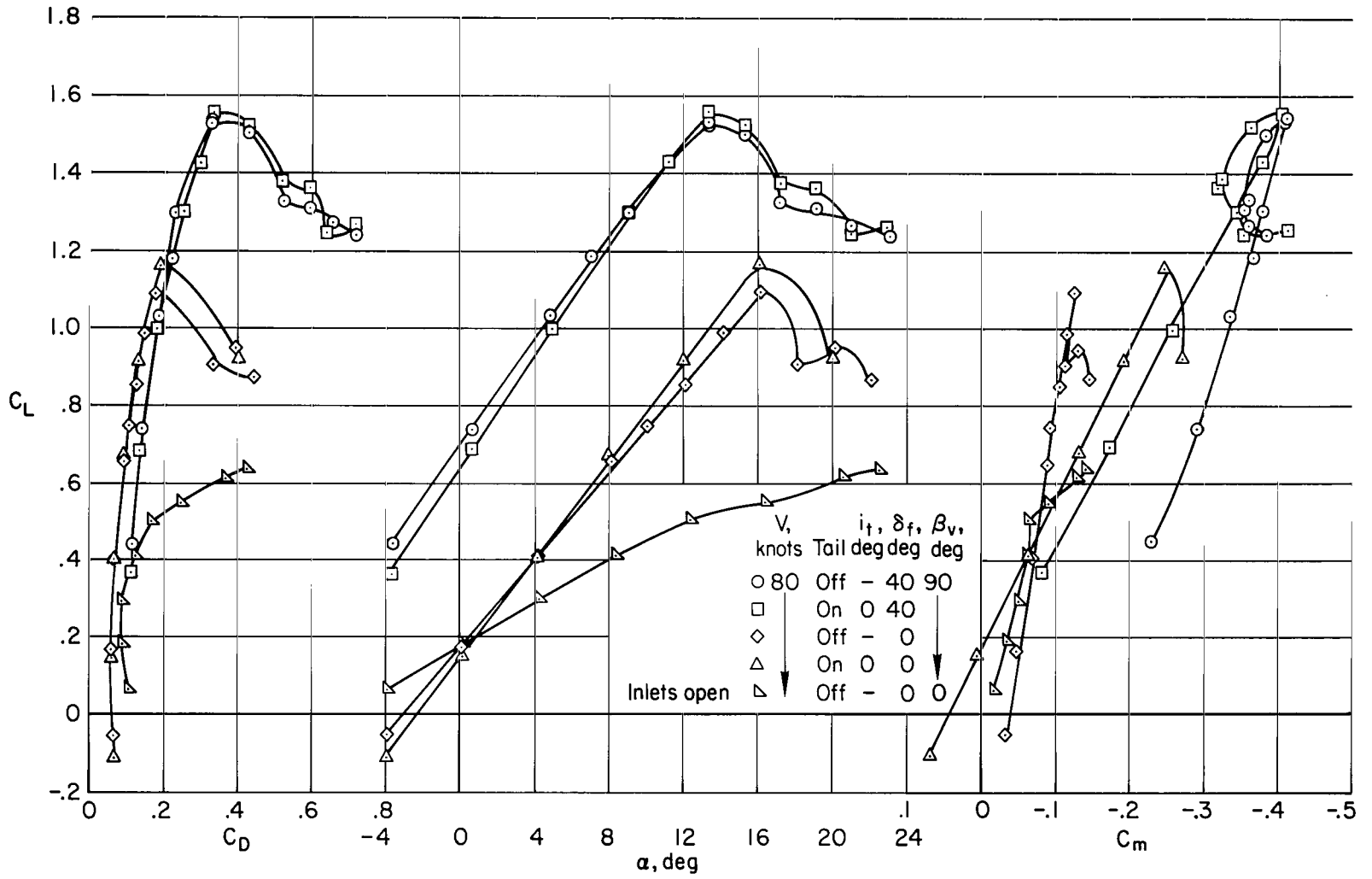


Figure 28.- Longitudinal characteristics with power off; lift-cruise nozzles off.

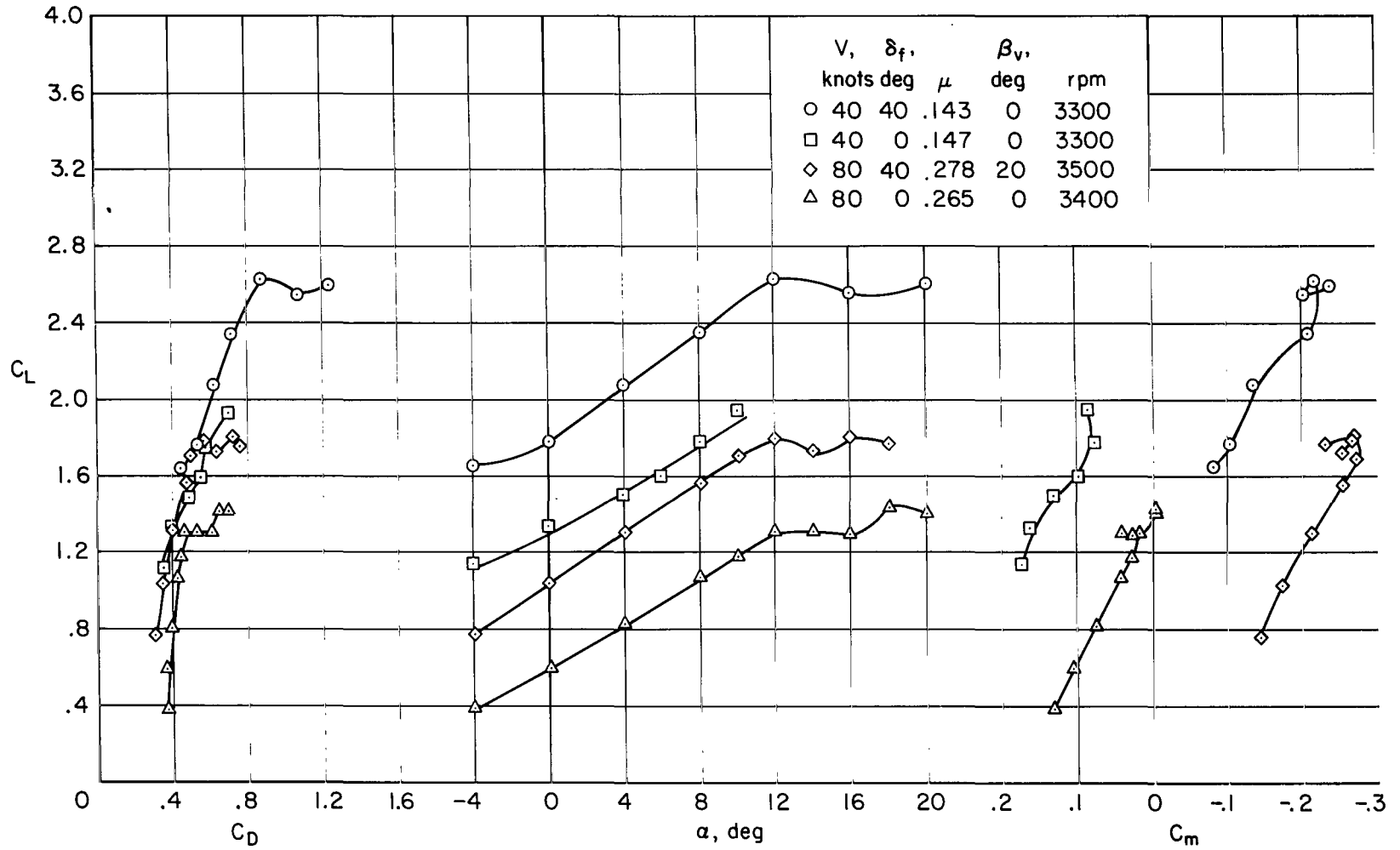
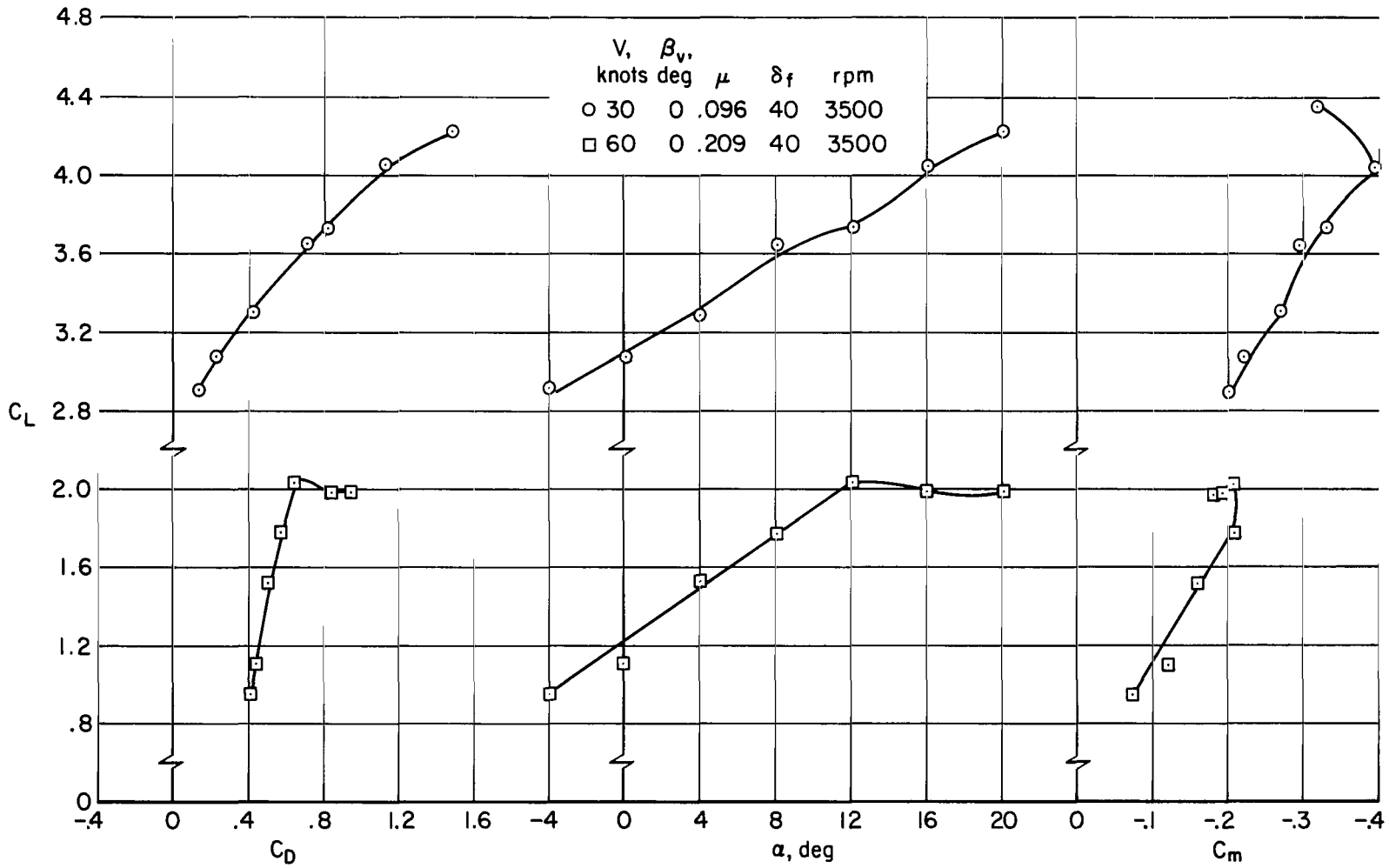
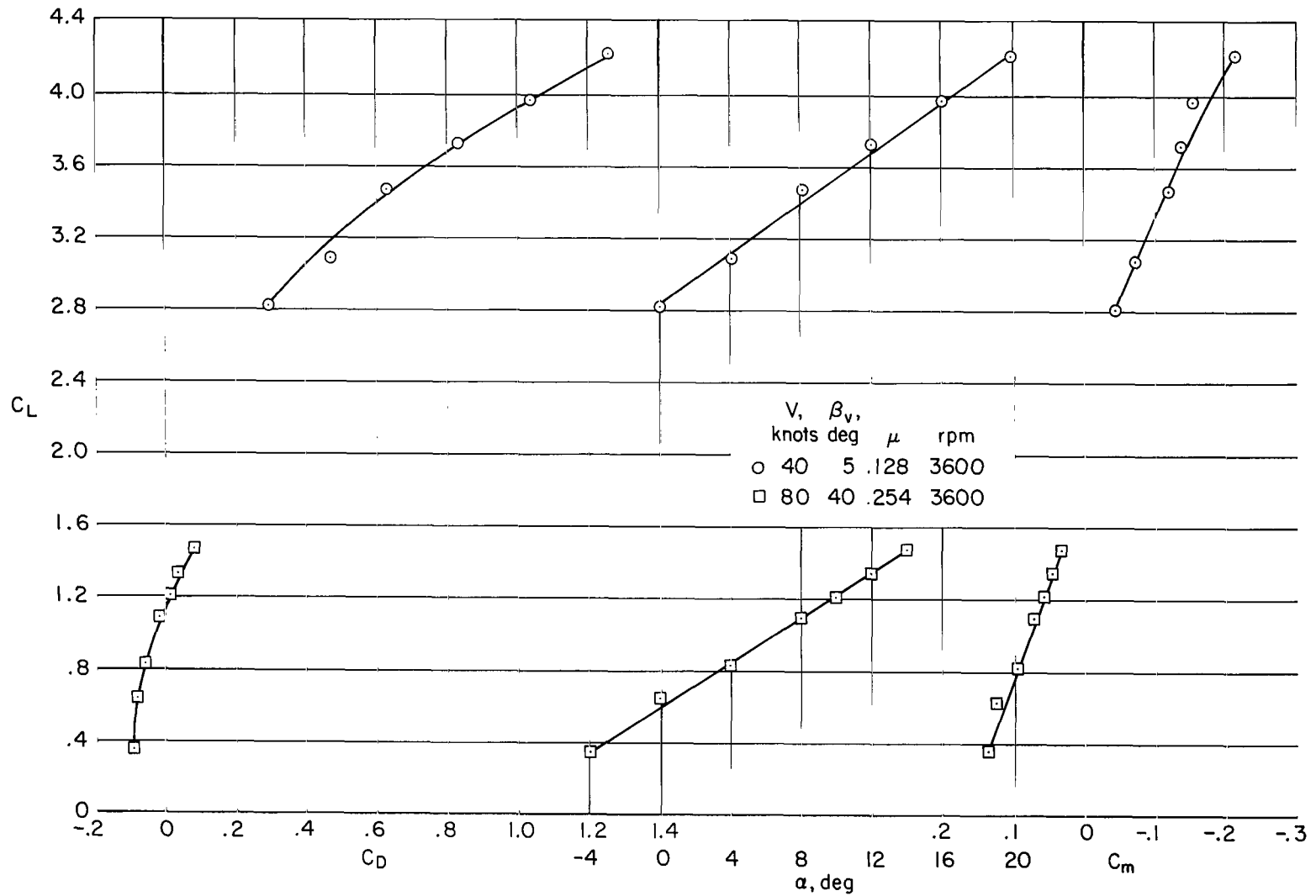
(a) $V = 40, 80$ knots .

Figure 29.- Longitudinal characteristics with two fans aft (inboard); tail off, lift-cruise nozzles off.



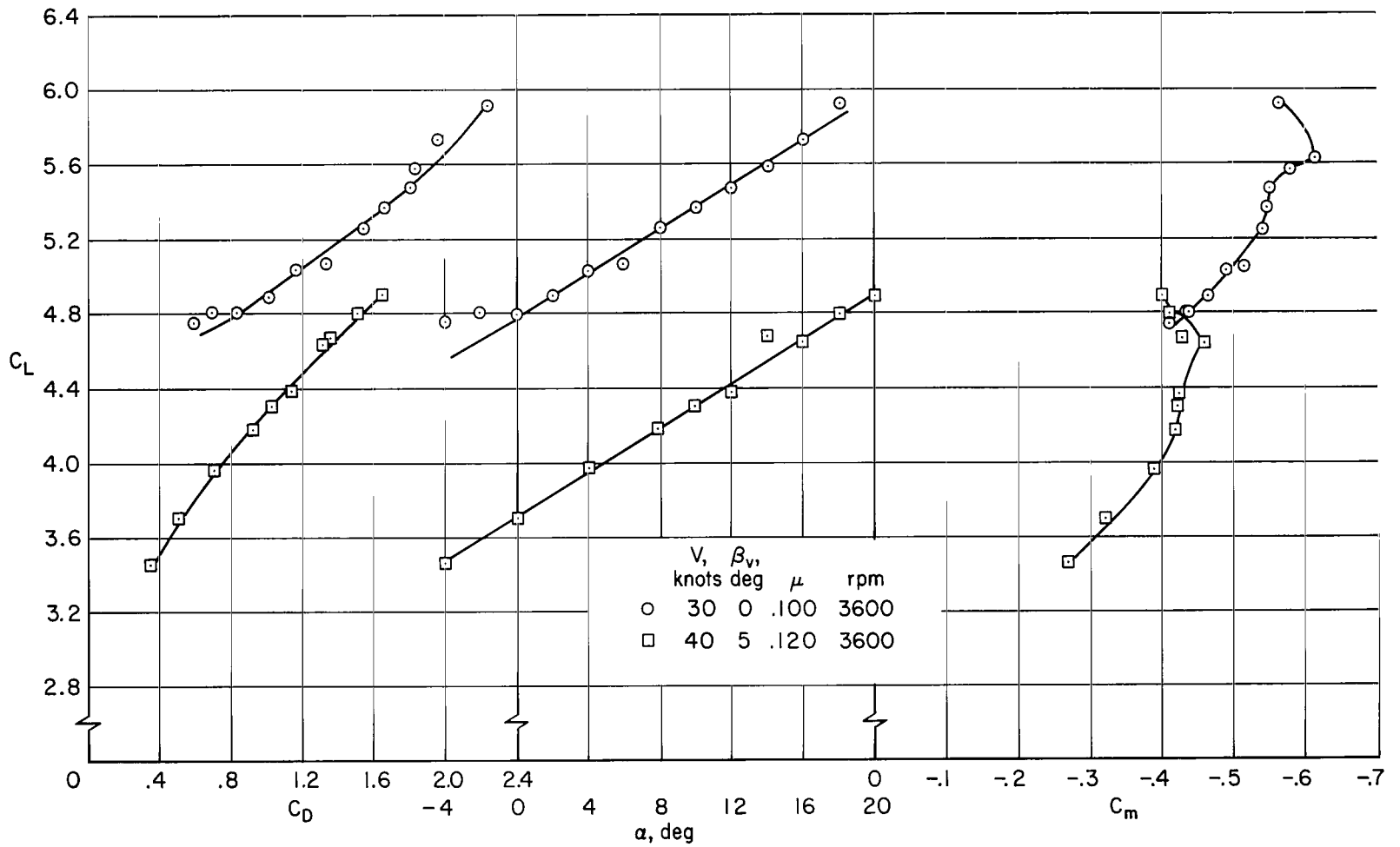
(b) $V = 30, 60$ knots.

Figure 29.- Concluded.



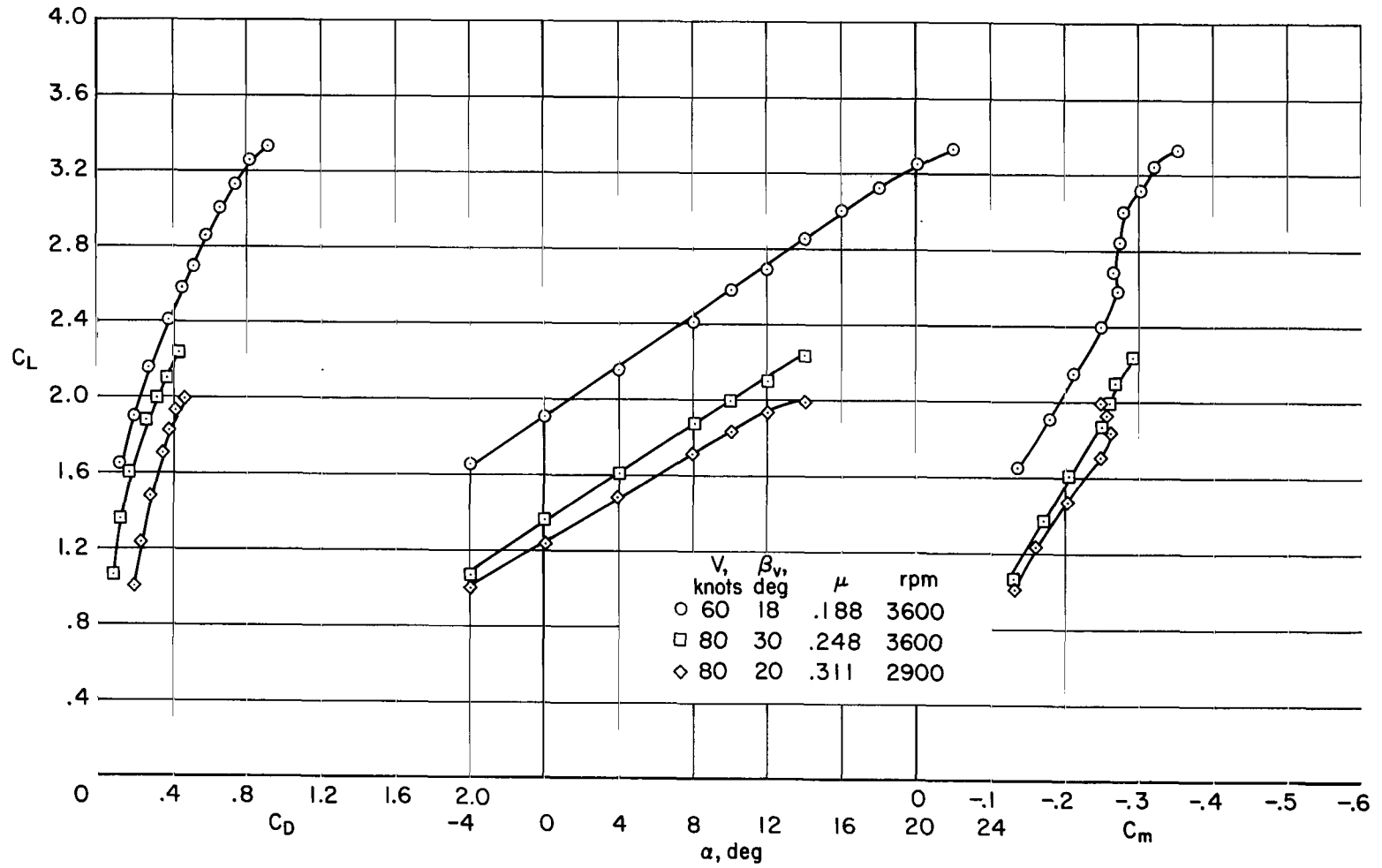
(a) $\delta_f = 0^\circ$

Figure 30.- Longitudinal characteristics with four fans aft (inboard and center); tail off, lift-cruise nozzles off.



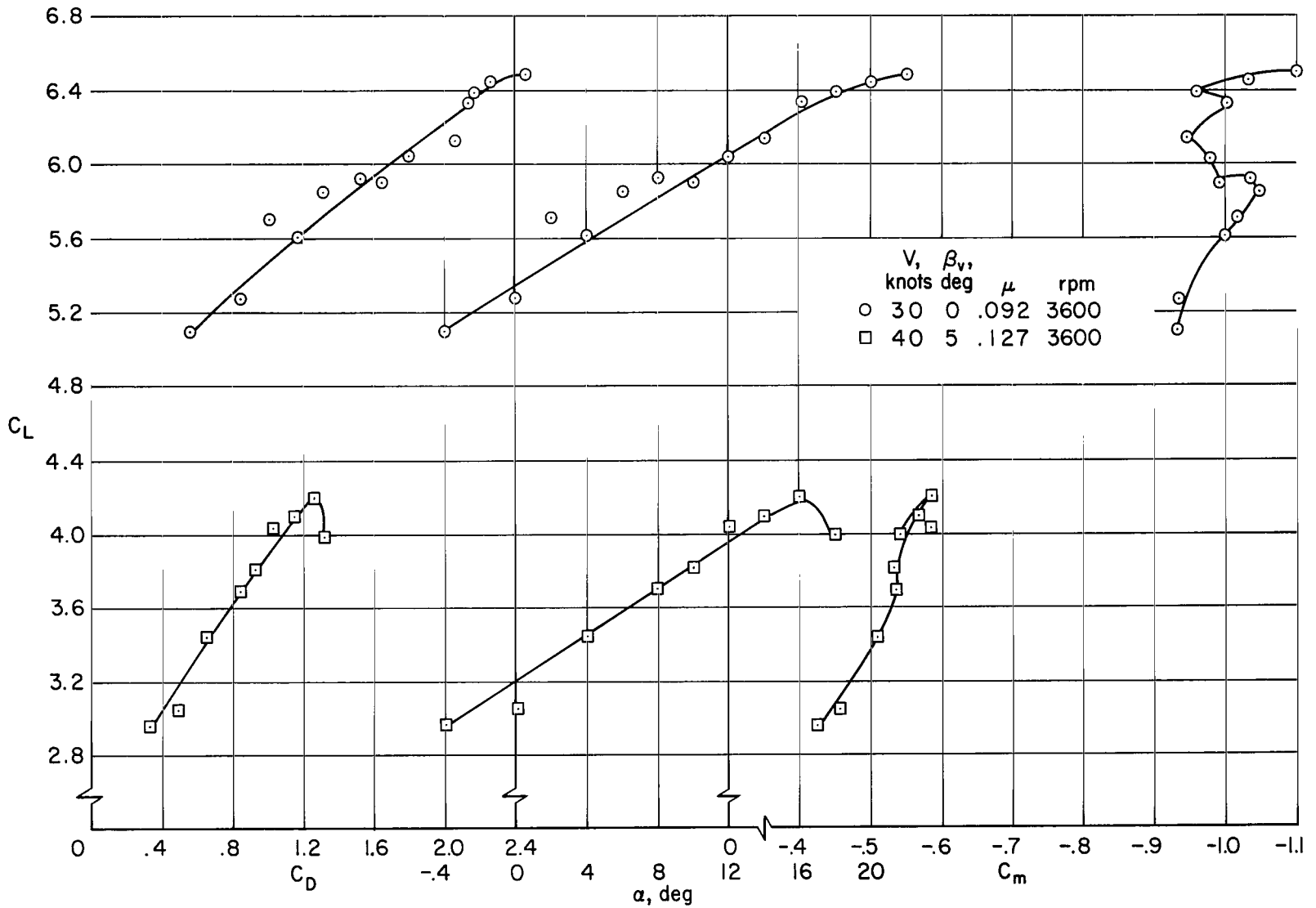
(b) $\delta_f = 40^\circ$

Figure 30.- Continued.



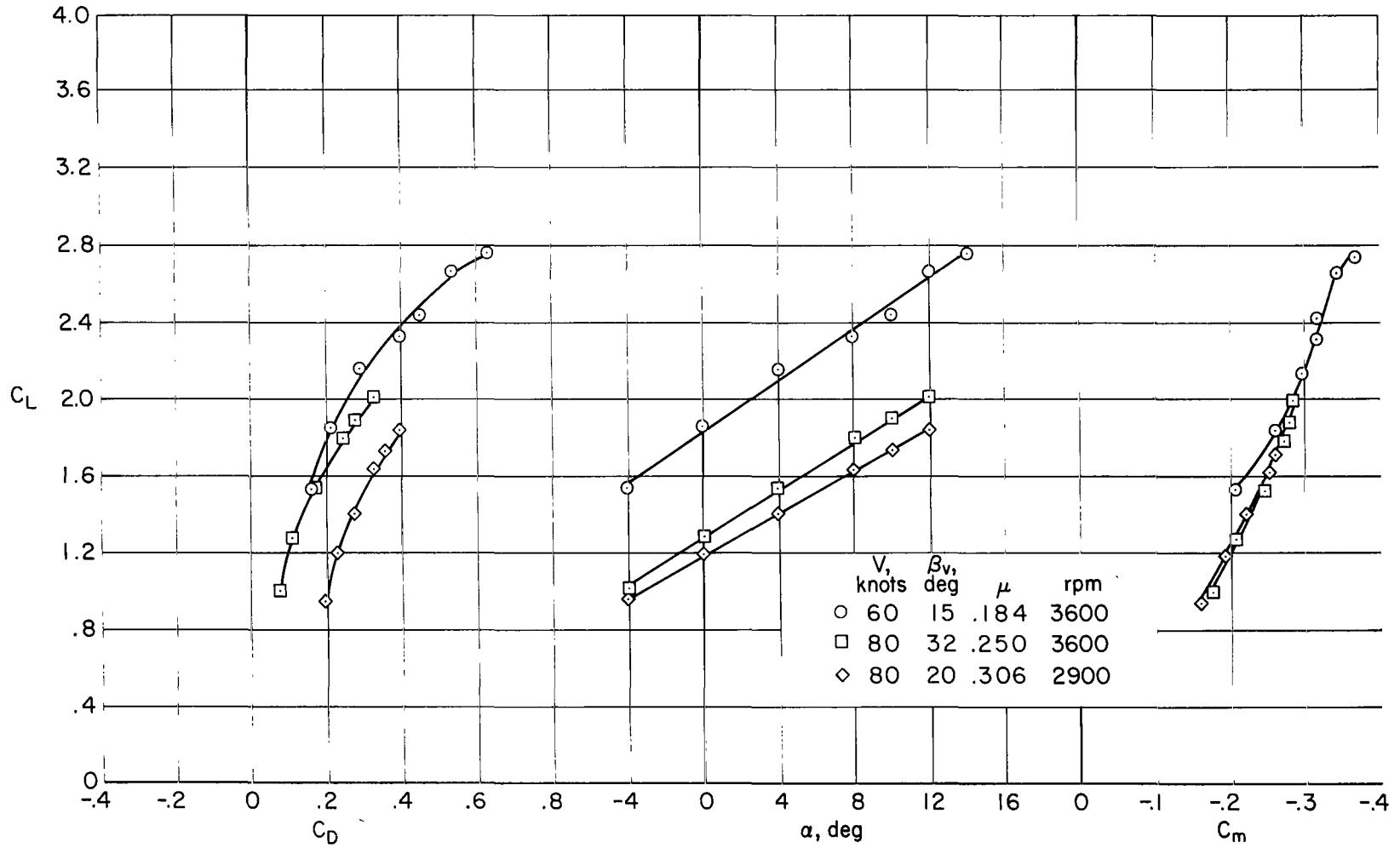
(c) $\delta_f = 40^\circ$

Figure 30.- Concluded.



(a) $V = 30, 40$ knots.

Figure 31.- Longitudinal characteristics with four fans aft (inboard and outboard); $\delta_F = 40^\circ$, tail off, lift-cruise nozzles off.



(b) $V = 60, 80$ knots .

Figure 31.- Concluded.

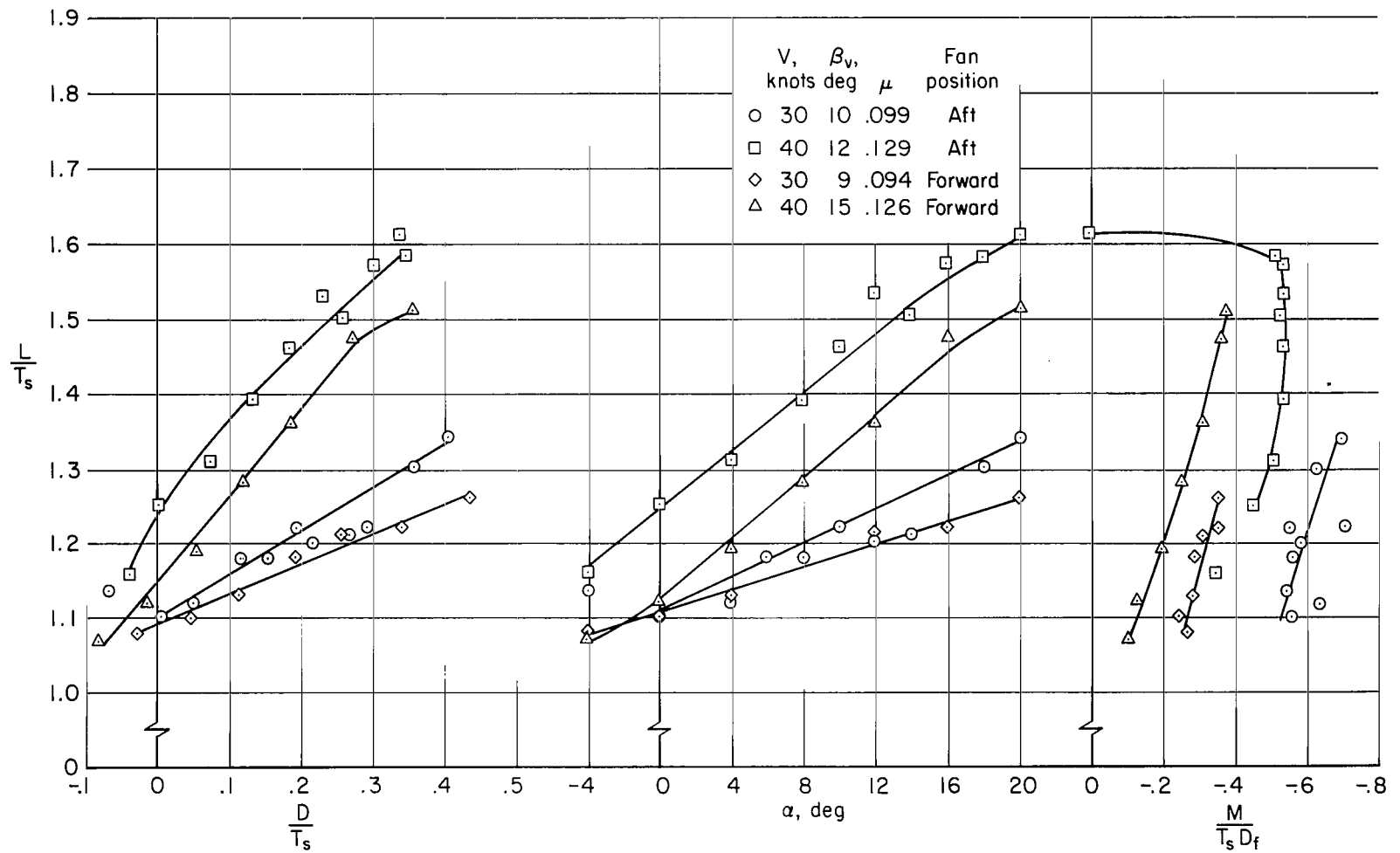
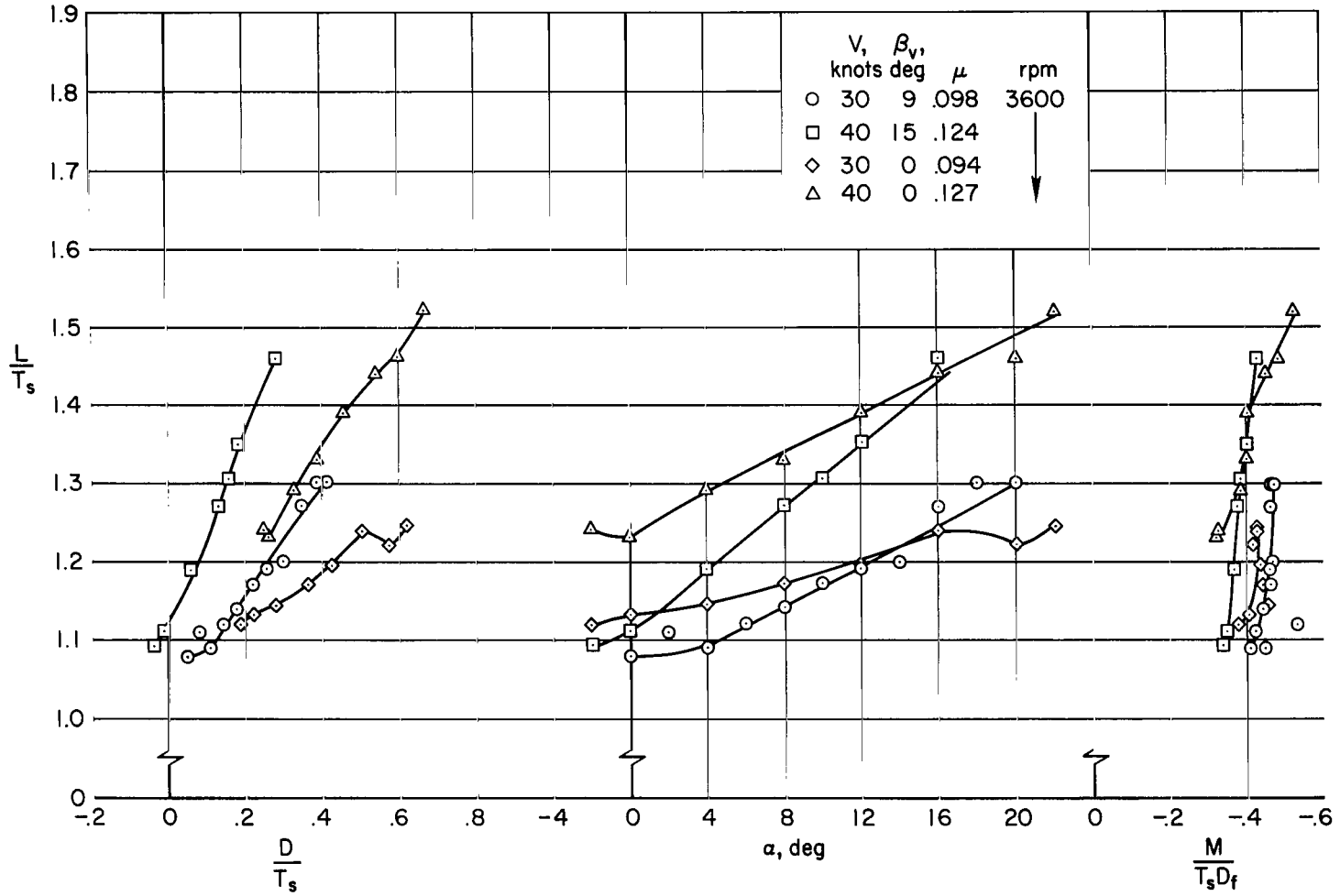
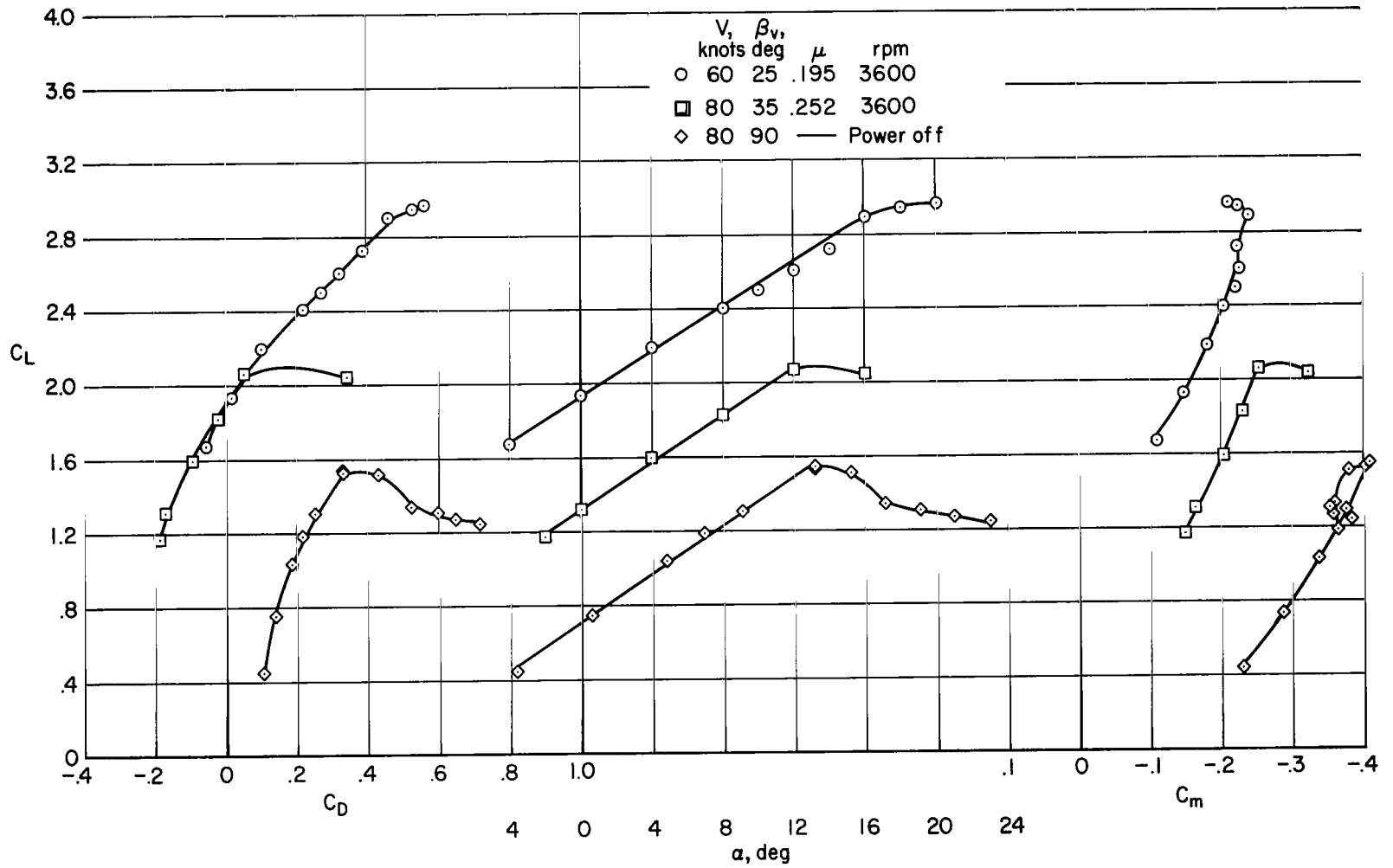


Figure 32.- Longitudinal characteristics with six fans; $\delta_f = 40^\circ$, tail on, $i_t = 0^\circ$, 3600 rpm, lift-cruise nozzles off.



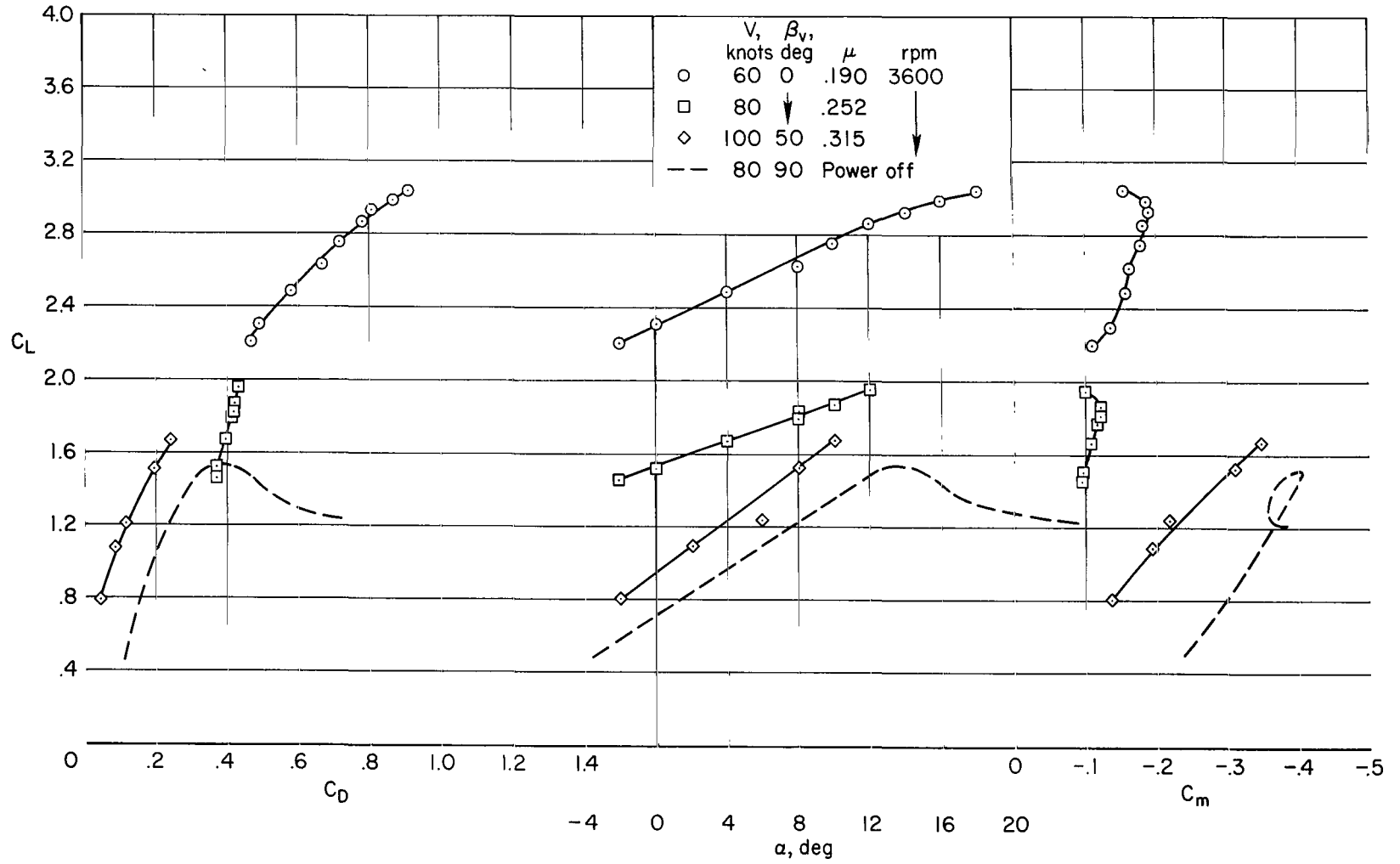
(a) Tail off.

Figure 33.- Longitudinal characteristics with six fans forward; $\delta_F = 40^\circ$, lift-cruise nozzles off.



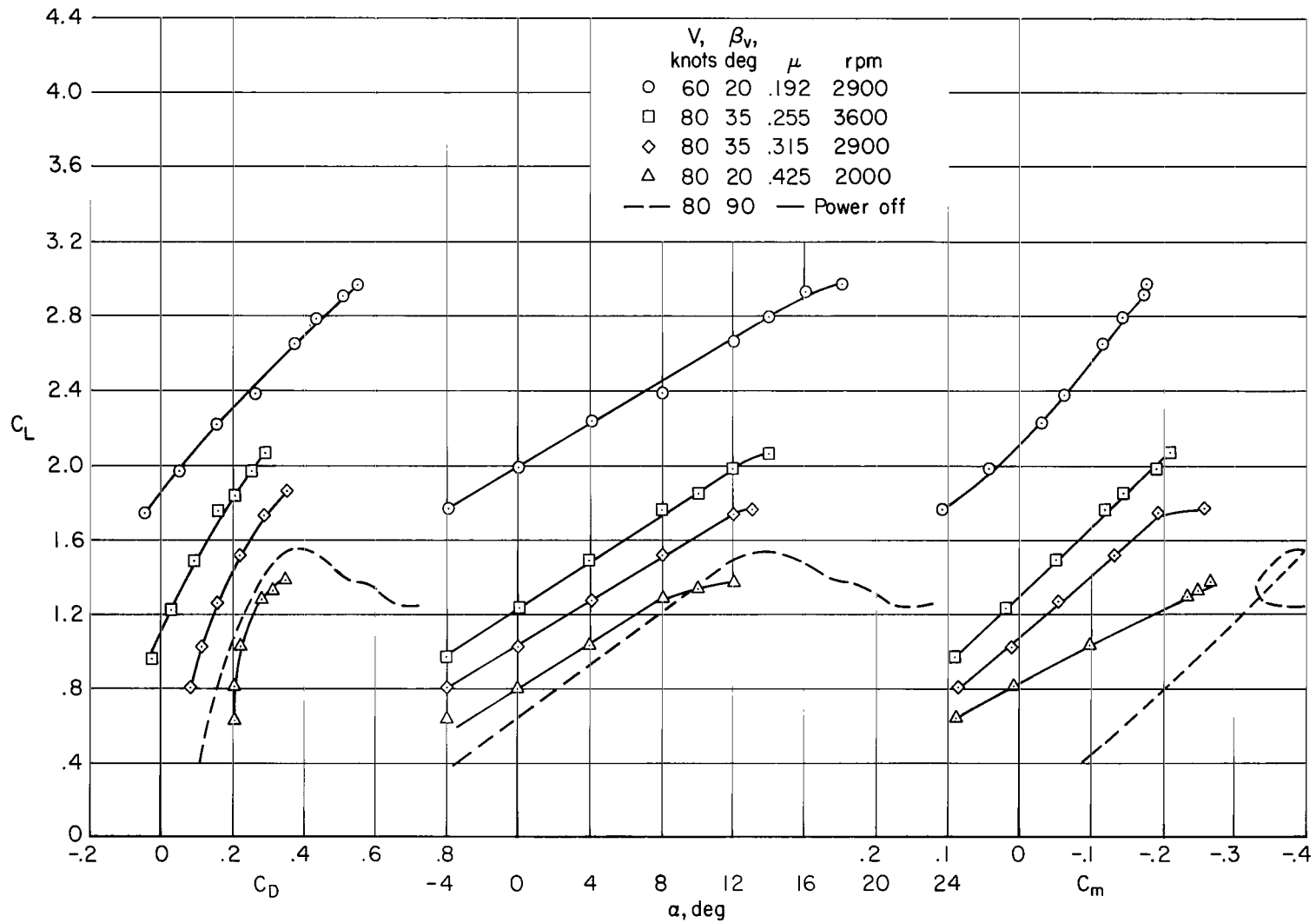
(b) Tail off.

Figure 33.- Continued.



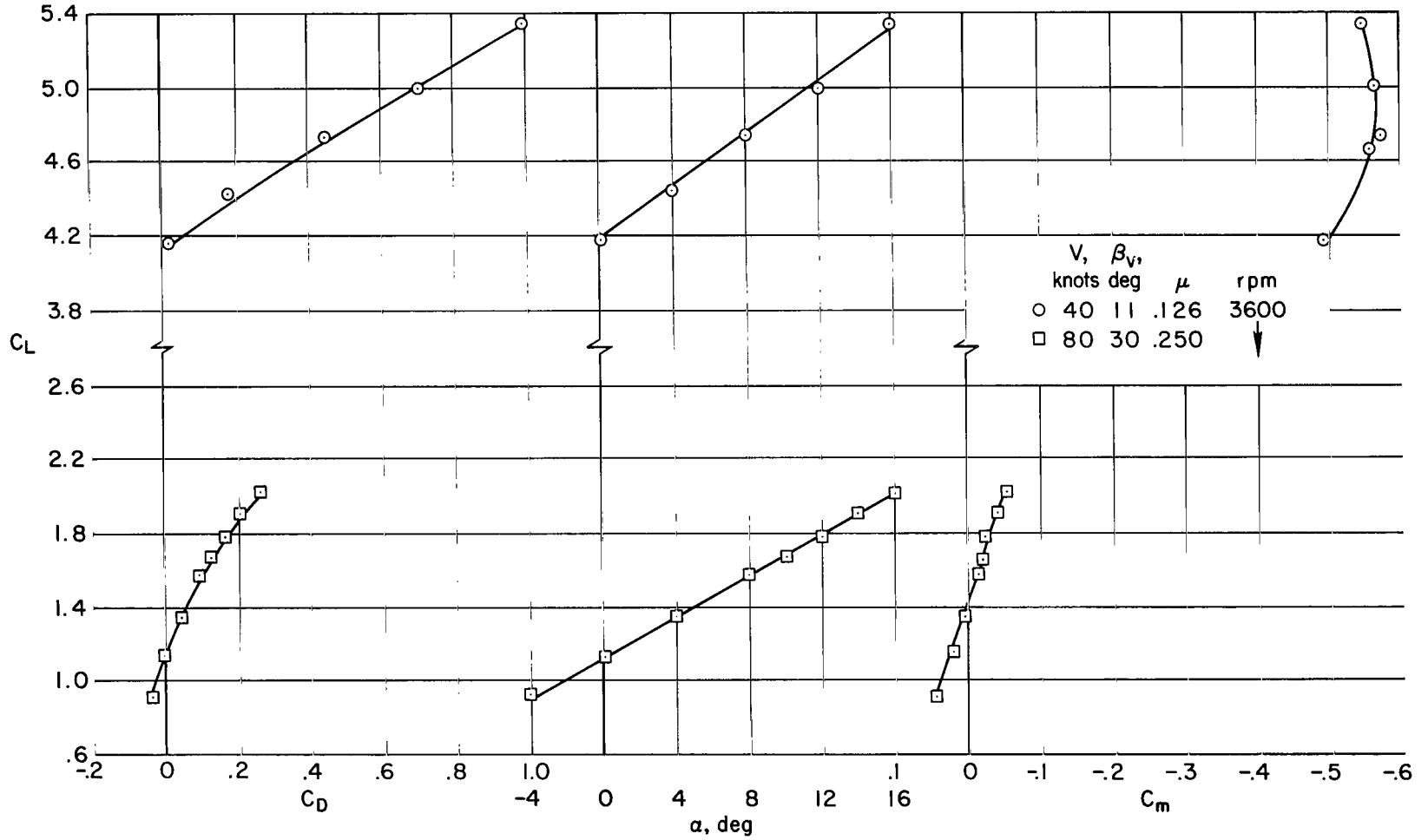
(c) Tail off.

Figure 33.- Continued.



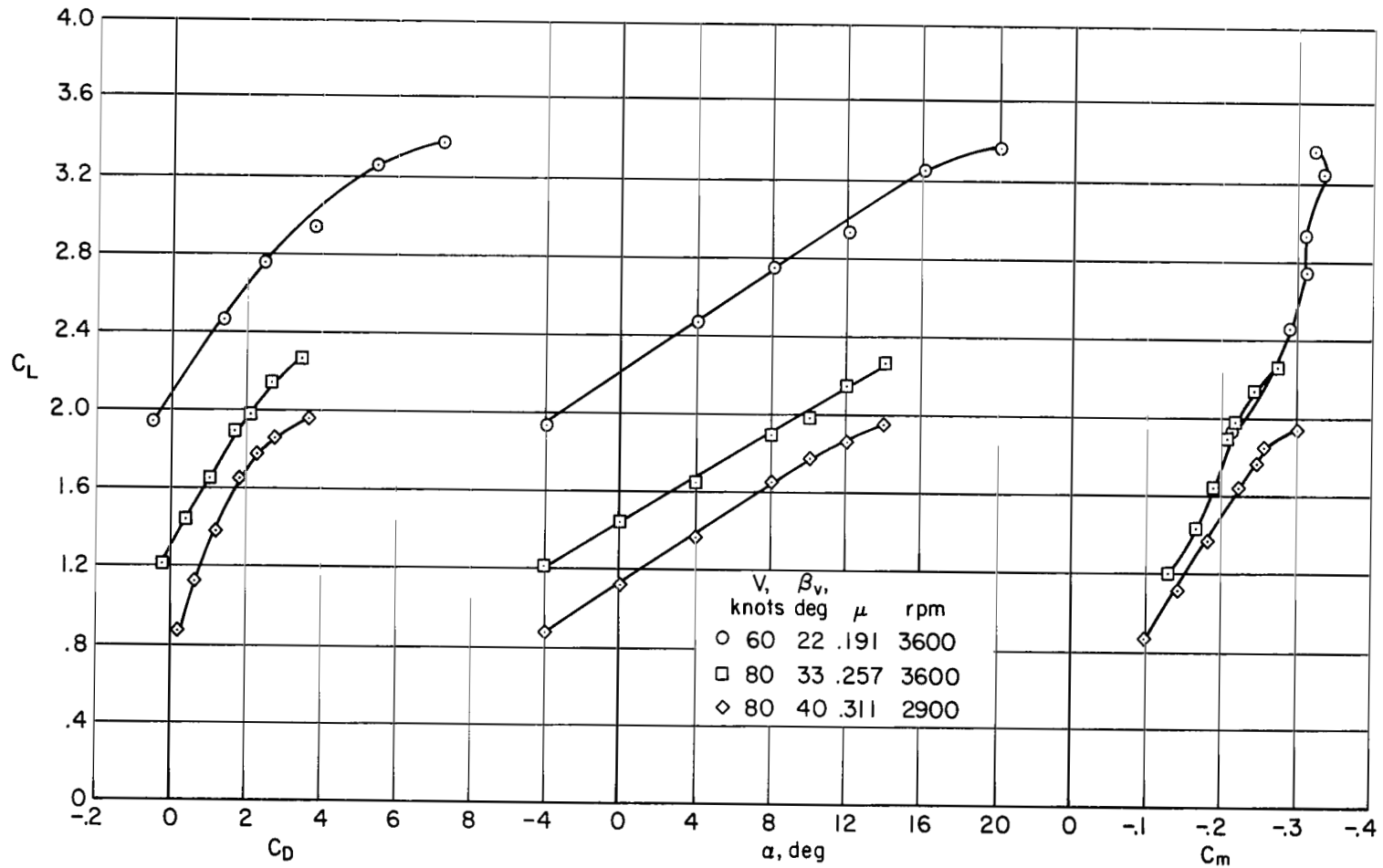
(d) Tail on, $i_t = 0^\circ$.

Figure 33.- Concluded.



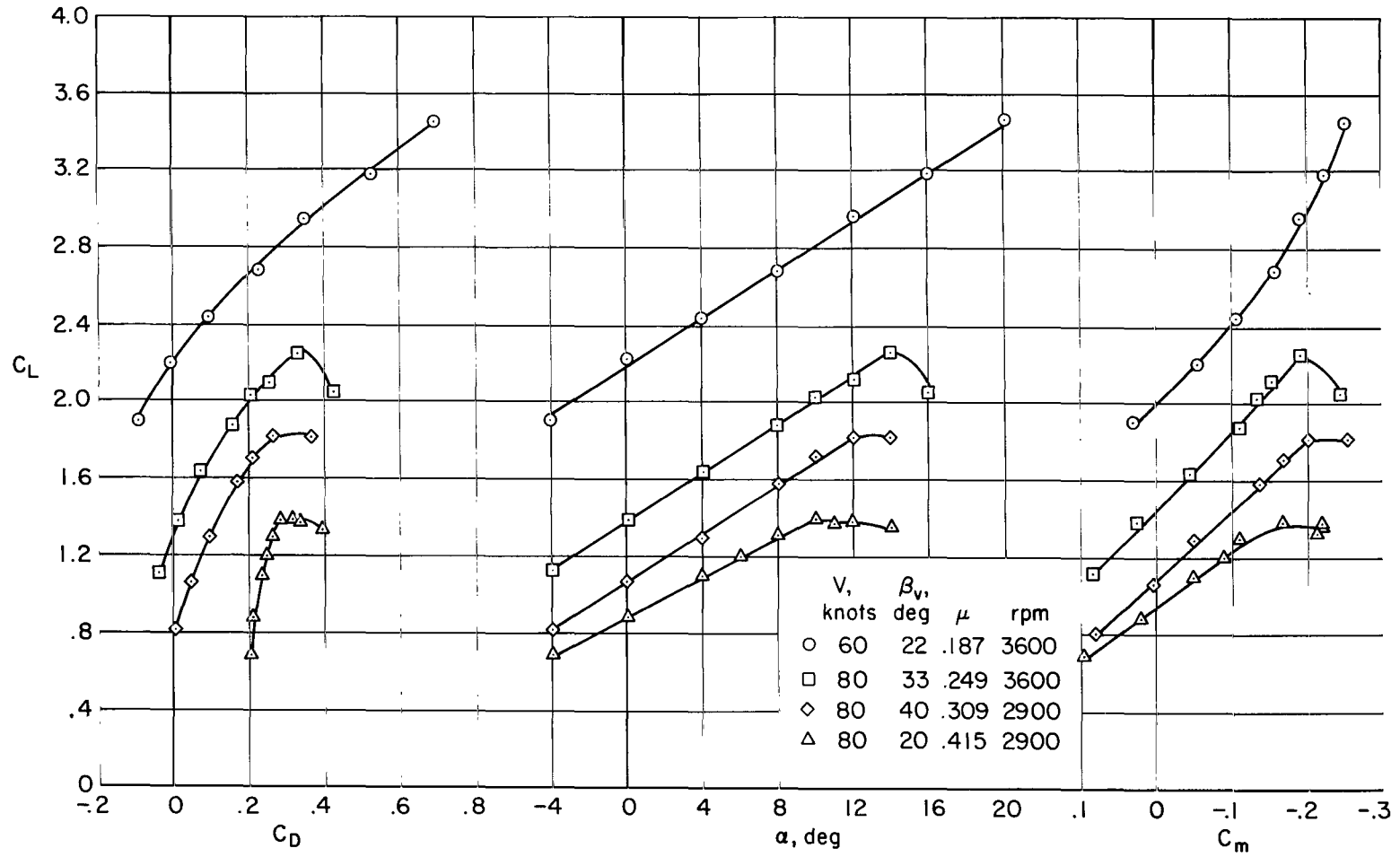
(a) Tail off, $\delta_f = 0^\circ$.

Figure 34.- Longitudinal characteristics with six fans aft; lift-cruise nozzles off.



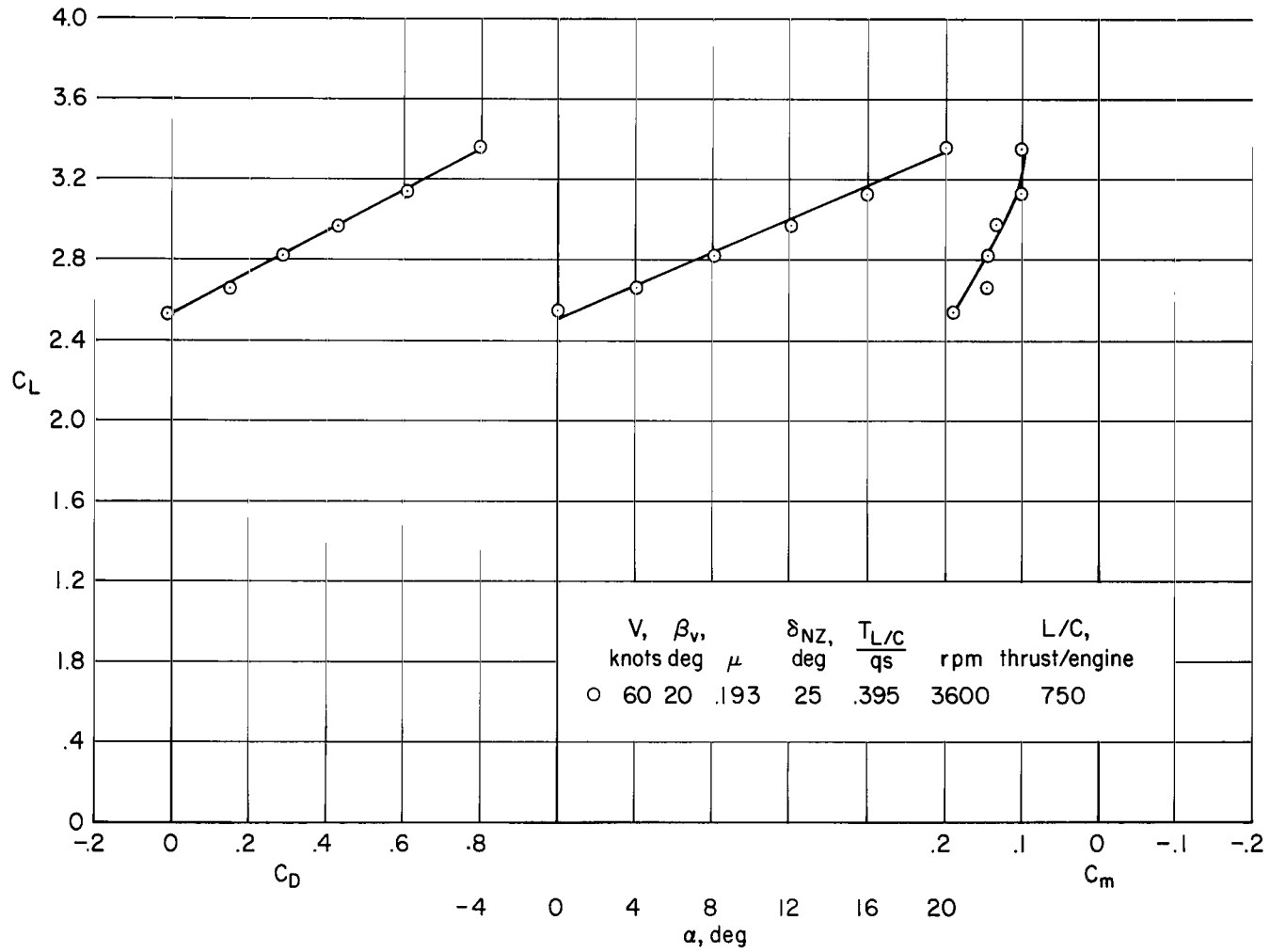
(b) Tail off, $\delta_f = 40^\circ$.

Figure 34.- Continued.



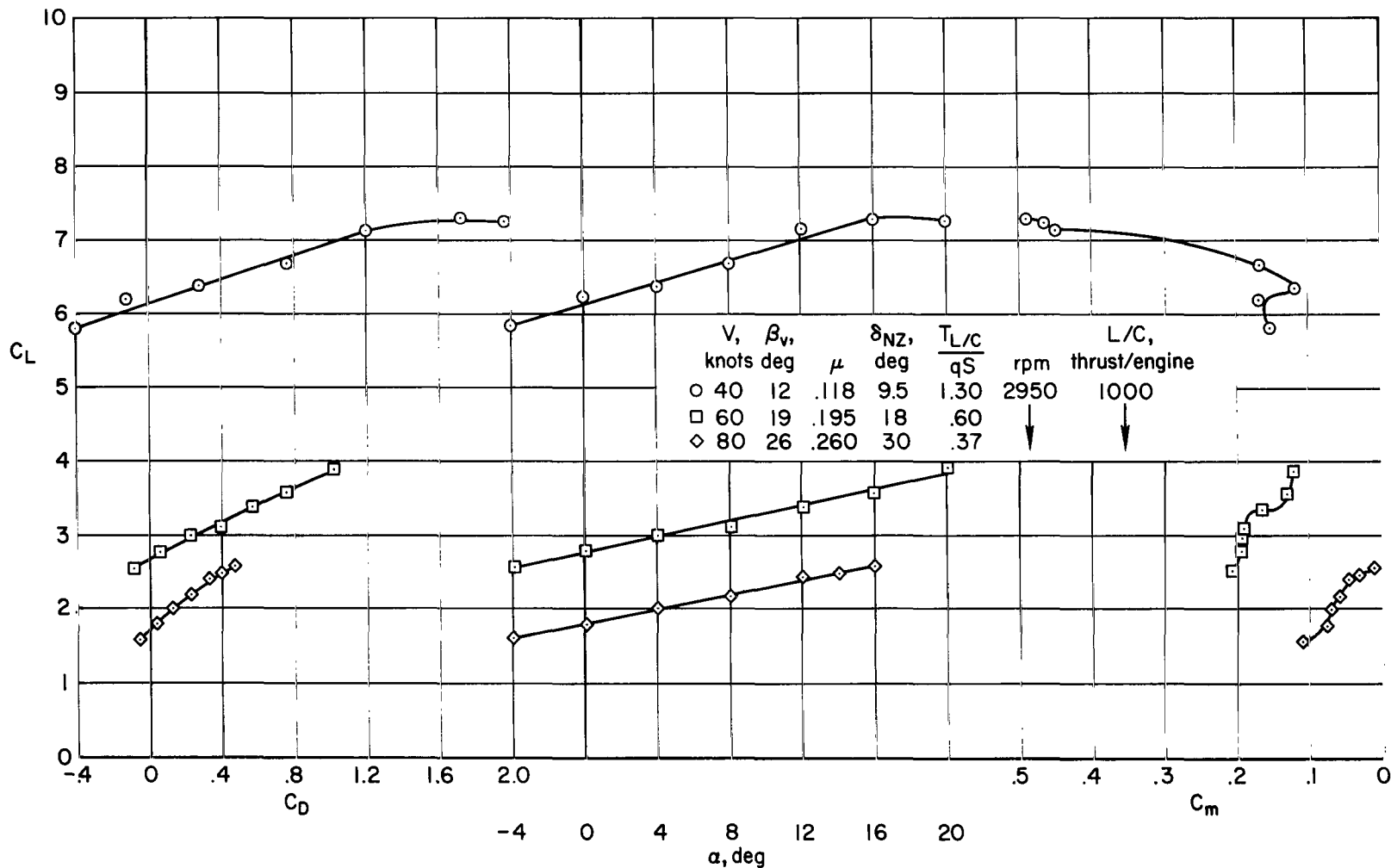
(c) Tail on, $i_t = 0^\circ$, $\delta_f = 40^\circ$.

Figure 34.- Concluded.



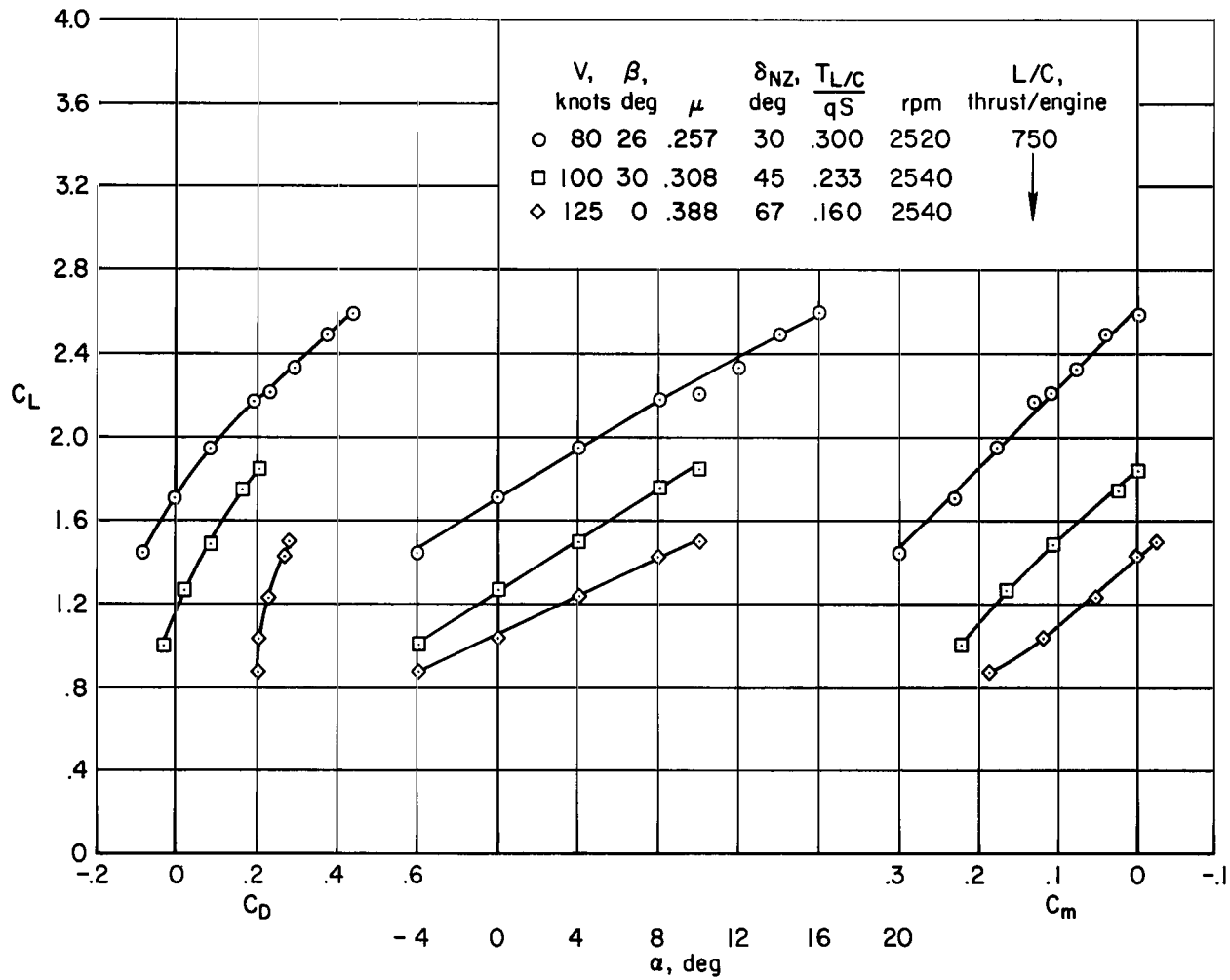
(a) Fans forward, tail off.

Figure 35.- Longitudinal characteristics with six fans; $\delta_F = 40^\circ$, lift-cruise nozzles on.



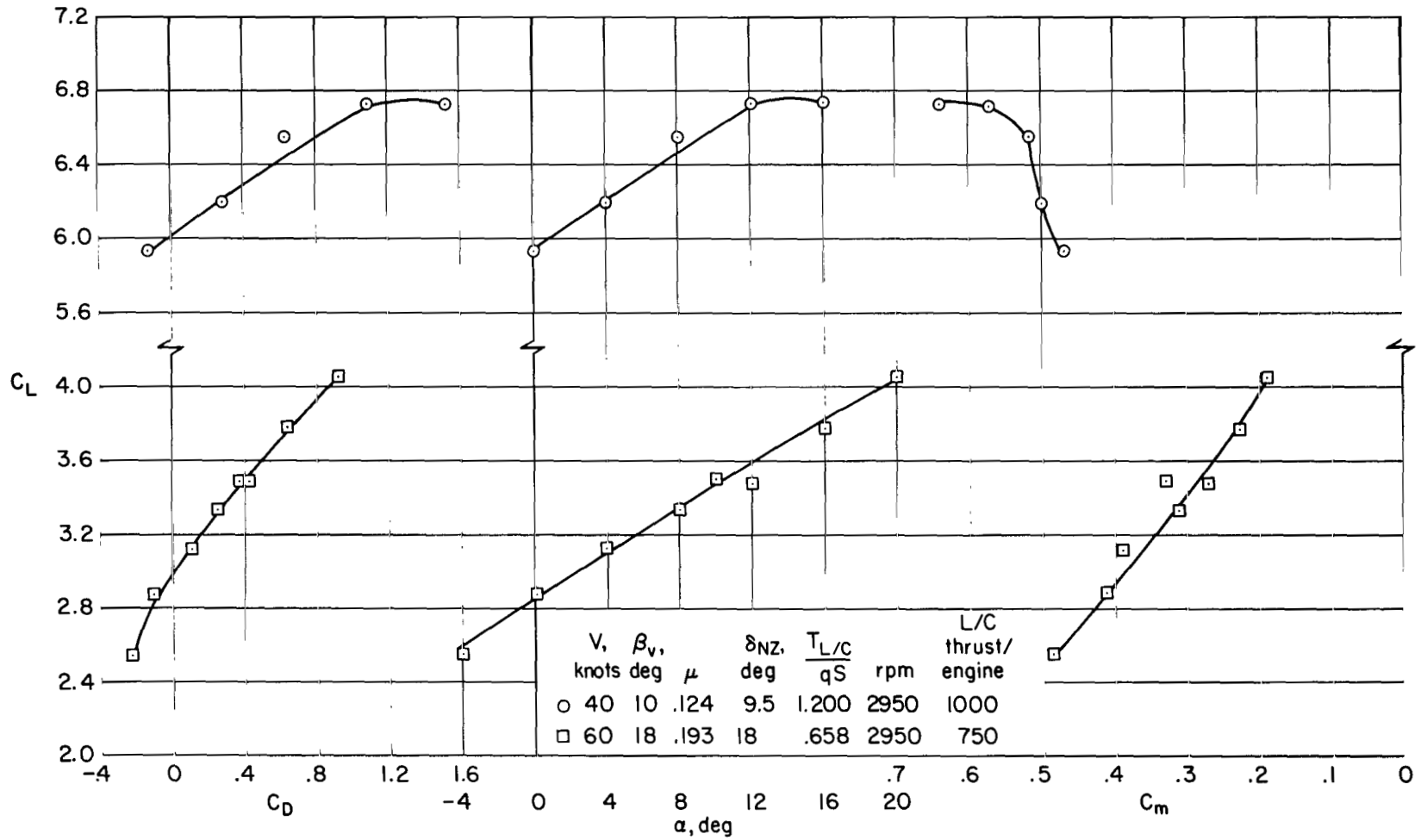
(b) Fans aft, tail off.

Figure 35.- Continued.



(c) Fans aft, tail on, $i_t = 0^\circ$.

Figure 35.- Continued.



(d) Fans aft, tail on, $i_t = 0^\circ$.

Figure 35.- Concluded.

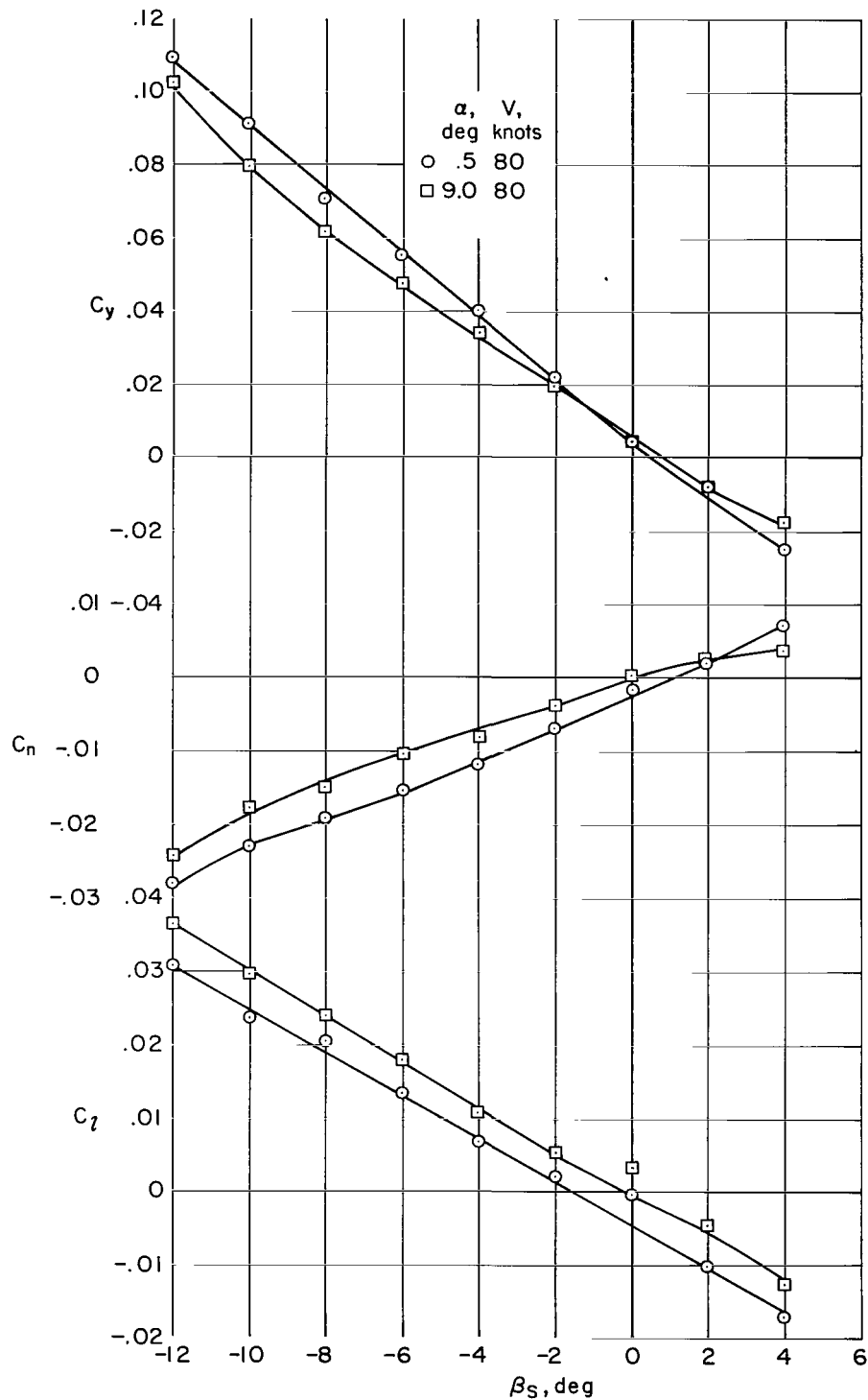
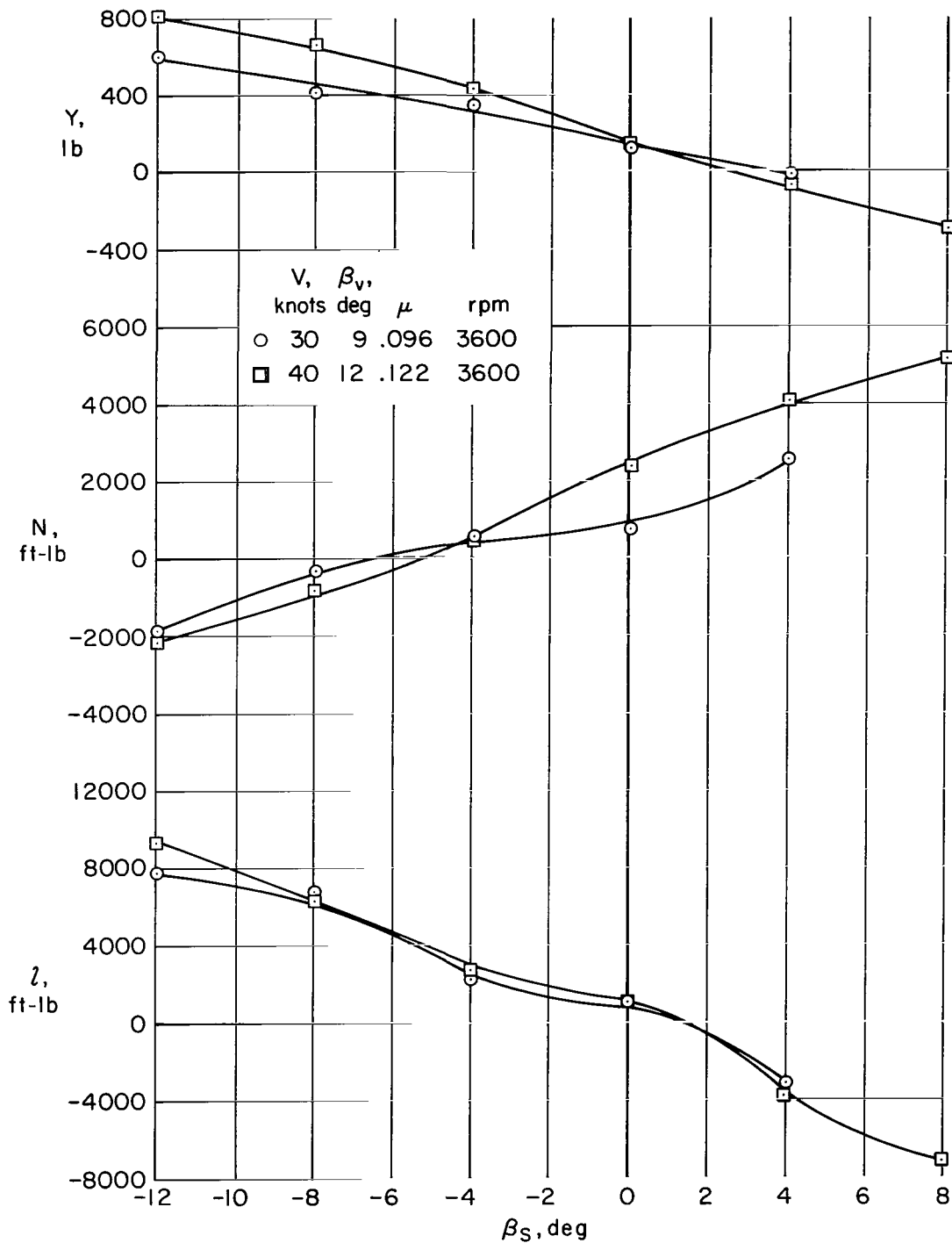
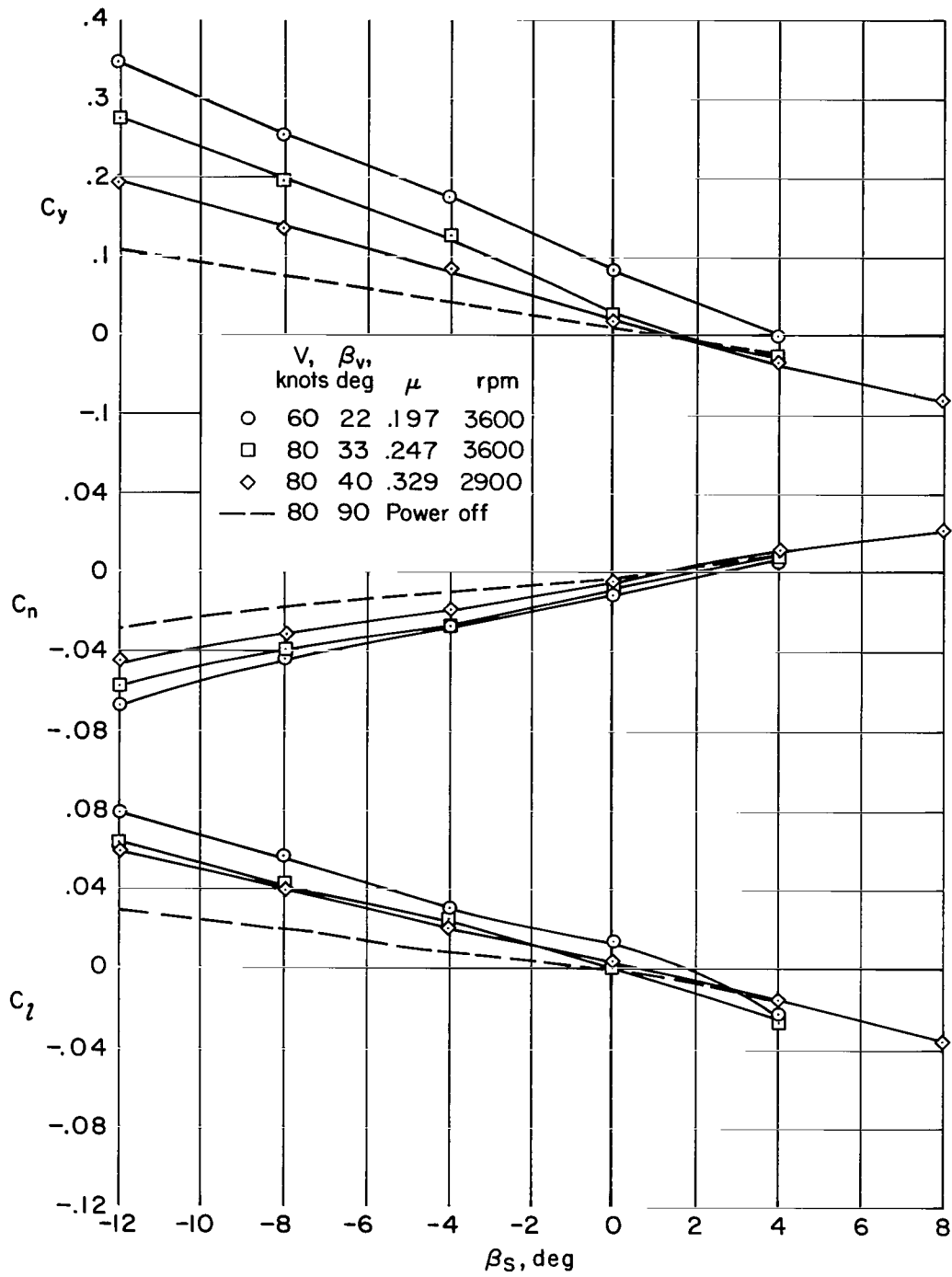


Figure 36.- Lateral-directional characteristics with power off; $\beta_v = 90^\circ$, $\delta_f = 40^\circ$, tail on, $i_t = 0^\circ$, fan inlets sealed, lift-cruise nozzles off.



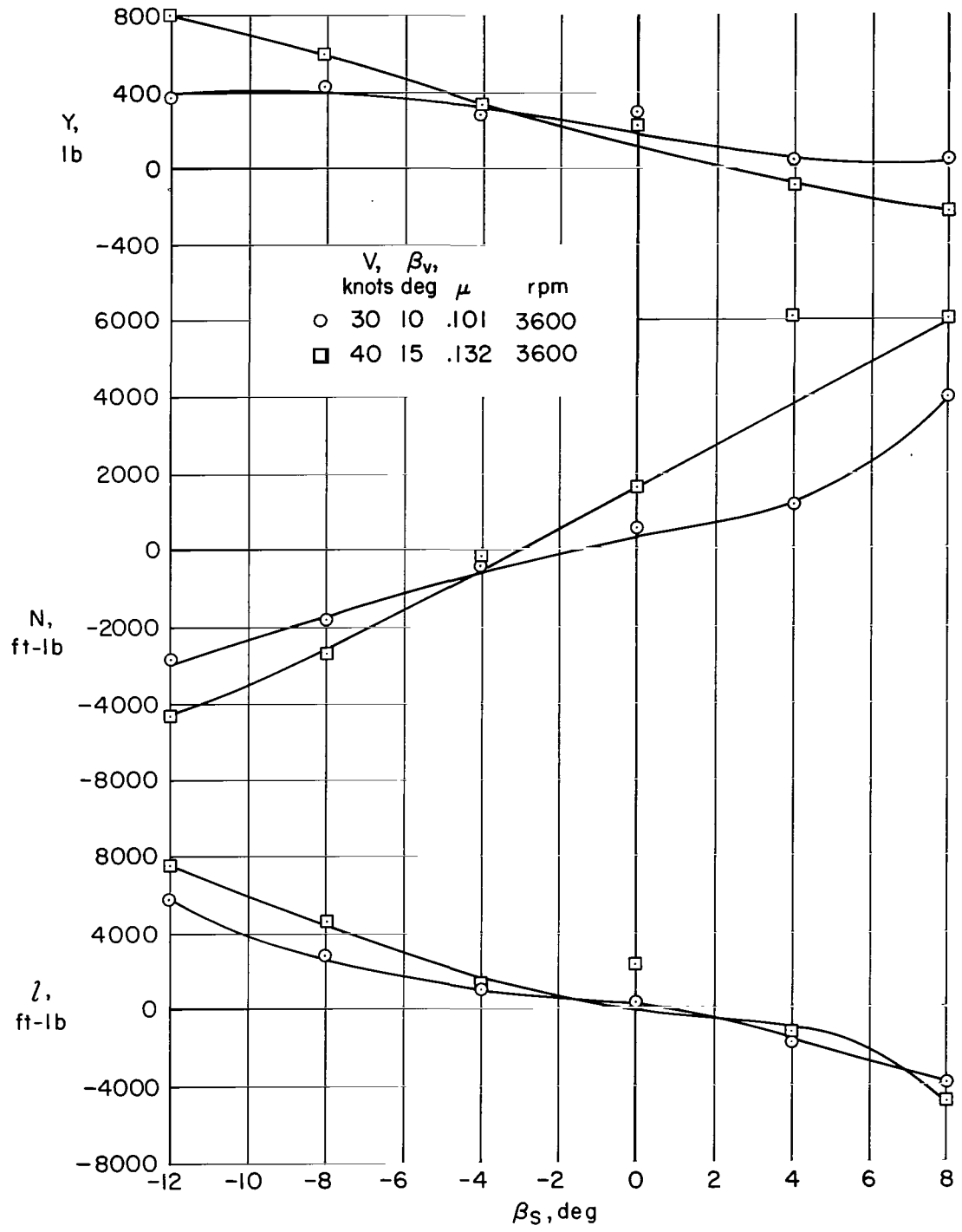
(a) $\alpha = 0^\circ$; forces and moments versus sideslip.

Figure 37.- Lateral-directional characteristics with six fans aft; $\delta_f = 40^\circ$, tail on, $i_t = 0^\circ$, lift-cruise nozzles off.



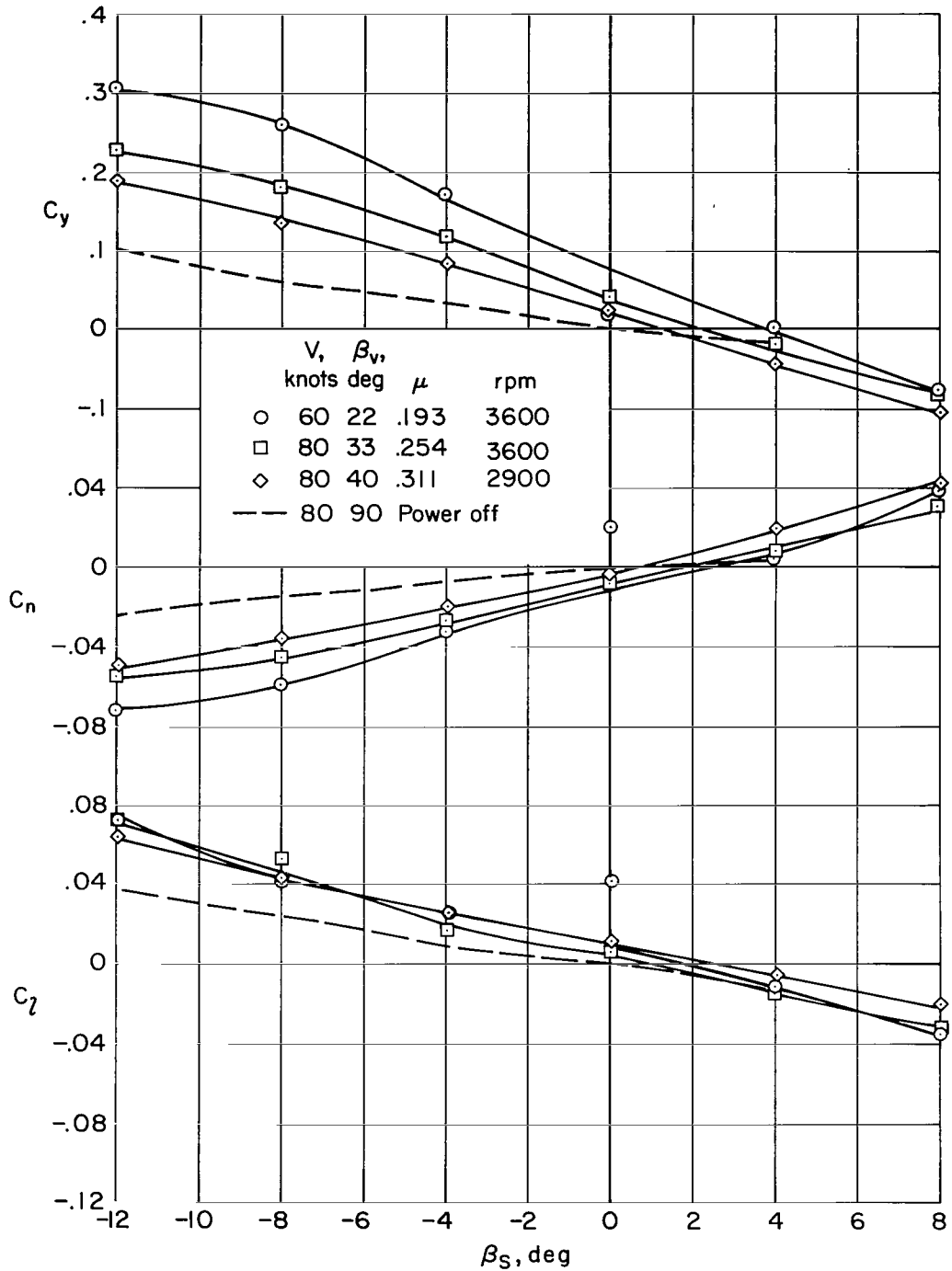
(b) $\alpha = 0^\circ$; C_y , C_n , C_l versus sideslip.

Figure 37.- Continued.



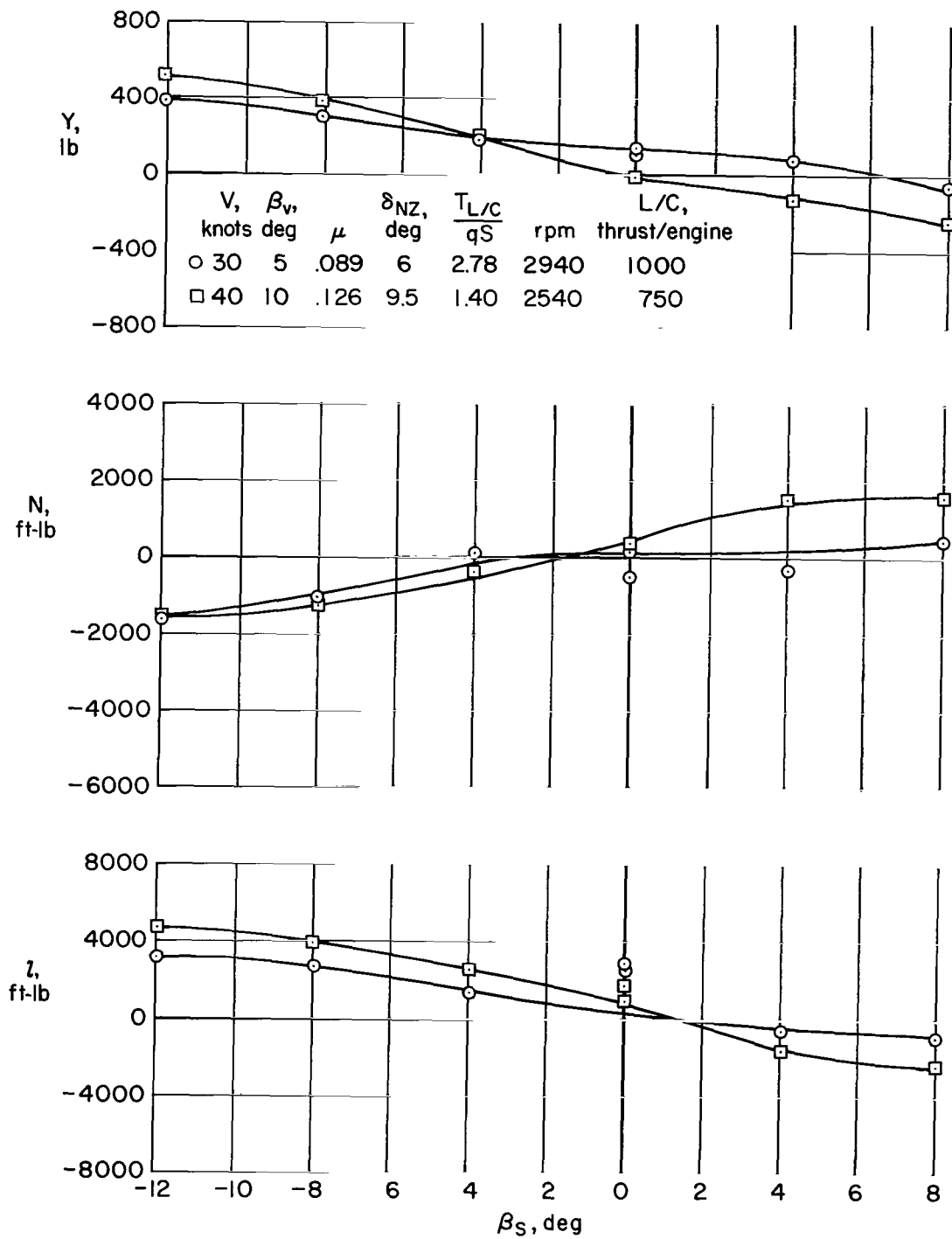
(c) $\alpha = 8^\circ$; forces and moments versus sideslip.

Figure 37.- Continued.



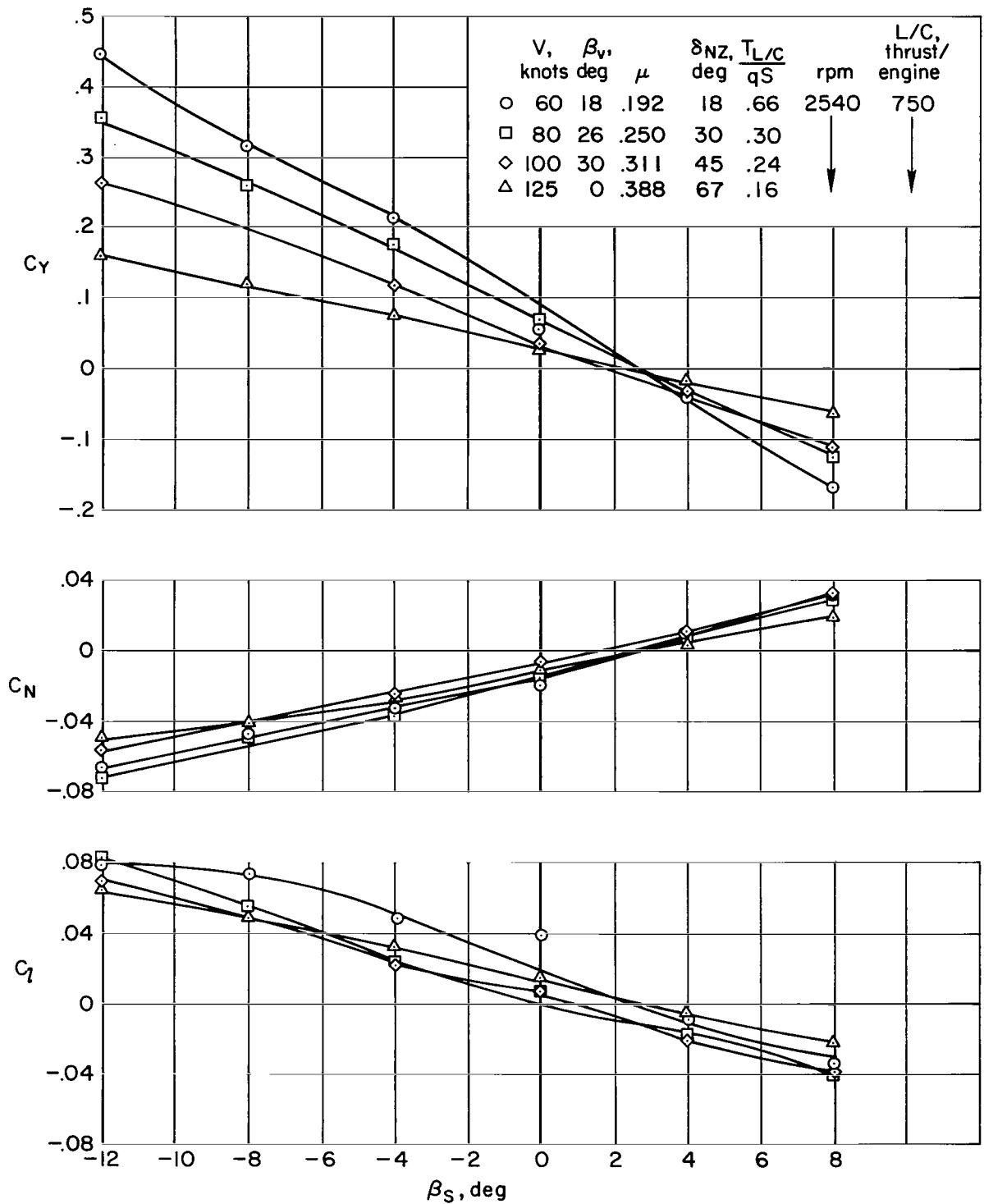
(d) $\alpha = 8^\circ$; C_y , C_n , C_l versus sideslip.

Figure 37.- Concluded.



(a) Forces and moments versus sideslip.

Figure 38.- Lateral-directional characteristics with six fans aft; $\alpha = 0^\circ$, $\delta_F = 40^\circ$, tail on, $i_t = 0^\circ$, lift-cruise nozzles on.



(b) C_y, C_n, C_l versus sideslip.

Figure 38.- Concluded.

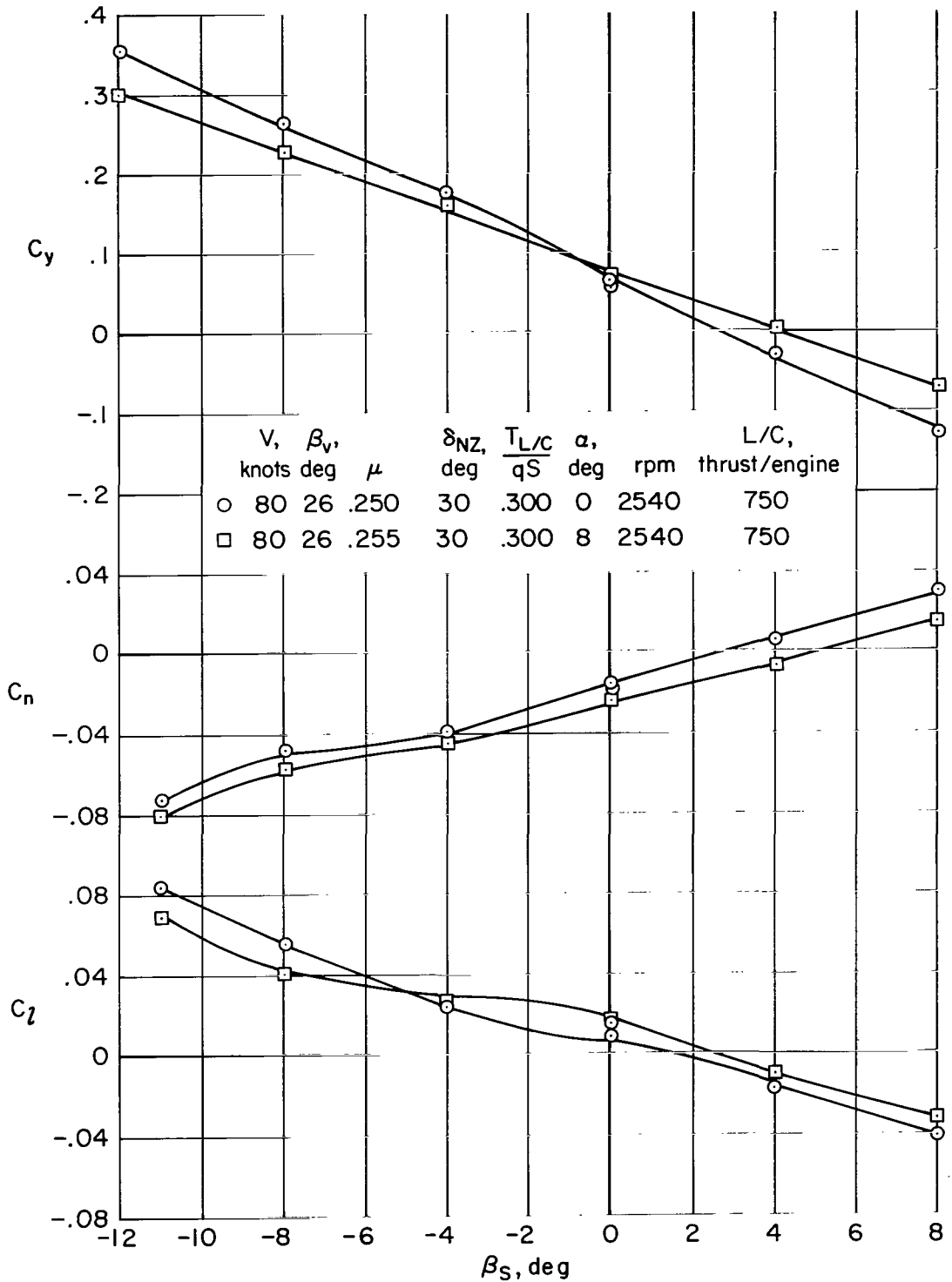
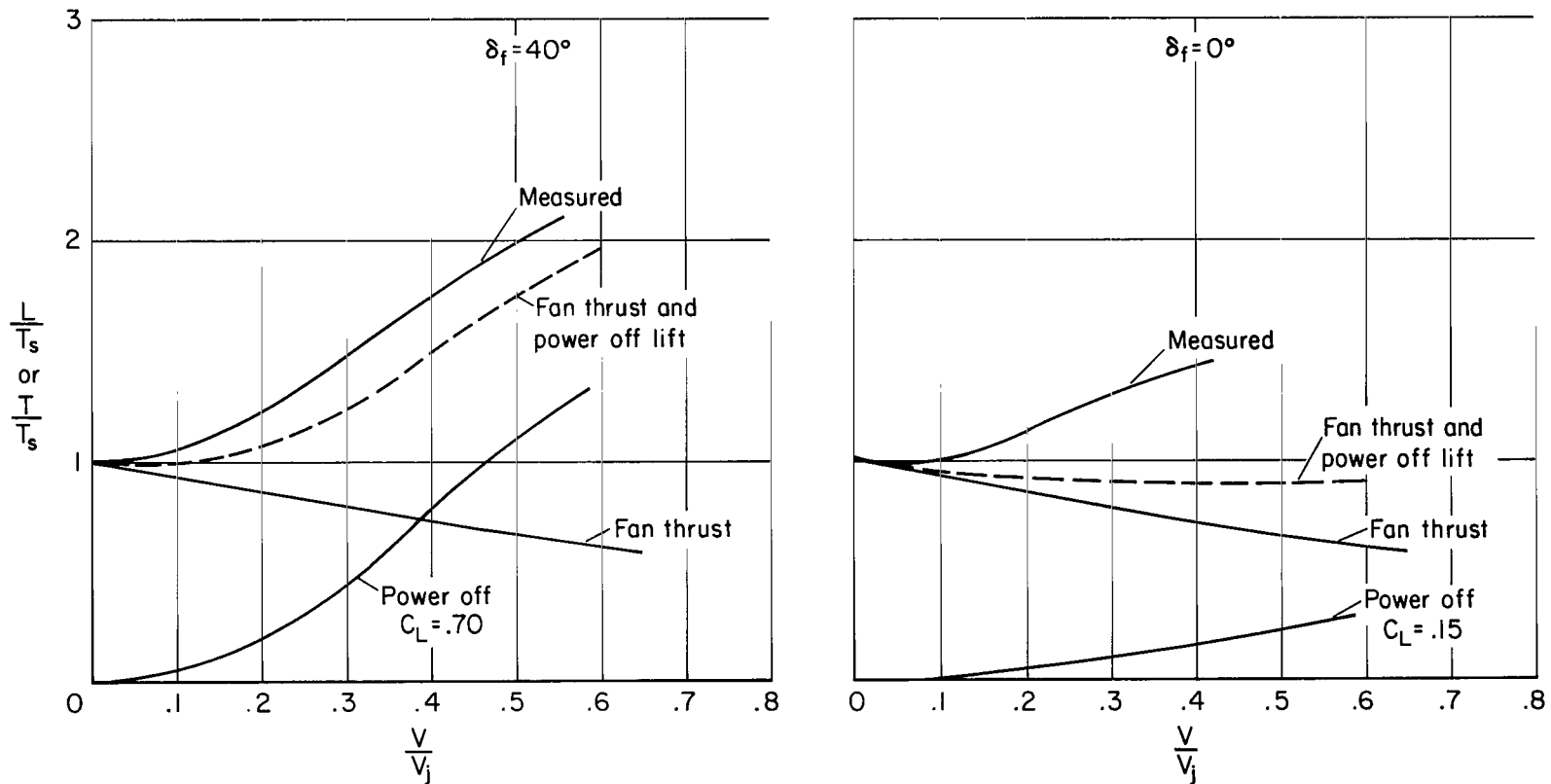
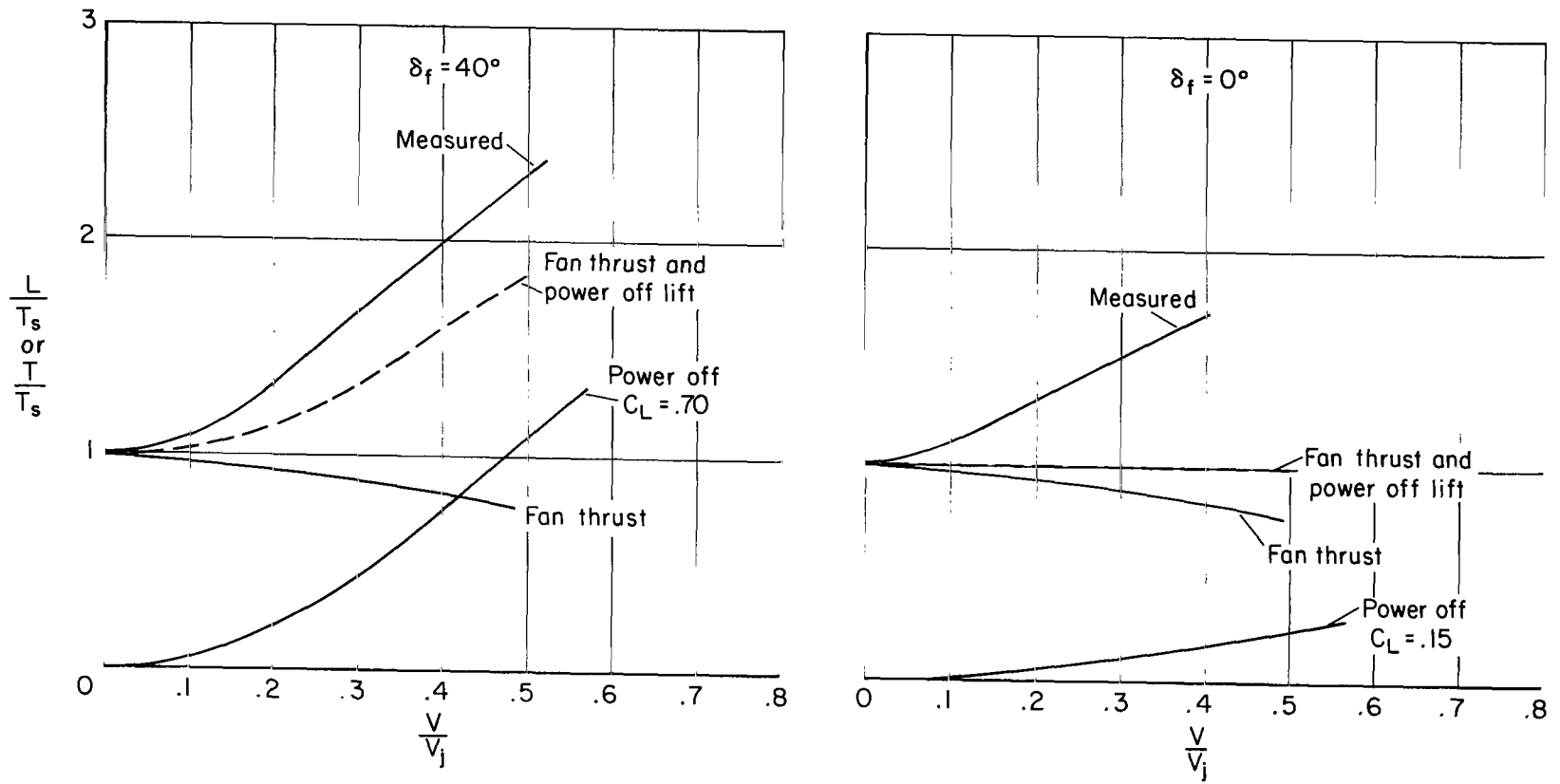


Figure 39.- Lateral-directional characteristics with six fans aft; $\delta_f = 40^\circ$, tail on, $i_t = 0^\circ$, lift-cruise nozzles on.



(a) Six fans forward.

Figure 40.- The effect of fan operation and forward speed on lift at constant fan rpm; $\alpha = 0^\circ$, $\beta_v = 0^\circ$, tail off, 3600 rpm.



(b) Six fans aft.

Figure 40.- Concluded.

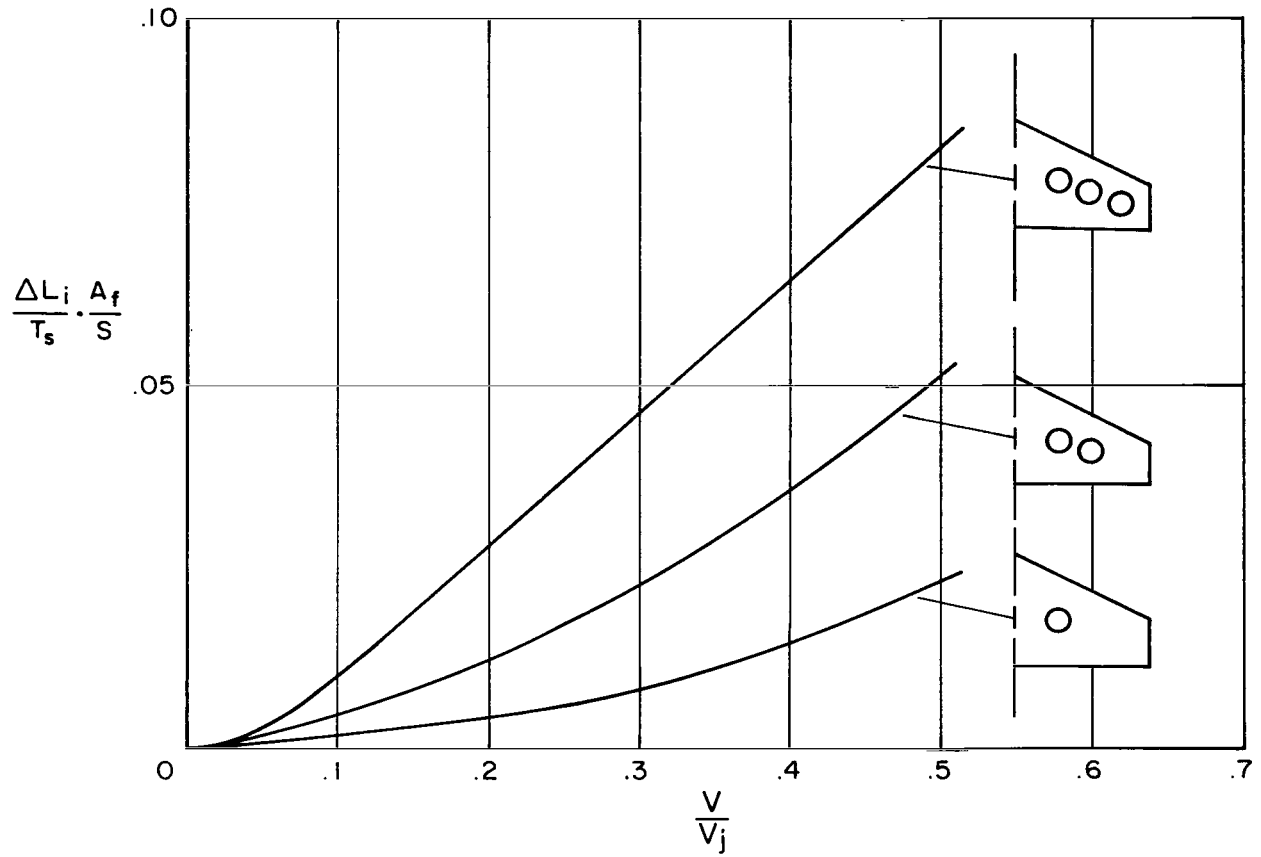


Figure 41.- The influence of spanwise distribution of lift fans on induced lift; $\delta_f = 0^\circ$, $\beta_v = 0^\circ$.

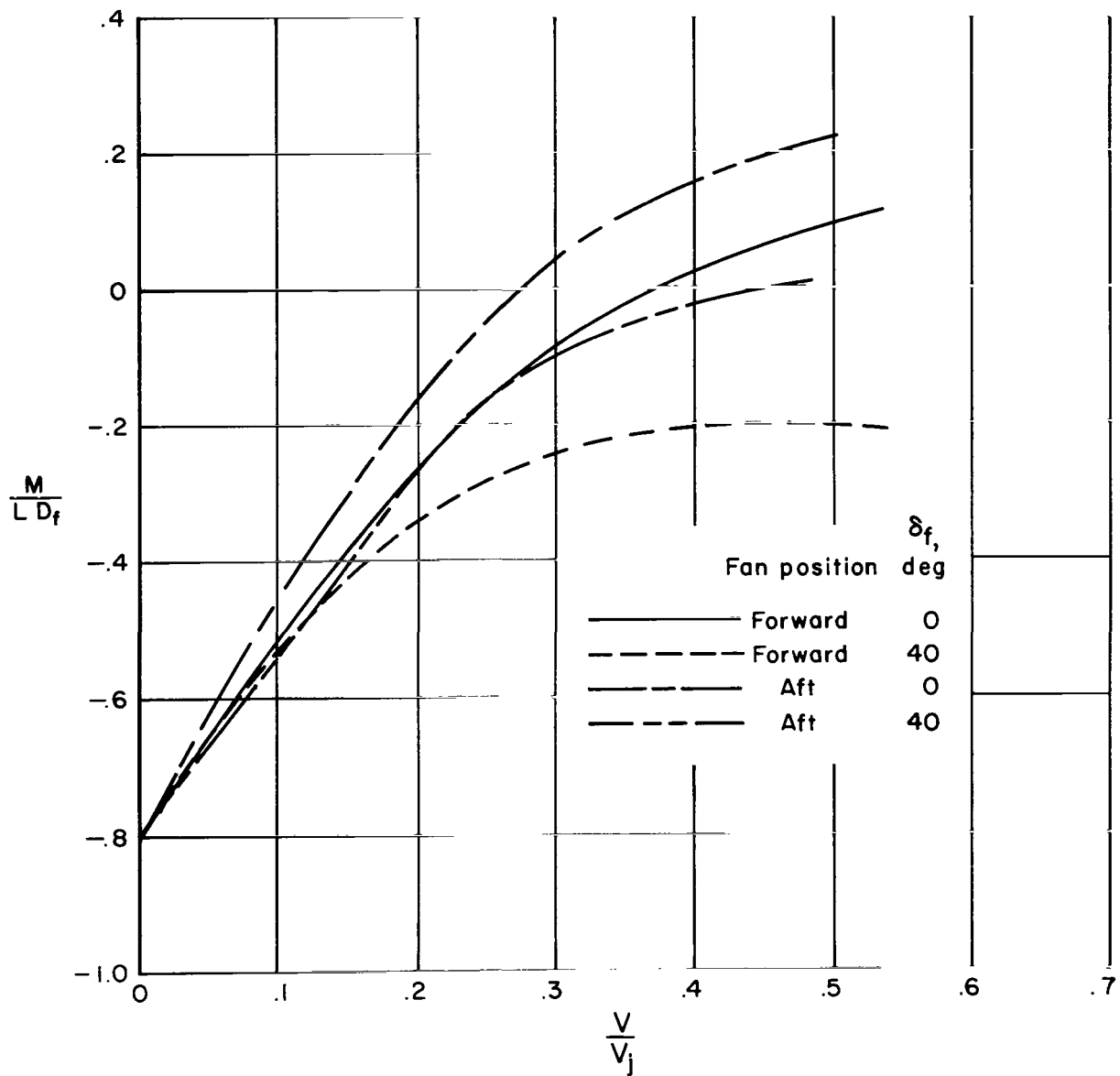


Figure 42.- The variation of pitching moment with forward speed; $\alpha = 0^\circ$, $\beta_V = 0^\circ$, six fans.

"The aeronautical and space activities of the United States shall be conducted so as to contribute . . . to the expansion of human knowledge of phenomena in the atmosphere and space. The Administration shall provide for the widest practicable and appropriate dissemination of information concerning its activities and the results thereof."

—NATIONAL AERONAUTICS AND SPACE ACT OF 1958

NASA SCIENTIFIC AND TECHNICAL PUBLICATIONS

TECHNICAL REPORTS: Scientific and technical information considered important, complete, and a lasting contribution to existing knowledge.

TECHNICAL NOTES: Information less broad in scope but nevertheless of importance as a contribution to existing knowledge.

TECHNICAL MEMORANDUMS: Information receiving limited distribution because of preliminary data, security classification, or other reasons.

CONTRACTOR REPORTS: Scientific and technical information generated under a NASA contract or grant and considered an important contribution to existing knowledge.

TECHNICAL TRANSLATIONS: Information published in a foreign language considered to merit NASA distribution in English.

SPECIAL PUBLICATIONS: Information derived from or of value to NASA activities. Publications include conference proceedings, monographs, data compilations, handbooks, sourcebooks, and special bibliographies.

TECHNOLOGY UTILIZATION PUBLICATIONS: Information on technology used by NASA that may be of particular interest in commercial and other non-aerospace applications. Publications include Tech Briefs, Technology Utilization Reports and Notes, and Technology Surveys.

Details on the availability of these publications may be obtained from:

SCIENTIFIC AND TECHNICAL INFORMATION DIVISION
NATIONAL AERONAUTICS AND SPACE ADMINISTRATION

Washington, D.C. 20546